Texas Utilities Generating Company
Comanche Peak Steam Electric Station
Unit 1

Report

Evaluation of Paint and Insulation Debris Effects on Containment Emergency Sump Performance

June 1984

Gibbs & Hill, Inc.
Engineers, Designers. Constructors
New York, New York

Texas Utilities Generating Company
Comanche Peak Steam Electric Station
Unit 1

Report

Evaluation of Paint and Insulation Debris Effects on Containment Emergency Sump Performance

June 1984

Gibbs & Hill, Inc.
Engineers, Designers, Constructors
New York, New York

ACKNOWLEDGEMENTS

1. Section 8 is contributed by Ebasco Services Inc.

2. Appendix 1 is contributed by Westinghouse Electric Corporation.

TABLE OF CONTENTS

EVALUATION OF PAINT AND INSULATION DEBRIS
EFFECTS ON CONTAINMENT EMERGENCY SUMP PERFORMANCE

LIST OF TABLES

LIST OF FIGURES

1.0 PURPOSE

The purpose of this report is to determine if the debris resulting from the postulated failure of paint and insulation inside the CPSES Unit 1 containment due to a LOCA will adversely affect performance of the containment emergency sumps and those engineered safeguards systems drawing suction therefrom.

2.0 SUMMARY

The detailed analysis of potential effects of coatings failure on the performance of all relevant plant safety systems indicated that the single most significant aspect of postulated coating failure will be the potential for blockage of the emergency sump screens by paint and insulation debris. The mechanism for and effect of such blockage on emergency sump performance are evaluated in detail in this report. The general methodology and logic used for determining the potential sump blockage are based on NUREG/CR-2791, NUREG/CR-3616 and NUREG-0897, Revision 1 (Draft).

The following step-by-step approach was used to evaluate the sump screen blockage effects. First, the water velocities inside the containment in each zone of the containment were determined. Next, the quantities of paint and insulation debris in each zone of the containment were calculated. The calculations determined that there is no potential for insulation debris to reach the sumps. Finally, the transport velocities for paint particles in each zone were calculated, and the quantity of paint transported to the sump screen was calculated.

Based on the conservatively assumed quantity of paint debris that could reach the sump screen, the screen blockage and pressure drops were evaluated. The analysis determined that about 90,000 sq ft (about 300 cu ft) of paint could reach the vicinity of the sump screen through mechanisms derived from the above NUREGs, and cause partial blockage. The extent of screen blockage by paint debris was calculated to be 35 to 50 percent of the screen area, well within the design basis for sump performance. The conclusion of the analysis is that this amount of screen blockage cannot cause any impact on plant safety.

To supplement the above methodology, other possible near sump effects were analyzed, assuming the various mechanisms for sump screen blockage. All these mechanisms evaluate paint particles impinging on the screen before settling to the floor of the containment. The analysis determined that paint debris within approximately ten feet of ten feet of the screen has the potential to impinge on the screen and be retained on the screen by flow forces, thereby blocking the screen. Using highly conservative assumptions, it was determined that up to 94 percent of the screen could be blocked. The sump blockage discussed in the previous paragraph and blockage due to the near sump effects discussed here are not additive. However, even in this worst possible case, the required level of sump performance would be unimpaired.

In addition to sump screen blockage, secondary effects of paint failure were analyzed. Most of such effects are only likely if there are very fine particles of paint debris which pass through the screen. The analysis of such effects leads to the conclusion that blockage of narrow passages in containment spray and RHR/SI

will not occur because these systems are designed to handle particles less than 1/8 inch in size. Further, impacts of very fine particles in the reactor systems are acceptable in that no significant buildup of fines in the core will occur.

The ECCS and its critical operating components were analyzed for potential erosion or corrosion degradation due to the postulated ingestion of zinc into the ECCS. The conclusion resulting from this evaluation and the related containment paint chemical analysis was that no significant erosion or corrosion damage to the ECCS or to its critical components would occur. No deleterious effects are postulated in the reactor core for the material concentrations assumed in this evaluation.

In addition, the analysis led to the conclusion that the design basis containment hydrogen generation will not increase because the original estimates of hydrogen generation in the FSAR conservatively assume that all zinc in the coatings react to produce hydrogen.

Finally, the analysis led to the conclusion that any failed paint would not tend to become airborne. In any event, the analysis reflected that any paint that did become airborne would have no adverse effects on plant filter systems.

3.0 SAFETY IMPACT OF POSTULATED PAINT FAILURE

3.1 Paint Characteristics

The major coating systems (paint) used inside the containment and their average DFT (dry film thicknesses) are presented in Table 3.1-1.

The steel coatings are manufactured by Carboline Co.; the concrete coatings are manufactured by Imperial Professional Coating Corporation, Inc.

Approximately 285,000 sq.ft. of concrete and 333,000 sq.ft. of steel are coated. The Carbozinc 11 is a self-curing zinc-filled inorganic coating, containing about 80% wt. solids, with a specific gravity of 4.0. The Phenoline 305 is a modified phenolic coating, containing about 81% wt. solids, with a specific gravity of 1.5. The Nutec 11 is a water-based epoxy coating, containing about 78% vol. solids, with a specific gravity of 1.8. Nutec 11S is the same as Nutec 11 except that it contains 51% wt. 30-140 mesh sand, and has a specific gravity of 1.8. Reactic 1201 is a polyamide epoxy coating, containing about 73% wt. solids, with a specific gravity of 1.5.

The Nutec 11S is used as a surfacer for concrete. Nutec 11 and Reactic 1201 are used as top coats.

All of these coatings have successfully passed the DBA test conforming to ANSI N101.2-1972, "Protective Coatings (Paints) for Light Water Nuclear Reactor Containment Facilities." Thus, these coatings can withstand the environmental conditions, such as, temperatures, pressures, chemical and radiation levels during a LOCA.

Paint impurities for the steel coatings are presented in Table 3.1-2.

Decomposition temperatures for all the containment coatings are ≥ 350 F. They are thermally stable for continuous exposure at 200 F. Carbozinc is thermally stable for continuous exposure at 750 F. The characteristics of all coating systems used at CPSES are summarized in Table 3.1-2.

Paint Failure Modes

Paint can fail by two general modes: chalking and flaking/peeling. Chalking is loss of the paint film by powdering to small (micrometer-size) particles. Flaking/peeling is loss of the paint film by flakes of small (usually <one inch) particles. Field and laboratory observations of the containment coatings used at Comanche Peak confirm that the failure modes are by flaking of small (1/8 - 1 inch) particles, except for the Carbozinc 11. The Carbozinc 11 failure mode is by chalking (powdering).

Other terminologies to explain coating failure used in the industry, such as blistering, intercoat delamination, cracking, undercutting (lifting of the paint film by substrate corrosion), checking, mud-cracking, alligatoring, erosion, wrinkling, pinpoint rusting and pitting, lead to either chalking or flaking/peeling.

Blistering, checking or mud-cracking can lead to failure by flaking/peeling of small size (< 1/2 inch) particles ("Good Painting Practice, Vol. 1, Steel Structures Painting Manual," SSPC 1982, Chapter 23; ASTM D772-47, "Standard Method of Evaluating Degree of Flaking (Scaling) of Exterior Paints," ASTM Vol. 06.01, 1984; ASTM E714-56, "Standard Method of Evaluating Degree of Blistering of Paints," ASTM Vol. 06.01, 1984; ASTM D660-44, "Standard Method of Evaluating Degree of Checking of Exterior Paints," ASTM Vol 06.01, 1984).

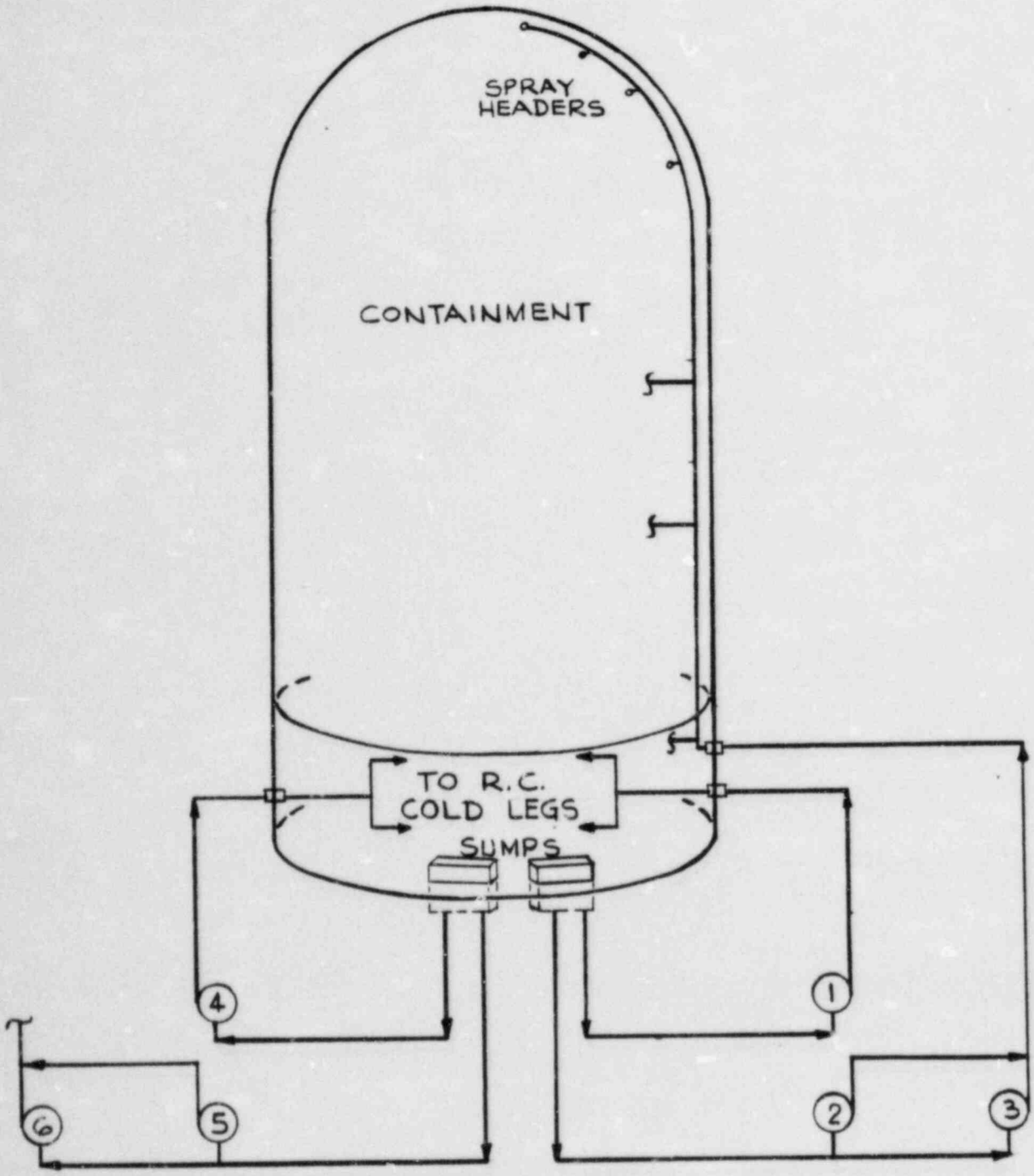

1. RHR PUMP
2. CONTAINMENT SPRAY PUMP } TRAIN "A"
3. " " "

4. RHR PUMP
5. CONTAINMENT SPRAY PUMP } TRAIN "B"
6. " " "

FIGURE 3.2-1
RECIRCULATION FLOW PATH

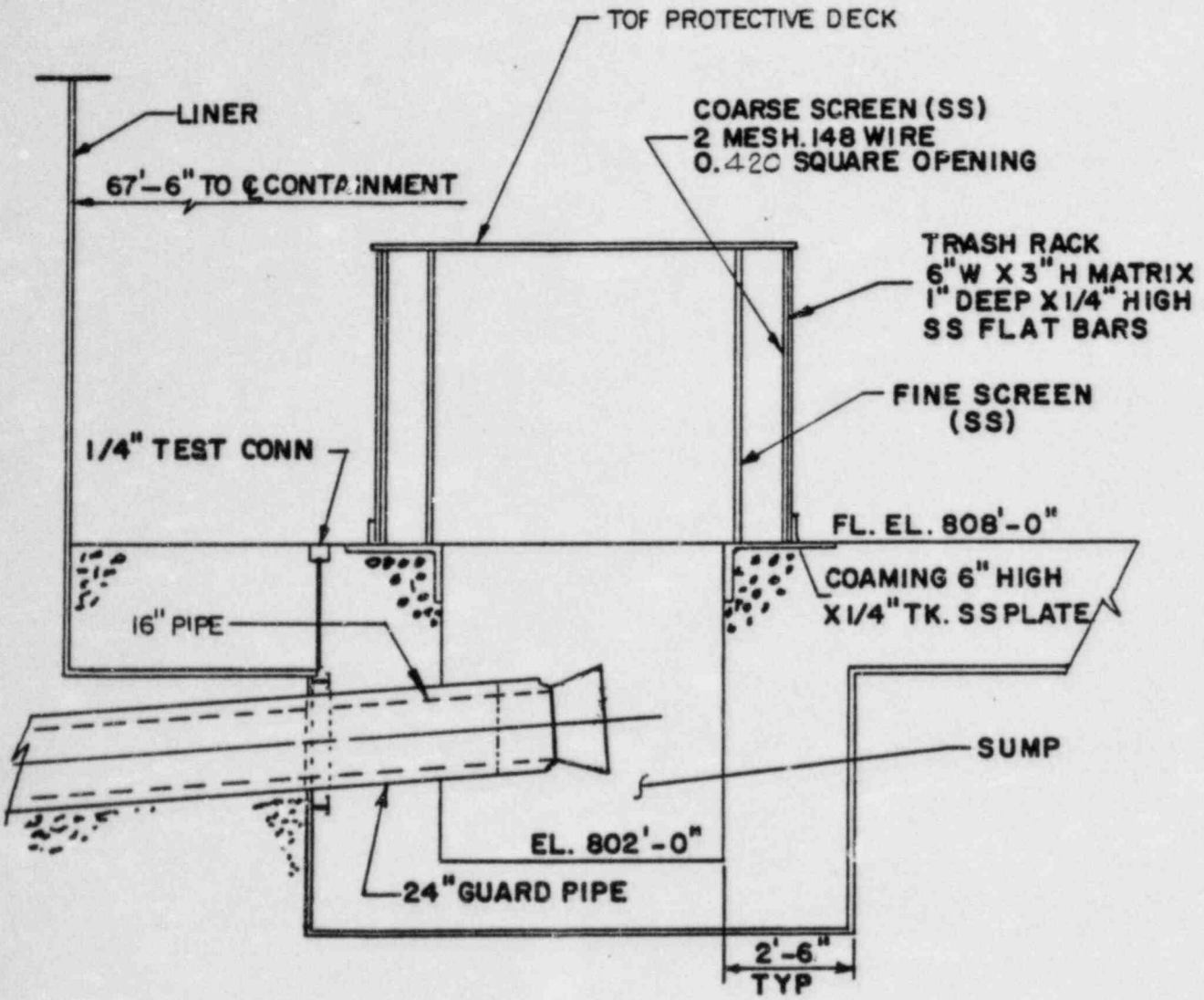

CONTAINMENT EMERGENCY SUMP

FIGURE 3.2-2

SCHEMATIC OF SUMP
CONTAINMENT SPRAY AND RHR/SI CONNECTIONS

TABLE 3.1-1

COATING SYSTEMS AT CPSES

Service	Type	Average DFT Mils[1]
1. Steel[2]:		
Primer	Carbozinc 11	3
Topcoat	Phenoline 305	5
2. Concrete[3]:		
Surfacer	Nutec 11 S	20
Topcoat	Nutec 11	12
	Reactic 1201	10

Notes:

(1) Dry film thickness in mils (1 mil equals .001 inch)
(2) Manufactured by Carboline Co.
(3) Manufactured by Imperial Professional Coating Corporation.

TABLE 3.1-2

CHARACTERISTICS OF COATINGS

Characteristic	Coating Type			
	Carbozinc 11	Phenoline 305	Nutec 11S & 11	Reactic 1201
1. Chemical:				
Solids (wt %)	80-85	81	78	73
Chlorides (ppm)	70-80	170-180	NA	NA
Halogens (ppm)	70-80	850-900	NA	NA
Lead (ppm)	1000 (max)	NA	NA	NA
2. Physical:				
Specific Gravity	4.0	1.5	1.6-2.0	1.5
Thermal Stability (°F)	750	>200	>200	>200
Decomposition (°F)	>750	>350	>350	>350

NA - not available

3.2 Potential Effects of Paint on Engineered Safeguards Performance

The potential effects of coatings failure on performance of plant engineered safeguards systems are evaluated in this report. Some of the area~ of likely concern are:

- Blockage of containment emergency sumps
- Blockage of containment spray and RHR/SI system flow passages
- Containment hydrogen generation
- Blockage of filters in containment air handling systems.
- Fouling of heat transfer surfaces

This report addresses each of these concerns and evaluates the impact on the plant safety systems.

Following a LOCA, the safety injection and RHR systems provide cooling water to the reactor core. The water supplied to the core spills on the containment floor. The containment spray system sprays water into the containment through nozzles in the dome of the containment and underneath the slabs of the major floors to remove heat and iodine from the containment atmosphere. Initially, both of these systems take water from the refueling water storage tank. When the refueling water storage tank contents are depleted, these systems are switched to recirculate water which has accumulated on the lowest level of the containment. Figure 3.2-1 shows, in simplified form, the flow path for these systems during recirculation.

The recirculation inlets to the RHR/SI and containment spray systems are protected by sump screens in the containment as shown in Figure 3.2-2. These screens comprise trash racks, coarse screens and fine screens.

The containment spray nozzles contain orifices 3/8" in diameter. The recirculation screens are sized to exclude particles larger than 1/8" diameter to avoid plugging of the spray nozzles. The remainder of the containment spray system is designed to accommodate 1/8" particles. For example, the containment spray pumps can pass such particles without clogging. The safety injection and RHR systems can also pass 1/8" particles, without clogging.

It is apparent that the screens might be blocked by large debris particles. Failed paint must be counted as a potential type of debris which could affect the screens.

Particles smaller than 1/8" can enter the systems and can cause other effects, such as erosion and accumulation in low velocity regions. These effects must therefore be investigated.

One possible influence of coatings on engineered safeguards system is hydrogen generation. The prime coat on steel surfaces is a zinc paint which, on exposure to hot water, can oxidize to zinc oxide, thereby releasing hydrogen gas from the water. It could be postulated that failure of the topcoat could expose the prime coat and therefore facilitate such hydrogen formation. However, the design basis hydrogen generation for the plant was calculated based on assuming that all the zinc in the coatings reacts to form hydrogen. Therefore, failure of the topcoat does not influence containment hydrogen generation estimates.

3.2.1 Airborne Paint Particles

It is concluded that airborne paint (failed paint that becomes airborne) is not a problem because of the following:

- All containment HVAC equipment shut down on accident initiation

- The containment Hydrogen Recombiners are not fed by fans and have no filters; they are fed by natural convection and do not have any catalyst. They are the thermal type which oxidize hydrogen (H_2) by electrically heated tubes.

There is a backup H_2 Purge System which is manually initiated and located outside the containment. This system would be operated in the event the containment H_2 exceeds a predetermined concentration. This system has fans and filters (100% redundant filter banks). However, these filters can be manually changed on high pressure drop. Therefore, airborne failed paint, even if it reached these filters, would not affect their operation since the filters can be changed if they clog.

During a LOCA failed paint would not tend to be airborne due to the scrubbing effect by the containment spray system, and the high density of the failed paint relative to containment atmosphere density.

3.2.2 Impact on NSSS Safety Systems

The effects of paint failure, specifically intrusion of paint fine particles into the NSSS safety systems was studied by Westinghouse. This report is presented in the Appendix-1 and summarized below.

The evaluation of the ECCS and its critical operating components revealed no potential erosion or corrosion degradation with respect to the postulated ingestion of zinc into the ECCS. The conclusions resulting from this evaluation and the related containment paint chemical analysis are as follows:

- No significant erosion or corrosion damage will occur to the ECCS or to its critical components.

- Leachable chloride concentration levels (for all containment panels) which could enter the ECCS are significantly below the chloride concentration levels which could cause cracking in sensitized austenitic stainless steel.

- No fluoride cracking of sensitized stainless steel will occur since any fluoride ions, if present, would form fluoroborates which have no affect on stainless steel.

- No deleterious effect are postulated in the reactor core for the material concentration assumed in this evaluation.

4.0 SUMP PERFORMANCE CRITERIA

4.1 Sump Performance

Figures 3.2-1 and 3.2-2 show the schematic of the Containment Emergency Sump and the Containment Spray and RHR/SI system connections to the sump. There are two sumps in each containment at Comanche Peak - one for train A and one for train B. Safety requirements can be met with one train operating. However, in normal post-LOCA conditions, both sumps will operate, and all pumps on each sump will operate. Design parameters for the sumps are shown in Table 4.1-1.

In this discussion, all elevations are referred to the containment basement level, 808 ft in the plant elevation reference. After a LOCA, water level in the containment will be a minimum of 6 ft 10 inches above this datum.

The containment spray pumps and the RHR pumps were tested at the manufacturers' shops. Shown in Table 4.1-2 are the minimum water levels in the containment required to accommodate the required NPSH, excluding the head losses across the screen. Head losses across the screen is considered later in this report.

Similar sumps were tested at the Western Canada Hydraulic Laboratories (WCHL) using a full scale model as reported in Reference 8. Most tests at WCHL were run with a water level of 2 ft 10 inches above datum. This level was selected to maximize the possibility of vortexing and to maximize head loss in the sumps.

Two series of WCHL tests should be noted in this analysis. First, there was a series of tests with "50 percent blockage." This was based on blockage of 50 percent of the screen below the 2 ft 10 inch level. Since the screen extends 5 ft 9 inches above datum, about 94 square feet of screen were available. Several "50 percent blockage" tests were run with different blockage configurations. Included among these blockage configurations was one where all screen area below 1 ft 5 inches was blocked.

Some tests were also run with approximately "90 percent blockage." These tests were run with 9 out of the 10 screens blocked off. This test established that sump performance was satisfactory even with only 19 square feet of screen available for flow.

Table 4.1-3 summarizes the WCHL test data for different sump blockages, flow velocities and corresponding screen pressure drops.

TABLE 4.1-1

SUMP DESIGN PARAMETERS

DESIGN FLOW, gpm		12,500
COARSE SCREEN		
Dimensions, ft.-in.	Length	30'8" Long radius 26'7" Short radius
	Width	7'10"
	Height	5'9"
Opening size, in.		0.420
Open area, %		70
FINE SCREEN		
Dimensions, ft.-in.	Length	30'3" Long radius 27'0.5" Short radius
	Width	6'10"
	Height	5'9"
Opening size, in.		0.115
Open area, %		64.6

TABLE 4.1-2

PUMP NPSH

	Pump	
	CSS	RHR
Flow at runout, gpm/pump	3900	5300
Pump centerline elevation	775'7"	776'6"
Water level required to provide minimum NPSH ft.(1)	0.62' above containment floor	2.2' above containment floor

(1) Does not include head loss in screens

TABLE 4.1-3

SUMMARY OF TEST DATA FOR SUMP PERFORMANCE
(Ref. Western Canada Hydraulic Laboratories)

Sump Screen Blockage, %[1]	Flow (gpm)	Screen Area (sq. ft.)	Pressure Drop (ft. of water)
0	12,200	188	0.005
50	16,600 - 17,600	94	0.020 - 0.035
50	9,500 - 10,500	94	0.005 - 0.01
88.3	16,000 - 19,000	22	0.271 - 0.454
89.8	18,500 - 19,500	21	0.314 - 0.34
91.5	18,500 - 19,500	16	0.4 - 0.44

[1] Below 2'10" Level

5.0 WATER VELOCITIES

Following the post-LOCA safety injection phase, when the contents of the RWST are exhausted, valving is aligned to provide for a recirculating flow of water from the containment emergency sumps.

The water flowing through various zones provides the motive force for the transport of debris to the containment emergency sumps. The available water velocity in a given area of the containment determines the transport potential for the debris.

The object of the water velocity analysis is to establish migration patterns for debris within the containment. The flow pattern within the containment is complex due to the presence of equipment supports, shield walls, openings in compartments, floor openings and related hydraulic resistances. The methodology used to estimate recirculation flow velocities within various regions of the containment is similar to that discussed in NUREG/CR-2791.

5.1 Sources of Water

The sources of water inside the containment following a LOCA determines the water level. The water level in turn determines the flow area for calculation of water velocities in various zones of the containment. The sources of water considered in this evaluation are given in Table 5.1-1. This table gives the maximum available water sources, the minimum and maximum amounts of water expected to be in the containment following a LOCA. The difference between the maximum and minimum water source is in the refueling water volume. The maximum water is based on the tank useable volume, i.e., 2 percent above high water level set point to the pump suction nozzle. The minimum water volume is based on the refueling water tank capacity from 2 percent below the high water level set point to 2 percent above the empty level set point (the empty level set point is 6 ft. 4 inches above the pumps suction nozzle.)

5.2 Water Levels at Sump Elevation (808 ft. EL)

The high and low water levels were calculated using the maximum and minimum water inventories given in Table 5.1-1. These calculations were based on the actual net volume available at 808 ft. EL. in the containment. The net volume was calculated by determining the gross volume and deducting the actual volumes of equipment, foundations and other components. The calculated high and low water levels are also presented in Table 5.1-1.

5.3 Velocities at Upper Elevation

Figure 5.3-1 shows a schematic of the containment spray system arrangement. The sprays are arranged in four zones. Each spray area covers the space above the floor in the zone. The spray flow rates given in Table 5.3-1 were used to determine the water velocities on each of the containment floors. Each floor in the containment is provided with 4-inch-high curbs all around. The pathways for spray cooler is only through openings in the floor for staircases, equipment hatches and grated openings.

The general methodology used for velocity determination is as follows:

a. The amount of spray flow collected on each floor was calculated using the spray flows and floor areas. The sprays which fall in open areas are attributed to the next lower floor.

   The total spray flow for each floor consists of net spray on the floor and the flow intercepted from floor above for both open areas and spill openings.

b. The flow discharge from each floor will be through the spill opening available. Average discharge in gallons per linear foot of spillway width was calculated for each floor.

c. The minimum water depth for each floor was calculated based on the critical depth. For flow discharging from a rectangular channel ending in free fall at a spill, critical depth occurs near the outlet, as shown in Figure 5.3-2 (Ref. 9 and 10).

$$D^3 = \frac{eQ^2}{gw^2}$$

where D = critical depth (ft)
Q = discharge (cfs)
g = accel. of gravity
w = width (ft)
e = energy coefficient

The energy coefficient (e) is applied to account for the non-uniform distribution of velocities. The energy coefficient varies from 1.03 to 2.0. An average coefficient of 1.5 was assumed. The assumption is reasonable and conservative because of the wide variation of flow conditions and obstructions which results in wide velocity fluctuations.

d. Flow depths and velocities for locations other than near the spill brink are approximated by deriving flow profiles using "backwater" procedures based on Manning's formula for open channel flow and Bernoulli's Theorem (Ref. 9 and 11).

   Friction allowance is based on a conservative roughness coefficient of 0.011 (Ref. 9) for smooth concrete, trowel finish.

Using the above methodology, flow velocities on each of the upper floor elevations are calculated and the results are presented in Tables 5.3-2 and 5.3-3. Table 5.3-2 gives flow velocities with two containment spray trains operating and Table 5.3-3 gives flow velocities for one train operation.

5.4 Water Velocity at the Sump Elevation

5.4.1 Water Flow Paths

The flow of fluids entering and exiting the containment during the recirculation phase of a LOCA were examined.

The RHR/SI (ECCS) and containment spray systems were each oriented as two completely redundant trains. Each train draws water from one of the containment emergency sumps. The containment spray and RHR flow rates are as shown on Table 5.4-1.

The flow rates corresponding to both one and two trains were considered in the water velocity determination. The spray flows at each elevation of the containment were evaluated in Section 5.3. All the spray flows from upper flows terminate on the 808'-0" elevation at various locations. Based on the discussions in Section 5.3, it was determined that the bulk of the spray flow terminates at azimuth 225°. For the purposes of this evaluation, it was conservatively assumed that the source of all the spray flow wil be at azimuth 225° and as shown on Figure 5.4-1. The flow from the RHR/SI system occurs through the postulated break in the coolant system. This break location was determined to be in Steam Generator Compartments No. 4. The location of this source of water is also shown on Figure 5.4-1.

Figures 5.4-2 and 5.4-3 show the flow paths to the sumps for the RHR/SI flow and the spray flow, respectively.

5.4.2 Water Velocity Analysis

The spray and RHR/SI flows were considered separately and then superimposed to yield the total velocity. The containment water inventory determines the height of water inside the containment which in turn determines the cross-sectional area available for flow. The available areas for flow were chosen by examining the containment and choosing cross-sections that presented maximum restriction to flow. These restriction were projected along the flow path until a more limiting restriction or a significant zone of larger flow area was encountered. Typical cross-sections examined for this evaluation are shown on Figures 5.4-4 and 5.4-5. Figure 5.4-4 and 5.4-5 represents the location of cross-sections within the containment and the steam generator compartments, respectively. Figures 5.4.-6 and 5.4-7 represent two typical cross-section within the steam generator compartment No. 4. Figures 5.4-8 represents a typical cross-section along the most restrictive channel to the sumps in the corridor outside the steam generator compartments.

Flow within the containment was assumed to be represented by a number of parallel open channel flows. Accordingly, pressure drop from the break region and spray source to the sump is constant for each flow path, and the summation of mass flows through the various paths equals the total flow. The magnitude of the flow rate through each channel is dependent upon the hydraulic resistance presented by the path.

As described in NUREG CR-2791, a flow resistance map of the containment floor was developed as shown on Figure 5.4-4. The map identifies channels (parallel resistance paths) and sub-channels (series resistances within a channel). A point source of flow was selected and the potential paths of flow to the sumps were determined. The source of RHR and SI water was postulated to be from a reactor coolant pipe break in steam generator compartment No. 4, which is closest to the sumps.

The resistances were determined as the length divided by the area of each sub-channel in the flow path. The area will vary depending on the water level chosen. The pathways are developed in the form of "circuit" diagrams or networks for the RHR/SI flows and spray flows as shown on Figures 5.4-9 and 5.4-10 respectively. The fraction of flow in each branch was determined by combining the resistances as in an electrical cicuit diagram and proportioning the flows by resolving the parallel and serial resistances. The resistances utilized are hydraulic and therefore the resistances relate to pressure drop in proportion to the square of the mass flow. By determining the total equivalent resistance, the total flow was apportioned to each channel. Velocity was then determined for each subchannel by dividing the channel flow rate by the subchannel area.

The velocity summary is presented on Tables 5.4-2 through 5.4-13.

Tables 5.4-2 through 5.4-9 show the flows and sub-channel resistance determinations. Tables 5.4-10 through 5.4-13 show the combined velocity summary for RHR/SI and spray systems operation.

The influence of various factors on the velocity was examined. It was determined that the effect of the cross-sectional area was the most significant factor. The cross-sectional area, in actuality, is subject to change as the water level in the containment varies. The total velocity was determined as the water level was varied between 814 feet and 817.5 feet. The results of this analysis are presented in Table 5.4-14.

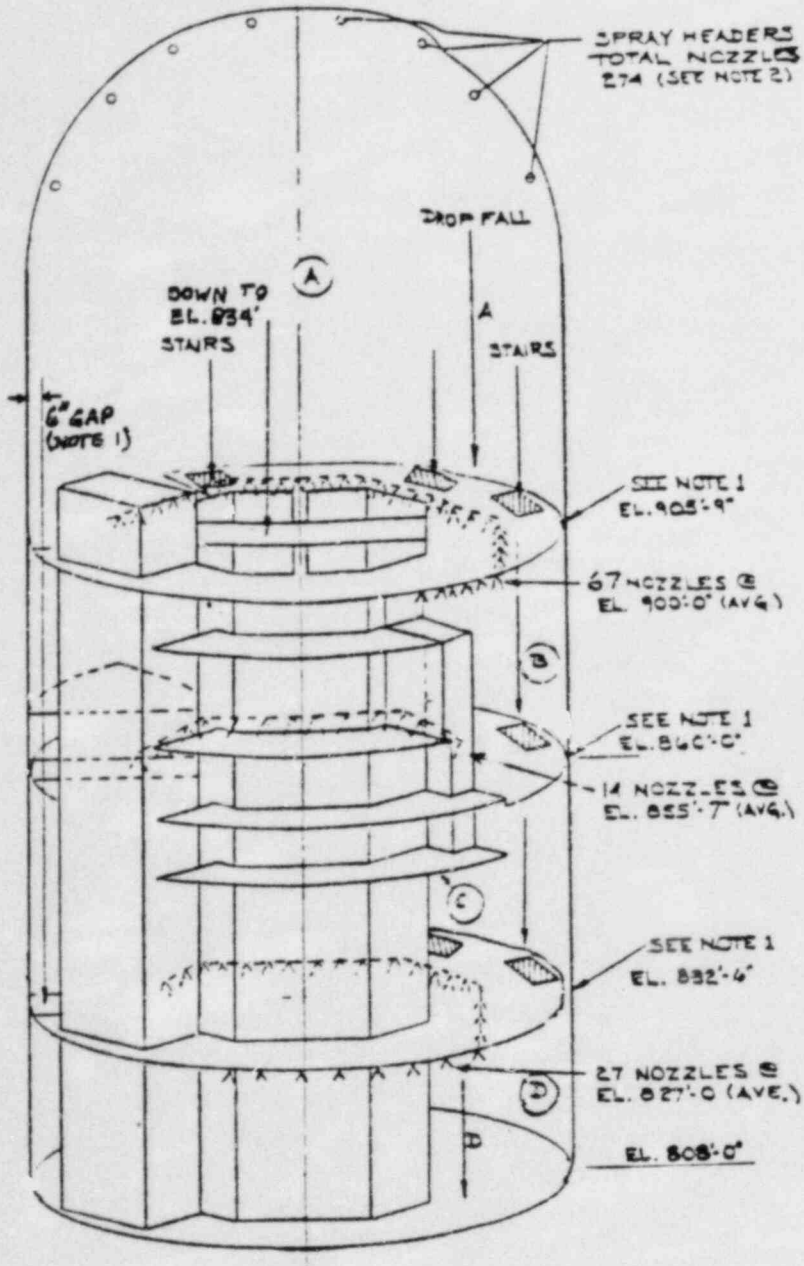

Notes: 1. 6" Gap between Floor & Containment Wall Allows for Dropfall Between Floors.

2. Number of Nozzles shown for each Floor is for One Train only.

FIGURE 5.3-1

CONTAINMENT SPRAY ZONES

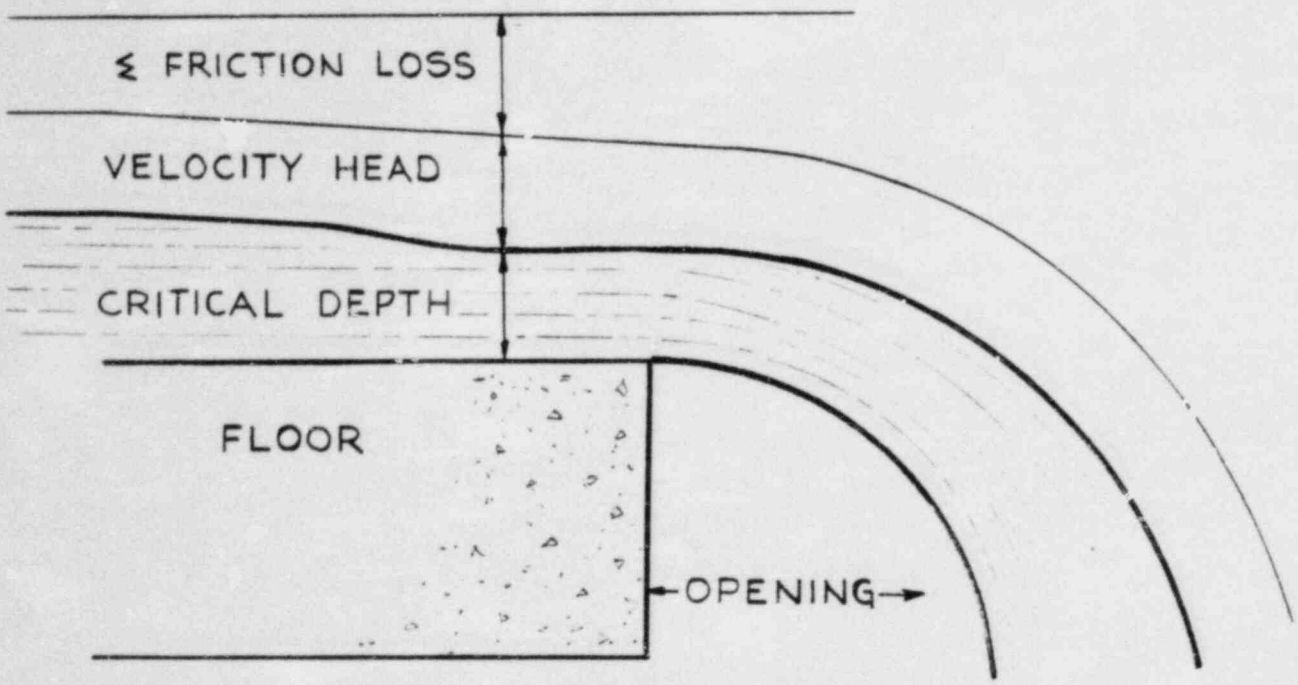

FIGURE 5.3-2
FREE FALL SPILLWAY

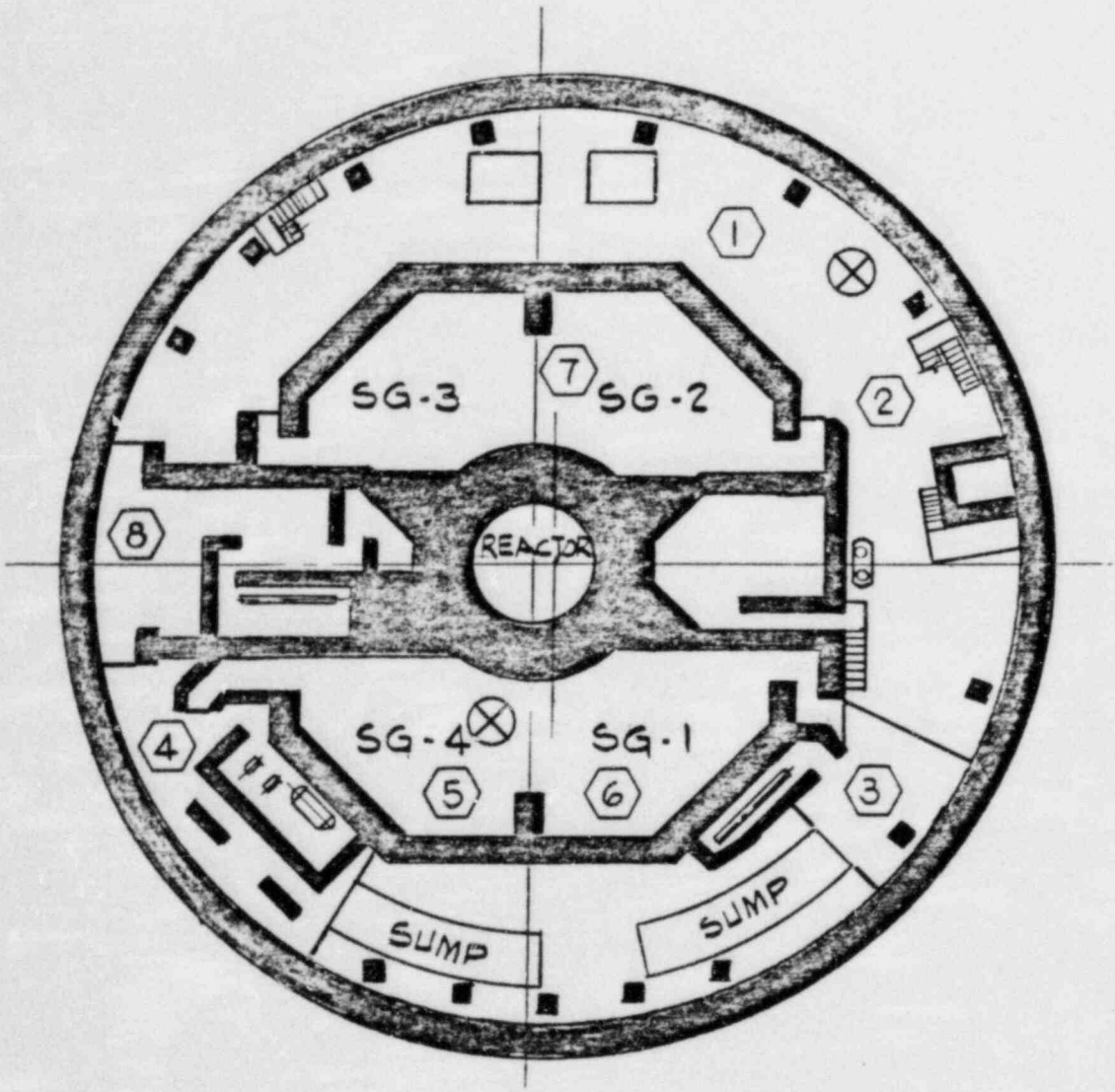

FIGURE 5.4-1
CONTAINMENT CHANNEL LOCATIONS
⊗ = SOURCE OF WATER

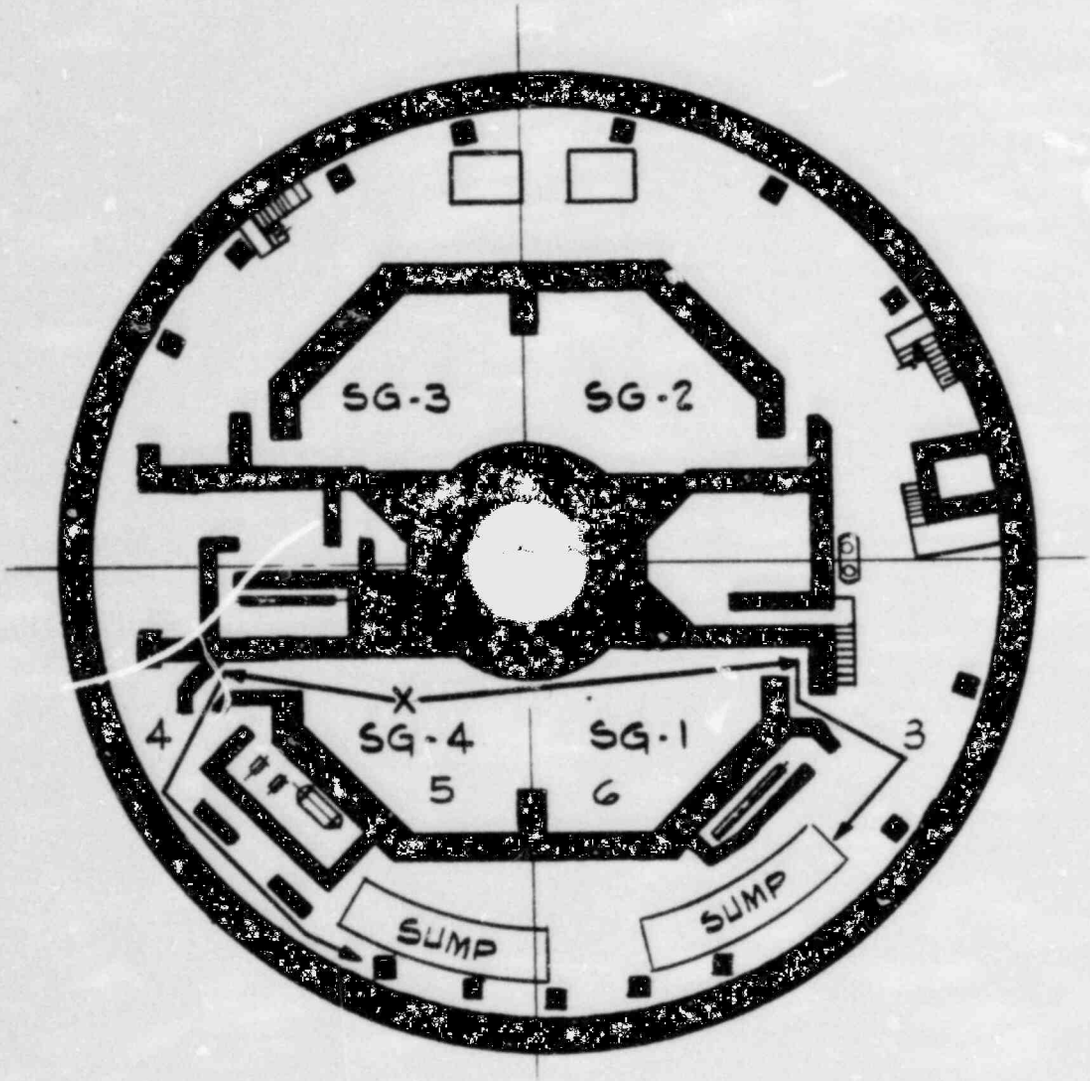

FIGURE 5.4-2
RHR/SI FLOW PATH
(X= BREAK LOCATION)

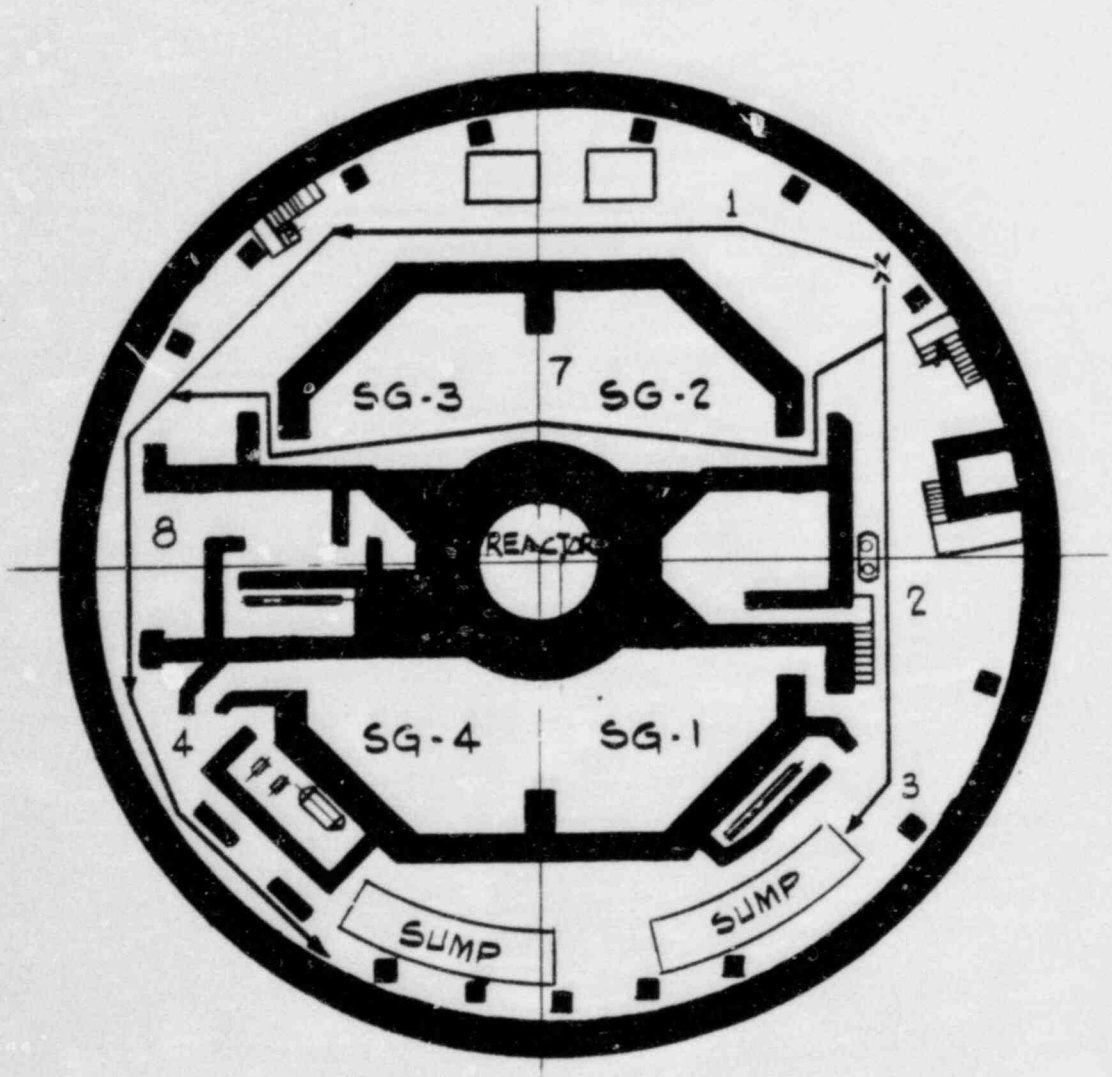

FIGURE 5.4-3
SPRAY FLOW PATH
(X = SPRAY SOURCE)

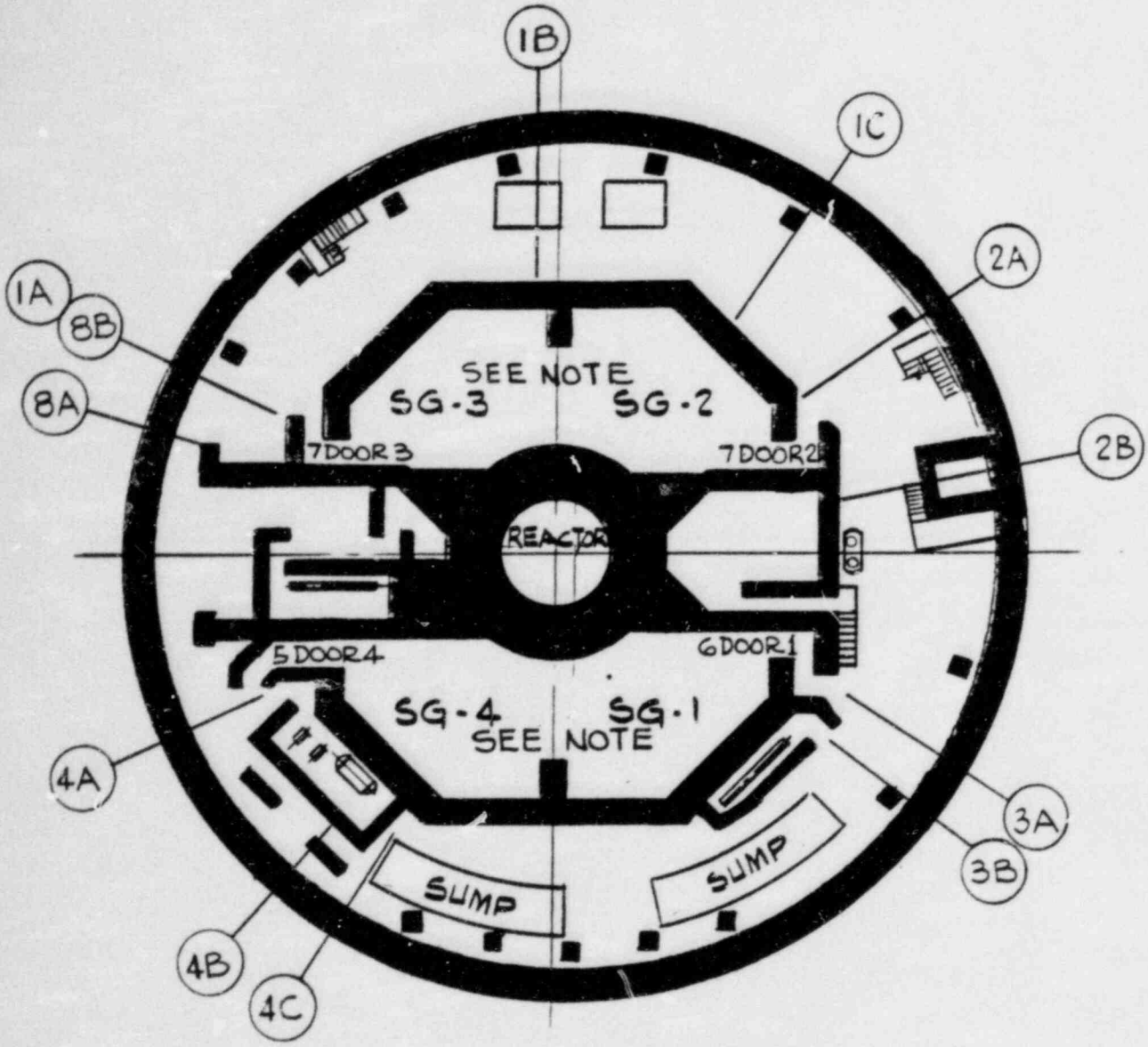

NOTE: SEE FIG. 5.4-5 FOR TYPICAL STEAM GEN. COMPARTMENT SECTIONS.

FIGURE 5.4-4
FLOW RESISTANCE MAP
SUB CHANNEL LOCATIONS

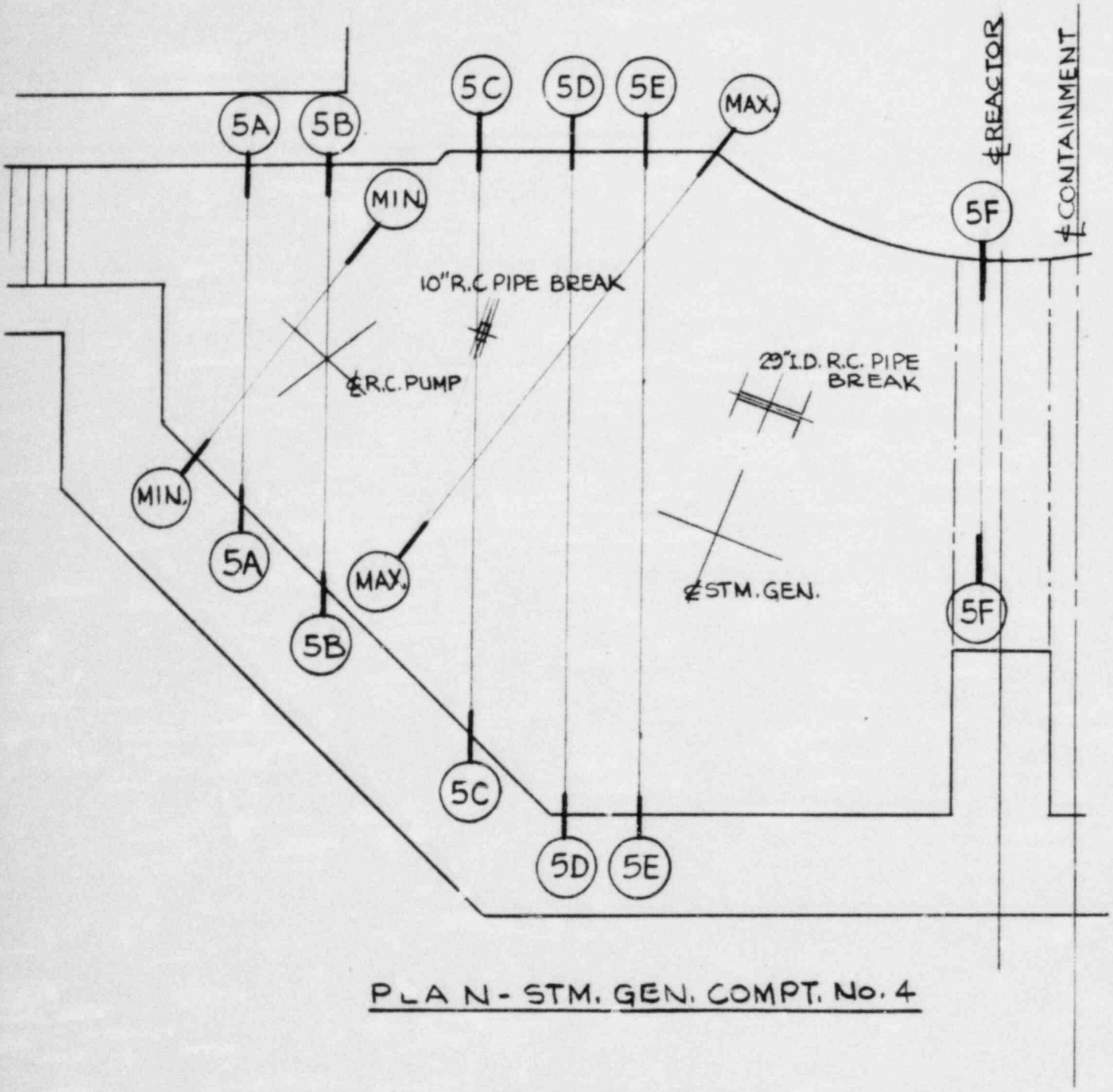

PLAN - STM. GEN. COMPT. No. 4

FIGURE 5.4-5
CROSS SECTION LOCATIONS

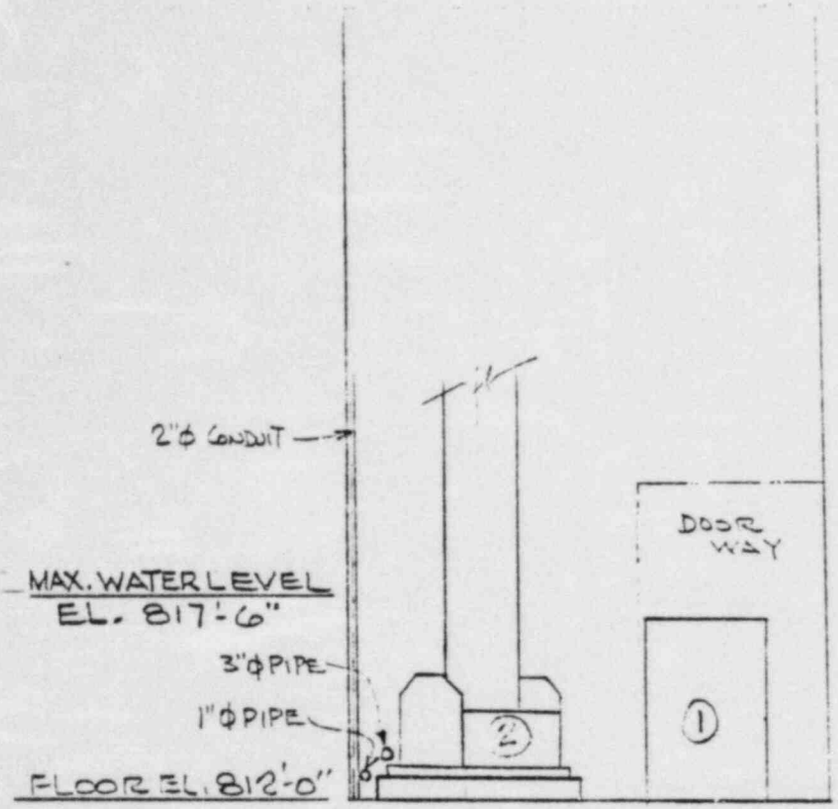

SECTION 5A-5A

TAKEN 3'-0" SOUTH OF DOORWAY

FIGURE 5.4-6

CONTAINMENT BLDG.

STEAM GEN. COMPARTMENT No. 4

CROSS SECTION 5A

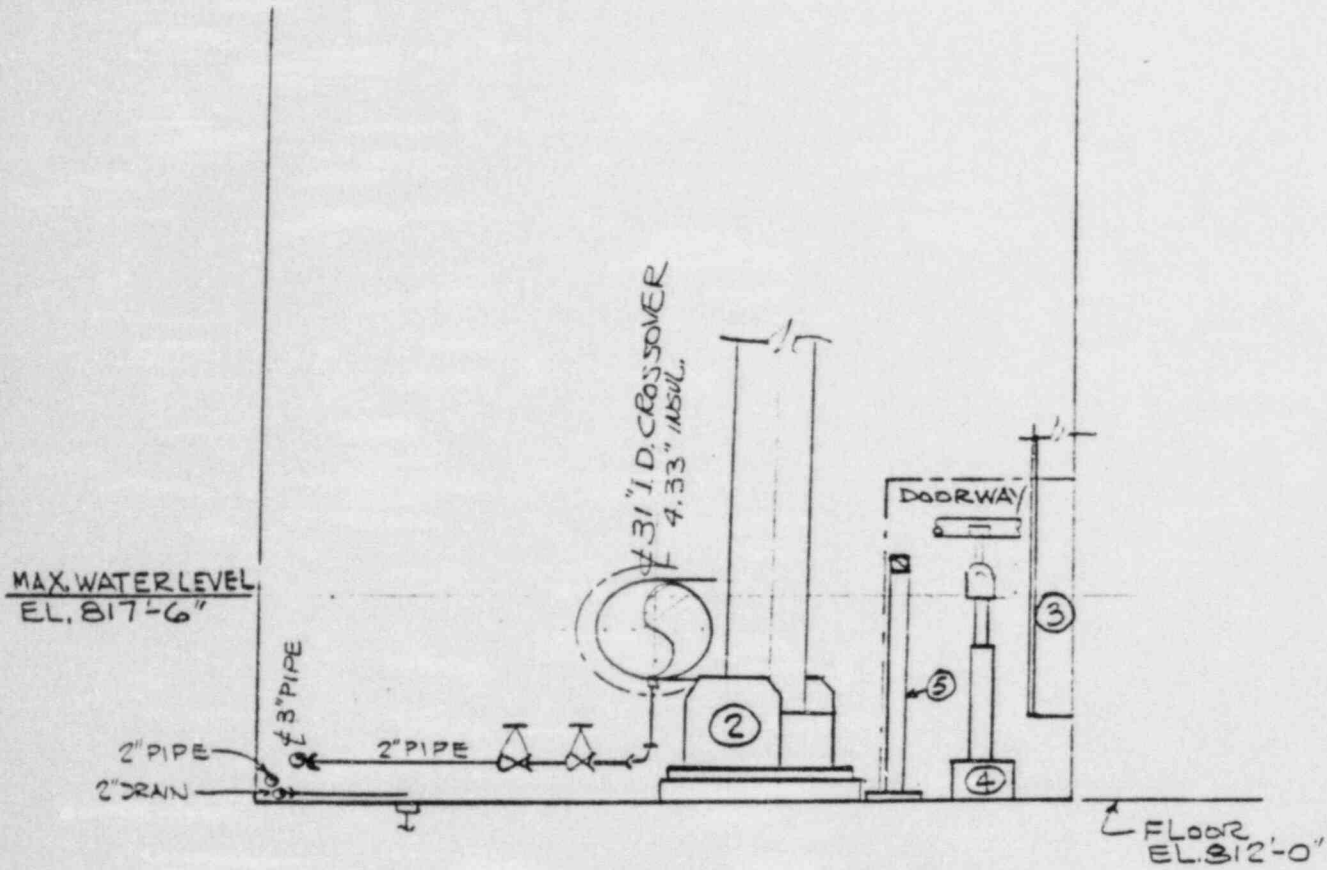

SECTION 5C-5C

TAKEN 11'-0" SOUTH OF DOORWAY

FIGURE 5.4-7
CONTAINMENT BLDG.
STEAM GEN. COMPARTMENT No. 4
CROSS SECTION 5C

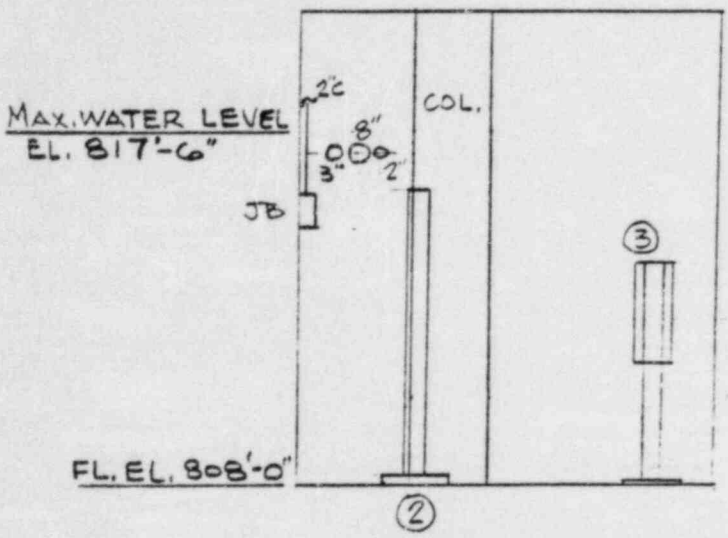

SECTION 4B-4B
TAKEN @ 60° AZIMUTH

FIGURE 5.4-8
CONTAINMENT BLDG.
CORRIDOR
CROSS SECTION 4B

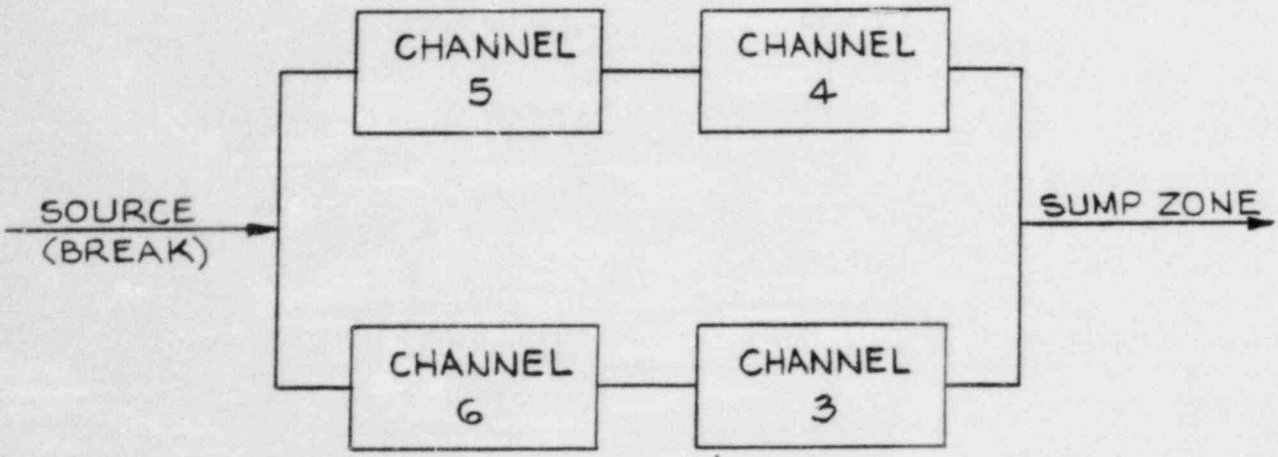

$$R_{EQ} = \left(\frac{1}{\sqrt{\frac{1}{R_4+R_5}} + \sqrt{\frac{1}{R_6+R_3}}} \right)^2$$

FIGURE 5.4-9
NETWORK DIAGRAM
RHR/SI SYSTEM

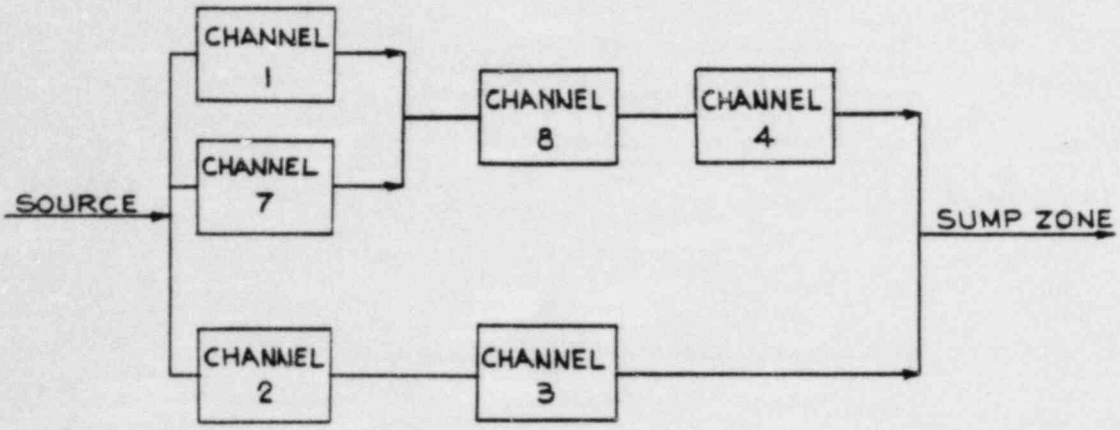

TOTAL NETWORK

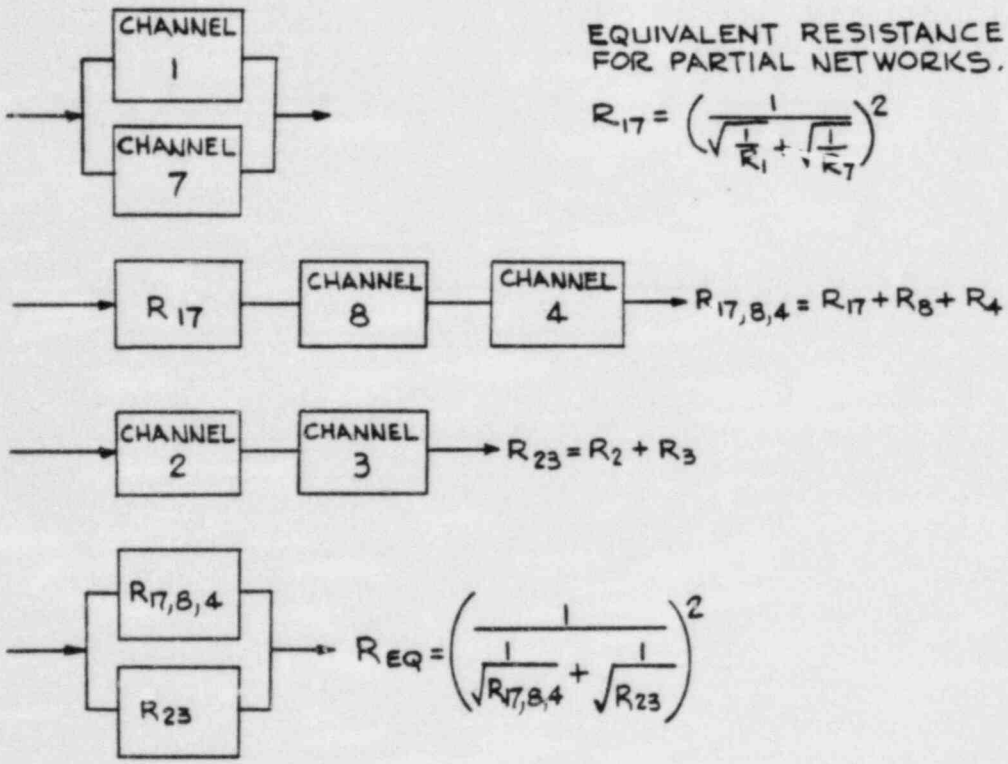

FIGURE 5.4-10
NETWORK DIAGRAM- SPRAY

TABLE 5.1-1

WATER INVENTORY AND LEVELS

Source	Available Capacity, cu.ft.	Maximum Quantity, cu.ft.	Minimum Quantity, cu.ft.
Reactor Coolant	12,740	12,740	12,740
Refueling Water Storage Tank	70,400	67,990	53,570
Accumulators	3,810	3,810	3,810
Miscellaneous	920	920	470
Total	87,370	85,460	70,590
Water Level (ft)(1)		817.5	814.8

Note:

(1) Based on calculation of actual net volumes available excluding equipment volumes, foundations, and other components.

TABLE 5.3-1

CONTAINMENT SPRAY DISTRIBUTION

Zone[1]	Floor Elevation	Flow gpm One Train	Two Trains
A	905	4165	8330
B	860	1018	2036
C	832	213	426
D	808	410	820

Note:

1. See Figure 5.3-1 for Zone locations.

TABLE 5.3-2

CALCULATION OF VELOCITIES
(Two Spray Trains)

Levels		Floor Elevation 905'-9"	860'-0"	832'6"
Open Area	sq.ft.	6,836	6,372	6,100
Non-Open Area	sq.ft.	7,478	7,942	8,214
Clear Floor Areas for Flow	sq.ft.	6,400	6,750	6,900
Flow on Floor Area	gpm	4,352	1,723	5,752
Spill Opening Perimeter	ft	62	74	110
Unit Discharge at Spill Openings (Average)	cfs/ft	0.156	0.0519	0.116
Water Depth	inches	1.2	1.5	1.08
Velocity at Spill Brink	fps	1.5	1.0	1.4
Velocity @ 5 ft. from Spill Brink	fps	0.6	0.5	1.1
Velocity @ 10 ft. from Spill Brink	fps	0.4	0.4	1.0

TABLE 5.3-3

CALCULATION OF VELOCITIES
(One Spray Train)

Levels		Floor Elevation 905'-9"	860'-0"	832'6"
Open Area	sq.ft.	6,836	6,372	6,100
Non-Open Area	sq.ft.	7,478	7,942	8,214
Clear Floor Areas for Flow	sq.ft.	6,400	6,750	6,900
Flow on Floor Area	gpm	2,176	861	2,875
Spill Opening Perimeter	ft	62	74	110
Unit Discharge at Spill Openings (Average)	cfs/ft	0.078	0.0259	0.058
Water Depth	inches	0.79	0.38	0.65
Velocity at Spill Brink	fps	1.2	0.8	1.1
Velocity @ 5 ft. from Spill Brink	fps	0.5	0.4	0.7
Velocity @ 10 ft. from Spill Brink	fps	0.3	0.3	0.7

TABLE 5.4-1

CONTAINMENT SPRAY AND RHR/SI FLOWS

Containment Spray	GPM	CFS
One Train	5,800	12.94
Two Trains	11,600	25.87
RHR/SI		
One Train	2,570	5.73
Two Trains	5,140	11.45

TABLE 5.4-2

SPRAY FLOW CONTRIBUTION (ONE TRAIN)
LOW WATER LEVEL (EL. 814.8 FT.)

SPRAY FLOW (CFS): 12.94

CHANNEL NO.	BRANCH NO.	LENGTH FT.	AREA SQ.FT.	RESIST. L/A,1/FT	FLOW CFS	VELOCITY FPS
7	DOOR 3	17.00	9.11	1.87	2.07	0.23
7	A3	3.00	15.35	0.20		0.13
7	B3	3.00	30.57	0.10		0.07
7	C3	5.00	39.17	0.13		0.05
7	D3	3.00	56.23	0.05		0.04
7	E3	16.00	56.96	0.28		0.04
7	F3	1.00	18.39	0.05		0.11
7	A2	3.00	15.35	0.20		0.13
7	B2	3.00	30.57	0.10		0.07
7	C2	5.00	39.17	0.13		0.05
7	D2	3.00	56.23	0.05		0.04
7	E2	16.00	56.96	0.28		0.04
7	F2	1.00	18.39	0.05		0.11
7	DOOR 2	14.00	9.11	1.54		0.23
	TOTAL CHANNEL RESISTANCE			5.02		
8	A	30.00	35.72	0.84	5.40	0.15
8	B	14.00	81.60	0.17		0.07
	TOTAL CHANNEL RESISTANCE			1.01		
1	A	55.00	81.60	0.67	3.33	0.04
1	B	29.00	27.20	1.07		0.12
1	C	23.00	115.60	0.20		0.03
	TOTAL CHANNEL RESISTANCE			1.94		
2	A	60.00	115.60	0.52	7.54	0.07
2	B	16.00	74.80	0.21		0.10
2	C	38.00	102.00	0.37		0.07
	TOTAL CHANNEL RESISTANCE			1.11		
3	A	24.00	143.96	0.17	7.54	0.05
3	B	10.00	85.47	0.12		0.09
	TOTAL CHANNEL RESISTANCE			0.28		
4	A	22.00	128.43	0.17	5.40	0.04
4	B	28.00	38.51	0.73		0.14
4	C	7.00	101.07	0.07		0.05
	TOTAL CHANNEL RESISTANCE			0.97		

TABLE 5.4-3

RHR/SI FLOW CONTRIBUTION (ONE TRAIN)
LOW WATER LEVEL (EL. 814.8 FT.)

RHR/SI FLOW (CFS): 5.73

CHANNEL NO.	BRANCH NO.	LENGTH FT.	AREA SQ.FT.	RESIST. L/A,1/FT	FLOW CFS	VELOCITY FPS
5	DOOR 4	17.00	9.11	1.87	2.63	0.29
5	A4	3.00	15.35	0.20		0.17
5	B4	3.00	30.57	0.10		0.09
5	C4	5.00	39.17	0.13		0.07
5	D4	3.00	56.23	0.05		0.05
5	E4	16.00	56.96	0.28		0.05
5	F4	1.00	18.39	0.05		0.14
	TOTAL CHANNEL RESISTANCE			2.68		
6	A1	3.00	15.35	0.20	3.10	0.20
6	B1	3.00	30.57	0.10		0.10
6	C1	5.00	39.17	0.13		0.08
6	D1	3.00	56.23	0.05		0.06
6	E1	16.00	56.96	0.28		0.05
6	F1	1.00	18.39	0.05		0.17
6	DOOR 1	14.00	9.11	1.54		0.34
	TOTAL CHANNEL RESISTANCE			2.35		
3	A	24.00	143.96	0.17	3.10	0.02
3	B	10.00	85.47	0.12		0.04
	TOTAL CHANNEL RESISTANCE			0.28		
4	A	22.00	128.43	0.17	2.63	0.02
4	B	28.00	38.51	0.73		0.07
4	C	7.00	101.07	0.07		0.03
	TOTAL CHANNEL RESISTANCE			0.97		

TABLE 5.4-4

SPRAY FLOW CONTRIBUTION (TWO TRAINS)
LOW WATER LEVEL (EL. 814.8 FT.)

SPRAY FLOW (CFS): 25.87

CHANNEL NO.	BRANCH NO.	LENGTH FT.	AREA SQ.FT.	RESIST. L/A,1/FT	FLOW CFS	VELOCITY FPS
7	DOOR 3	17.00	9.11	1.87	4.13	0.45
7	A3	3.00	15.35	0.20		0.27
7	B3	3.00	30.57	0.10		0.14
7	C3	5.00	39.17	0.13		0.11
7	D3	3.00	56.23	0.05		0.07
7	E3	16.00	56.96	0.28		0.07
7	F3	1.00	18.39	0.05		0.22
7	A2	3.00	15.35	0.20		0.27
7	B2	3.00	30.57	0.10		0.14
7	C2	5.00	39.17	0.13		0.11
7	D2	3.00	56.23	0.05		0.07
7	E2	16.00	56.96	0.28		0.07
7	F2	1.00	18.39	0.05		0.22
7	DOOR 2	14.00	9.11	1.54		0.45
	TOTAL CHANNEL RESISTANCE			5.02		
8	A	30.00	35.72	0.84	10.79	0.30
8	B	14.00	81.60	0.17		0.13
	TOTAL CHANNEL RESISTANCE			1.01		
1	A	55.00	81.60	0.67	6.65	0.08
1	B	29.00	27.20	1.07		0.24
1	C	23.00	115.60	0.20		0.06
	TOTAL CHANNEL RESISTANCE			1.94		
2	A	60.00	115.60	0.52	15.08	0.13
2	B	16.00	74.80	0.21		0.20
2	C	38.00	102.00	0.37		0.15
	TOTAL CHANNEL RESISTANCE			1.11		
3	A	24.00	143.96	0.17	15.08	0.10
3	B	10.00	85.47	0.12		0.18
	TOTAL CHANNEL RESISTANCE			0.28		
4	A	22.00	128.43	0.17	10.79	0.08
4	B	28.00	38.51	0.73		0.28
4	C	7.00	101.07	0.07		0.11
	TOTAL CHANNEL RESISTANCE			0.97		

TABLE 5.4-5

RHR/SI FLOW CONTRIBUTION (TWO TRAINS)
LOW WATER LEVEL (EL. 814.8 FT.)

RHR/SI FLOW (CFS): 11.45

CHANNEL NO.	BRANCH NO.	LENGTH FT.	AREA SQ.FT.	RESIST. L/A,1/FT	FLOW CFS	VELOCITY FPS
5	DOOR 4	17.00	9.11	1.87	5.26	0.58
5	A4	3.00	15.35	0.20		0.34
5	B4	3.00	30.57	0.10		0.17
5	C4	5.00	39.17	0.13		0.13
5	D4	3.00	56.23	0.05		0.09
5	E4	16.00	56.96	0.28		0.09
5	F4	1.00	18.39	0.05		0.29
	TOTAL CHANNEL RESISTANCE			2.68		
6	A1	3.00	15.35	0.20	6.19	0.40
6	B1	3.00	30.57	0.10		0.20
6	C1	5.00	39.17	0.13		0.16
6	D1	3.00	56.23	0.05		0.11
6	E1	16.00	56.96	0.28		0.11
6	F1	1.00	18.39	0.05		0.34
6	DOOR 1	14.00	9.11	1.54		0.68
	TOTAL CHANNEL RESISTANCE			2.35		
3	A	24.00	143.96	0.17	6.19	0.04
3	B	10.00	85.47	0.12		0.07
	TOTAL CHANNEL RESISTANCE			0.28		
4	A	22.00	128.43	0.17	5.26	0.04
4	B	28.00	38.51	0.73		0.14
4	C	7.00	101.07	0.07		0.05
	TOTAL CHANNEL RESISTANCE			0.97		

TABLE 5.4-6

SPRAY FLOW CONTRIBUTION (ONE TRAIN)
HIGH WATER LEVEL (EL. 817.5 FT.)

SPRAY FLOW (CFS): 12.94

CHANNEL NO.	BRANCH NO.	LENGTH FT.	AREA SQ.FT.	RESIST. L/A,1/FT	FLOW CFS	VELOCITY FPS
7	DOOR 3	17.00	17.90	0.95	2.31	0.13
7	A3	3.00	30.15	0.10		0.08
7	B3	3.00	60.05	0.05		0.04
7	C3	5.00	76.95	0.06		0.03
7	D3	3.00	110.46	0.03		0.02
7	E3	16.00	111.88	0.14		0.02
7	F3	1.00	36.13	0.03		0.06
7	A2	3.00	30.15	0.10		0.08
7	B2	3.00	60.05	0.05		0.04
7	C2	5.00	76.95	0.06		0.03
7	D2	3.00	110.46	0.03		0.02
7	E2	16.00	111.88	0.14		0.02
7	F2	1.00	36.13	0.03		0.06
7	DOOR 2	14.00	17.90	0.78		0.13
	TOTAL CHANNEL RESISTANCE			2.56		
8	A	30.00	49.90	0.60	5.45	0.11
8	B	14.00	114.00	0.12		0.05
	TOTAL CHANNEL RESISTANCE			0.72		
1	A	55.00	114.00	0.48	3.14	0.03
1	B	29.00	38.00	0.76		0.08
1	C	23.00	161.50	0.14		0.02
	TOTAL CHANNEL RESISTANCE			1.39		
2	A	60.00	161.50	0.37	7.49	0.05
2	B	16.00	104.50	0.15		0.07
2	C	38.00	142.50	0.27		0.05
	TOTAL CHANNEL RESISTANCE			0.79		
3	A	24.00	201.12	0.12	7.49	0.04
3	B	10.00	119.41	0.08		0.06
	TOTAL CHANNEL RESISTANCE			0.20		
4	A	22.00	179.43	0.12	5.45	0.03
4	B	28.00	53.80	0.52		0.10
4	C	7.00	141.20	0.05		0.04
	TOTAL CHANNEL RESISTANCE			0.69		

TABLE 5.4-7

RHR/SI FLOW CONTRIBUTION (ONE TRAIN)
HIGH WATER LEVEL (EL. 817.5 FT.)

RHR/SI FLOW (CFS): 5.73

CHANNEL NO.	BRANCH NO.	LENGTH FT.	AREA SQ.FT.	RESIST. L/A,1/FT	FLOW CFS	VELOCITY FPS
5	DOOR 4	17.00	17.90	0.95	2.59	0.14
5	A4	3.00	30.15	0.10		0.09
5	B4	3.00	60.05	0.05		0.04
5	C4	5.00	76.95	0.06		0.03
5	D4	3.00	110.46	0.03		0.02
5	E4	16.00	111.88	0.14		0.02
5	F4	1.00	36.13	0.03		0.07
	TOTAL CHANNEL RESISTANCE			1.36		
6	A1	3.00	30.15	0.10	3.14	0.10
6	B1	3.00	60.05	0.05		0.05
6	C1	5.00	76.95	0.06		0.04
6	D1	3.00	110.46	0.03		0.03
6	E1	16.00	111.88	0.14		0.03
6	F1	1.00	36.13	0.03		0.09
6	DOOR 1	14.00	17.90	0.78		0.18
	TOTAL CHANNEL RESISTANCE			1.19		
3	A	24.00	201.12	0.12	3.14	0.02
3	B	10.00	119.41	0.08		0.03
	TOTAL CHANNEL RESISTANCE			0.20		
4	A	22.00	179.43	0.12	2.59	0.01
4	B	28.00	53.80	0.52		0.05
4	C	7.00	141.20	0.05		0.02
	TOTAL CHANNEL RESISTANCE			0.69		

TABLE 5.4-8

SPRAY FLOW CONTRIBUTION (TWO TRAINS)
HIGH WATER LEVEL (EL. 817.5 FT.)

SPRAY FLOW (CFS): 25.87

CHANNEL NO.	BRANCH NO.	LENGTH FT.	AREA SQ.FT.	RESIST. L/A,1/FT	FLOW CFS	VELOCITY FPS
7	DOOR 3	17.00	17.90	0.95	4.62	0.26
7	A3	3.00	30.15	0.10		0.15
7	B3	3.00	60.05	0.05		0.08
7	C3	5.00	76.95	0.06		0.06
7	D3	3.00	110.46	0.03		0.04
7	E3	16.00	111.88	0.14		0.04
7	F3	1.00	36.13	0.03		0.13
7	A2	3.00	30.15	0.10		0.15
7	B2	3.00	60.05	0.05		0.08
7	C2	5.00	76.95	0.06		0.06
7	D2	3.00	110.46	0.03		0.04
7	E2	16.00	111.88	0.14		0.04
7	F2	1.00	36.13	0.03		0.13
7	DOOR 2	14.00	17.90	0.78		0.26
	TOTAL CHANNEL RESISTANCE			2.56		
8	A	30.00	49.90	0.60	10.90	0.22
8	B	14.00	114.00	0.12		0.10
	TOTAL CHANNEL RESISTANCE			0.72		
1	A	55.00	114.00	0.48	6.27	0.06
1	B	29.00	38.00	0.76		0.17
1	C	23.00	161.50	0.14		0.04
	TOTAL CHANNEL RESISTANCE			1.39		
2	A	60.00	161.50	0.37	14.97	0.09
2	B	16.00	104.50	0.15		0.14
2	C	38.00	142.50	0.27		0.11
	TOTAL CHANNEL RESISTANCE			0.79		
3	A	24.00	201.17	0.12	14.97	0.07
3	B	10.00	119.41	0.08		0.13
	TOTAL CHANNEL RESISTANCE			0.20		
4	A	22.00	179.43	0.12	10.90	0.06
4	B	28.00	53.80	0.52		0.20
4	C	7.00	141.20	0.05		0.08
	TOTAL CHANNEL RESISTANCE			0.69		

TABLE 5.4-9

RHR/SI FLOW CONTRIBUTION (TWO TRAINS)
HIGH WATER LEVEL (EL. 817.5 FT.)

RHR/SI FLOW (CFS): 11.45

CHANNEL NO.	BRANCH NO.	LENGTH FT.	AREA SQ.FT.	RESIST. L/A,1/FT	FLOW CFS	VELOCITY FPS
5	DOOR 4	17.00	17.90	0.95	5.18	0.29
5	A4	3.00	30.15	0.10		0.17
5	B4	3.00	60.05	0.05		0.09
5	C4	5.00	76.95	0.06		0.07
5	D4	3.00	110.46	0.03		0.05
5	E4	16.00	111.88	0.14		0.05
5	F4	1.00	36.13	0.03		0.14
	TOTAL CHANNEL RESISTANCE			1.36		
6	A1	3.00	30.15	0.10	6.27	0.21
6	B1	3.00	60.05	0.05		0.10
6	C1	5.00	76.95	0.06		0.08
6	D1	3.00	110.46	0.03		0.06
6	E1	16.00	111.88	0.14		0.06
6	F1	1.00	36.13	0.03		0.17
6	DOOR 1	14.00	17.90	0.78		0.35
	TOTAL CHANNEL RESISTANCE			1.19		
3	A	24.00	201.12	0.12	6.27	0.03
3	B	10.00	119.41	0.08		0.05
	TOTAL CHANNEL RESISTANCE			0.20		
4	A	22.00	179.43	0.12	5.18	0.03
4	B	28.00	53.80	0.52		0.10
4	C	7.00	141.20	0.05		0.04
	TOTAL CHANNEL RESISTANCE			0.69		

TABLE 5.4-10
TOTAL VELOCITY-ONE TRAIN, LOW LEVEL

WATER HT= 814.80 FLOWS,CFS:SPRAY= 12.94 ,RHR/SI= 5.73

CHANNEL NO.	BRANCH NO.	SPRAY FLOW CFS	SPRAY VELOCITY FPS	RHR/SI FLOW CFS	RHR/SI VELOCITY FPS	TOTAL VELOCITY FPS
5	DOOR 4	0.00	0.00	2.63	0.29	0.29
5	A4		0.00		0.17	0.17
5	B4		0.00		0.09	0.09
5	C4		0.00		0.07	0.07
5	D4		0.00		0.05	0.05
5	E4		0.00		0.05	0.05
5	F4		0.00		0.14	0.14
6	A1	0.00	0.00	3.10	0.20	0.20
6	B1		0.00		0.10	0.10
6	C1		0.00		0.08	0.08
6	D1		0.00		0.06	0.06
6	E1		0.00		0.05	0.05
6	F1		0.00		0.17	0.17
6	DOOR 1		0.00		0.34	0.34
7	DOOR 3	2.07	0.23	0.00	0.00	0.23
7	A3		0.13		0.00	0.13
7	B3		0.07		0.00	0.07
7	C3		0.05		0.00	0.05
7	D3		0.04		0.00	0.04
7	E3		0.04		0.00	0.04
7	F3		0.11		0.00	0.11
7	A2		0.13		0.00	0.13
7	B2		0.07		0.00	0.07
7	C2		0.05		0.00	0.05
7	D2		0.04		0.00	0.04
7	E2		0.04		0.00	0.04
7	F2		0.11		0.00	0.11
7	DOOR 2		0.23		0.00	0.23
8	A	5.39	0.15	0.00	0.00	0.15
8	B		0.07		0.00	0.07
1	A	3.33	0.04	0.00	0.00	0.04
1	B		0.12		0.00	0.12
1	C		0.03		0.00	0.03
2	A	7.54	0.07	0.00	0.00	0.07
2	B		0.10		0.00	0.10
2	C		0.07		0.00	0.07
3	A	7.54	0.05	3.10	0.02	0.07
3	B		0.09		0.04	0.12
4	A	5.39	0.04	2.63	0.02	0.06
4	B		0.14		0.07	0.21
4	C		0.05		0.03	0.08

TABLE 5.4-11
TOTAL VELOCITY-TWO TRAINS, LOW LEVEL

WATER HT= 814.80 FLOWS,CFS:SPRAY= 25.87 ,RHR/SI= 11.45

CHANNEL NO.	BRANCH NO.	SPRAY FLOW CFS	SPRAY VELOCITY FPS	RHR/SI FLOW CFS	RHR/SI VELOCITY FPS	TOTAL VELOCITY FPS
5	DOOR 4	0.00	0.00	5.26	0.58	0.58
5	A4		0.00		0.34	0.34
5	B4		0.00		0.17	0.17
5	C4		0.00		0.13	0.13
5	D4		0.00		0.09	0.09
5	E4		0.00		0.09	0.09
5	F4		0.00		0.29	0.29
6	A1	0.00	0.00	6.19	0.40	0.40
6	B1		0.00		0.20	0.20
6	C1		0.00		0.16	0.16
6	D1		0.00		0.11	0.11
6	E1		0.00		0.11	0.11
6	F1		0.00		0.34	0.34
6	DOOR 1		0.00		0.68	0.68
7	DOOR 3	4.13	0.45	0.	0.00	0.45
7	A3		0.27		0.00	0.27
7	B3		0.14		0.00	0.14
7	C3		0.11		0.00	0.11
7	D3		0.07		0.00	0.07
7	E3		0.07		0.00	0.07
7	F3		0.22		0.00	0.22
7	A2		0.27		0.00	0.27
7	B2		0.14		0.00	0.14
7	C2		0.11		0.00	0.11
7	D2		0.07		0.00	0.07
7	E2		0.07		0.00	0.07
7	F2		0.22		0.00	0.22
7	DOOR 2		0.45		0.00	0.45
8	A	10.79	0.30	0.00	0.00	0.30
8	B		0.13		0.00	0.13
1	A	6.65	0.08	0.00	0.00	0.08
1	B		0.24		0.00	0.24
1	C		0.06		0.00	0.06
2	A	15.08	0.13	0.00	0.00	0.13
2	B		0.20		0.00	0.20
2	C		0.15		0.00	0.15
3	A	15.08	0.10	6.19	0.04	0.15
3	B		0.18		0.07	0.25
4	A	10.79	0.08	5.26	0.04	0.12
4	B		0.28		0.14	0.42
4	C		0.11		0.05	0.16

TABLE 5.4-12
TOTAL VELOCITY-ONE TRAIN, HIGH LEVEL

WATER HT= 817.50 FLOWS,CFS:SPRAY= 12.94 ,RHR/SI= 5.73

CHANNEL NO.	BRANCH NO.	SPRAY FLOW CFS	SPRAY VELOCITY FPS	RHR/SI FLOW CFS	RHR/SI VELOCITY FPS	TOTAL VELOCITY FPS
5	DOOR 4	0.00	0.00	2.59	0.14	0.14
5	A4		0.00		0.09	0.09
5	B4		0.00		0.04	0.04
5	C4		0.00		0.03	0.03
5	D4		0.00		0.02	0.02
5	E4		0.00		0.02	0.02
5	F4		0.00		0.07	0.07
6	A1	0.00	0.00	3.14	0.10	0.10
6	B1		0.00		0.05	0.05
6	C1		0.00		0.04	0.04
6	D1		0.00		0.03	0.03
6	E1		0.00		0.03	0.03
6	F1		0.00		0.09	0.09
6	DOOR 1		0.00		0.18	0.18
7	DOOR 3	2.31	0.13	0.00	0.00	0.13
7	A3		0.08		0.00	0.08
7	B3		0.04		0.00	0.04
7	C3		0.03		0.00	0.03
7	D3		0.02		0.00	0.02
7	E3		0.02		0.00	0.02
7	F3		0.06		0.00	0.06
7	A2		0.08		0.00	0.08
7	B2		0.04		0.00	0.04
7	C2		0.03		0.00	0.03
7	D2		0.02		0.00	0.02
7	E2		0.02		0.00	0.02
7	F2		0.06		0.00	0.06
7	DOOR 2		0.13		0.00	0.13
8	A	5.45	0.11	0.00	0.00	0.11
8	B		0.05		0.00	0.05
1	A	3.14	0.03	0.00	0.00	0.03
1	B		0.08		0.00	0.08
1	C		0.02		0.00	0.02
2	A	7.49	0.05	0.00	0.00	0.05
2	B		0.07		0.00	0.07
2	C		0.05		0.00	0.05
3	A	7.49	0.04	3.14	0.02	0.05
3	B		0.06		0.03	0.09
4	A	5.45	0.03	2.59	0.01	0.04
4	B		0.10		0.05	0.15
4	C		0.04		0.02	0.06

TABLE 5.4-13
TOTAL VELOCITY-TWO TRAINS, HIGH LEVEL

WATER HT= 817.50 FLOWS,CFS:SPRAY= 25.87 ,RHR/SI= 11.45

CHANNEL NO.	BRANCH NO.	SPRAY FLOW CFS	SPRAY VELOCITY FPS	RHR/SI FLOW CFS	RHR/SI VELOCITY FPS	TOTAL VELOCITY FPS
5	DOOR 4	0.00	0.00	5.18	0.29	0.29
5	A4		0.00		0.17	0.17
5	B4		0.00		0.09	0.09
5	C4		0.00		0.07	0.07
5	D4		0.00		0.05	0.05
5	E4		0.00		0.05	0.05
5	F4		0.00		0.14	0.14
6	A1	0.00	0.00	6.27	0.21	0.21
6	B1		0.00		0.10	0.10
6	C1		0.00		0.08	0.08
6	D1		0.00		0.06	0.06
6	E1		0.00		0.06	0.06
6	F1		0.00		0.17	0.17
6	DOOR 1		0.00		0.35	0.35
7	DOOR 3	4.62	0.26	0.00	0.00	0.26
7	A3		0.15		0.00	0.15
7	B3		0.08		0.00	0.08
7	C3		0.06		0.00	0.06
7	D3		0.04		0.00	0.04
7	E3		0.04		0.00	0.04
7	F3		0.13		0.00	0.13
7	A2		0.15		0.00	0.15
7	B2		0.08		0.00	0.08
7	C2		0.06		0.00	0.06
7	D2		0.04		0.00	0.04
7	E2		0.04		0.00	0.04
7	F2		0.13		0.00	0.13
7	DOOR 2		0.26		0.00	0.26
8	A	10.90	0.22	0.00	0.00	0.22
8	B		0.10		0.00	0.10
1	A	6.27	0.06	0.00	0.00	0.06
1	B		0.17		0.00	0.17
1	C		0.04		0.00	0.04
2	A	14.97	0.09	0.00	0.00	0.09
2	B		0.14		0.00	0.14
2	C		0.11		0.00	0.11
3	A	14.97	0.07	6.27	0.03	0.11
3	B		0.13		0.05	0.18
4	A	10.90	0.06	5.18	0.03	0.09
4	B		0.20		0.10	0.30
4	C		0.08		0.04	0.11

TABLE 5.4-14
SENSITIVITY ANALYSIS
TWO TRAINS VS. WATER LEVEL

CHANNEL NO.	BRANCH NO.	VELOCITIES (FPS) VERSUS WATER ELEVATIONS (FT) 814.00	814.80	815.00	815.50	816.50	817.50
5	DOOR 4	0.81	0.58	0.54	0.46	0.35	0.29
5	A4	0.48	0.34	0.32	0.27	0.21	0.17
5	B4	0.24	0.17	0.16	0.14	0.11	0.09
5	C4	0.19	0.13	0.13	0.11	0.08	0.07
5	D4	0.13	0.09	0.09	0.07	0.06	0.05
5	E4	0.13	0.09	0.09	0.07	0.06	0.05
5	F4	0.40	0.29	0.27	0.23	0.18	0.14
6	A1	0.56	0.40	0.38	0.32	0.25	0.21
6	B1	0.28	0.20	0.19	0.16	0.13	0.10
6	C1	0.22	0.16	0.15	0.13	0.10	0.08
6	D1	0.15	0.11	0.10	0.09	0.07	0.06
6	E1	0.15	0.11	0.10	0.09	0.07	0.06
6	F1	0.47	0.34	0.31	0.27	0.21	0.17
6	DOOR 1	0.94	0.68	0.63	0.55	0.43	0.35
7	DOOR 3	0.59	0.45	0.43	0.38	0.31	0.26
7	A3	0.35	0.27	0.25	0.22	0.18	0.15
7	B3	0.18	0.14	0.13	0.11	0.09	0.08
7	C3	0.14	0.11	0.10	0.09	0.07	0.06
7	D3	0.10	0.07	0.07	0.06	0.05	0.04
7	E3	0.09	0.07	0.07	0.06	0.05	0.04
7	F3	0.29	0.22	0.21	0.19	0.15	0.13
7	A2	0.35	0.27	0.25	0.22	0.18	0.15
7	B2	0.18	0.14	0.13	0.11	0.09	0.08
7	C2	0.14	0.11	0.10	0.09	0.07	0.06
7	D2	0.10	0.07	0.07	0.06	0.05	0.04
7	E2	0.09	0.07	0.07	0.06	0.05	0.04
7	F2	0.29	0.22	0.21	0.19	0.15	0.13
7	DOOR 2	0.59	0.45	0.43	0.38	0.31	0.26
8	A	0.34	0.30	0.29	0.27	0.24	0.22
8	B	0.15	0.13	0.13	0.12	0.11	0.10
1	A	0.10	0.08	0.08	0.07	0.06	0.06
1	B	0.29	0.24	0.24	0.22	0.19	0.17
1	C	0.07	0.06	0.06	0.05	0.04	0.04
2	A	0.15	0.13	0.13	0.12	0.10	0.09
2	B	0.23	0.20	0.20	0.18	0.16	0.14
2	C	0.17	0.15	0.14	0.13	0.12	0.11
3	A	0.17	0.15	0.14	0.13	0.12	0.11
3	B	0.28	0.25	0.24	0.23	0.20	0.18
4	A	0.14	0.12	0.12	0.11	0.10	0.09
4	B	0.47	0.42	0.40	0.38	0.33	0.30
4	C	0.18	0.16	0.15	0.14	0.13	0.11

6.0 PAINT DEBRIS GENERATION AND TRANSPORT

6.1 Paint Debris Generation

Most of the coating systems in the containment at CPSES are LOCA qualified and are expected to withstand the service conditions during normal plant operation and post-LOCA operations. However, for the purpose of this evaluation it is postulated that all the coating systems in the containment fail. An extremely conservative worst case scenario was postulated where all the coatings (100 percent) inside the containment fail and form debris. This assumption, although unrealistic, provides for an analytical approach to evaluate the effects of the coating failures on plant safety systems.

In addition to the assumption that all the paint fails, another extremely conservative and equally unrealistic worst case assumption was made for the particle size distribution of the failed paint. For the paint debris transport analysis, it was assumed that all the paint fails as 1/8-inch particles. This is the smallest particle size which cannot pass through the sump screens and is the most transportable. Thus, this assumption is extremely conservative for sump blockage analysis purposes.

Table 6.1-1 summarizes the estimated quantities of paint used in CPSES Unit 1 containment in various locations. The quantity of paint debris at each elevation of the containment was apportioned based on the available paint directly above the floor area. The paint from the vertical surfaces was assumed to fall vertically to the floor surface below. In all cases very conservative assumptions were used to maximize the paint debris transport to the sumps. For example, all the paint on vertical surfaces of the containment liner (up to the spring line) was assumed to be deposited on the lowest floor (El. 808'-0").

6.2 Paint Transport

The NUREG/CR-2791 methodology addresses short term and long term transport of insulation debris inside the containment. The short term transport is associated with the initiating event such as pipe whip, pipe impact and jet impingement. For the purposes of the evaluation of paint debris transport, the short term transport was not considered because it was conservatively assumed that all the paint fails.

The long term transport begins at the initiation of the recirculation phase of the post-LOCA operation. Dislodged paint is subjected to a circulating water flow during the operation of the containment recirculation pumps. Fluid velocity, debris density, and debris size were analyzed to determine if long term transport occurs.

This section establishes the transport velocity required to move the paint particles.

6.2.1 Paint Transport Velocity

Using the basic concepts of NUREG/CR-2791 for insulation debris, the transport velocity for paint particles was derived. First, tumbling motion was considered. A model of the forces on a cylindrical paint particle with its surface area perpendicular to the water flow was developed (see Figure 6.2-1). F_A is the force available to tumble or flip the paint particle so that its surface area will be parallel to the water flow. To tumble, the available force (F_A) must exceed the friction between the particle and the floor ($\mu s\ F_N$), where μs is the static friction coefficient and F is the force exerted by the paint particle normal to the floor, its weight. To find the minimum velocity to tumble the paint particle, F_A was set equal to $\mu s\ F_N$.

$$F_A = \frac{C_D \, Ap \, Pw \, \bar{v}^2}{2gc}$$

$$F_N = (Pm-Pw) \, V_M \, (g/gc)$$

F_L = 0 for tumbling per NUREG/CR-2791

$$F_r = \mu s \, (F_N - F_L) = \mu s \, F_N$$

$$Ap = \pi d^2/4$$

$$V_M = (\pi d^2/4)t$$

$$\frac{C_D \, (\pi d^2/4) Pw \, \bar{v}^2}{2 \, gc} = \left[(Pm-Pw) \, (\pi d^2/4)t\right]\mu s$$

Equation 1

$$\text{Tumble Velocity} = \bar{v} = \left[\frac{\mu s (Pm-Pw)(t) \, 2gc}{C_D \cdot Pw}\right]^{0.5}$$

F_L = lift force

Pw = density of water

Pm = density of material

V_M = volume of material

Ap = area normal to flow

$\bar{v}$ = average water velocity

C_D = drag coefficient

d = diameter of particle

t = thickness of particle

g = gravitational force

gc = Newton's constant

Similarly, the model for slide velocity was developed as shown on Figure 6.2-2. For a particle to slide, F_A should be greater than the force required to move the particle. The major differences in the derivation are that the friction coefficient used is now the dynamic coefficient, the lift force (F_L) will be equal to (F_A) and areas normal to the flow Ap now equals (d•t). Thus,

$$F_A = \frac{C_D \, (d \cdot t) \, Pw \, \bar{v}^2}{2gc}$$

$$F_N = (Pm - Pw) V_M (g/gc)$$

$$F_L = F_A$$

$$F_A = \mu d \, (F_N - F_A)$$

$$(1 + \mu d) \, F_A = \mu d \, F_N$$

$$\frac{(1 + \mu d) \, C_D \, (d \cdot t) \, Pw \, \bar{v}^2}{2gc} = \mu d \left[(Pm-Pw) \, (\pi d^2/4 \cdot t)\right]$$

$$\text{Slide Velocity} = \bar{v} = \left[\frac{\mu d \, (Pm-Pw) \, (\pi d/4) \, 2gc}{(1 + \mu d) \, C_D \cdot Pw}\right]^{0.5}$$

Tables 6.2-1 through 6.2-9 show the expected transport velocities for several different particles sizes, paint densities, containment conditions, and three particle thicknesses. It should be noted that while the density of each coating used is known in the dry film, the density of failed particles is not. The failed particles' density will include topcoat with all or some smaller portion of its primer or concrete surfacers. Thus a regime of failed particle density was conservatively assumed to envelope the known individual material densities. This regime varies from a specific gravity of 1.5 for Reactic 1201 topcoat to 4.0 for Carbozinc 11 primer. Failed point particles' thicknesses were also conservatively assumed at 3, 5, 10, 20 and 30 mils, which envelopes the lowest acceptable thickness to an almost excessive topcoat thickness. The particle size regime considers particles from 1/16-inch to 128-inch diameter. The sump screen opening size is 1/8-inch; thus a large variety of particle sizes which are capable of blocking the openings were considered. Both the tumble and slide transport velocities were calculated and presented in Tables 6.2-1 through 6.2-9, 6.2-19 and 6.2-20. Tables 6.2-10 through 6.2-18 show the effect of varying the friction and drag coefficients. The following conclusions can be drawn from the data presented in these tables:

- The thickness of the paint particle has no effect on its transport velocity.
- The smaller the paint particle size, the higher is the potential for its transport.
- The greater the relative density difference between the paint and the water, the lower is the potential for transport.
- The higher the drag coefficient between the paint particle and the moving water, the higher is the potential for transport.
- Variation in the friction coefficient between paint particle and concrete floor of the containment does not significantly affect the transport velocity.

6.2.2 Fine Particle Transport Considerations

For completeness, the transport velocity for very fine (dust) particles which could be generated from the failure of the coating systems was analyzed. Specifically, the behavior of particles of concrete coating, sand (used as a filler in the concrete surfacer) and zinc dust (used in the steel primer) were examined. This analysis provides a quantitative basis for evaluating the safety impact of paint failure other than sump screen blockage.

6.2.2.1 Sand in Concrete Coatings

The concrete is covered with a thick film coating system consisting of Nutec 11S, Nutec 11, and Reactic 1201 with a total coating dry film thickness of about 30 mils. The Nutec 11S is different from Nutec 11 in that it has a sand filler material. The sand constitutes approximately 51 weight percent of the dry film and varies in particle size from 30-140 mesh. The transport velocity determination of 20 and 30 mil thick particles of the previously described density and particle size regimes was performed. This analysis is presented on Tables 6.2-19 and 6.2-20. In addition, for sand particle transport, velocities were evaluated by varying the sand specific gravity from 1.4 to 2.2. The transport velocities determined are shown on Table 6.2-21.

6.2.2.2 Zinc in Inorganic Zinc Primer

The steel primer for CPSES is a self-curing inorganic zinc type coating with about 85 percent by weight of zinc in the dry film. The zinc is added as a basic component of the primer in the form of fine dust. The zinc dust particle size is commonly 5-10 microns; however, a particle size distribution by sieve analysis shows that particle sizes will vary from two to 50 microns with the bulk in 5-20 micron range.

Because failure of the steel primer could liberate zinc dust particles, a tranport velocity analysis was performed for this material. The analysis envelopes the expected particle size and uses both the known density of pure zinc (S.G. = 7.1) and the density of the primer dry film (S.G. = 4.0). Due to the extremely small particle sizes, very small velocities can transport the zinc dust.

Table 6.2-22 gives the transport velocities for different particle sizes up to 50 microns.

6.2.3 Paint Transport from Upper Floors

The quantity of paint that can be transported to El. 808'-0" floor (sump floor) and the location (azimuth) where the paint will be deposited is evaluated. This evaluation is based on the results of the calculations for: water velocities at upper elevations (Section 5.3), paint transport velocities (Section 6.2.1), and the quantity of paint available in each area (Section 6.1).

The water velocities on the upper floors range from 0.3 to 1.2 ft/sec (refer to Tables 5.3-2 and 5.3-3). If the available water velocities exceed the critical velocity required to transport a paint particle, then the particle is conservatively

assumed to be transported towards the sumps. Table 6.2-23 summarizes the results presented in Tables 6.2-1 through 6.2-18. The data presented in Table 6.2-23 is for very conservatively assumed containment water temperature of 200 F (higher temperatures give higher critical velocities for transport). The lowest critical velocity for transport of 0.27 ft/sec is for 1/8-inch-size particles of the Phenoline 305 and Reactic 1201 coatings. The critical velocity for 1/8 inch size, Carbozinc 11 particles exceeds 0.57 ft/sec. Also, the critical velocity for transport increases with increase in particle size. The transport velocity for one inch size particles varies from 0.75 to 1.62.

For the purpose of this analysis, a very conservative critical velcocity of 0.27 ft/sec was used. This is the lowest value in the table and is based on the assumption that all the paint fails at 1/8-inch particles. Based on this very conservative critical velocity value and the complexity of evaluating accurate flow velocities on the upper floors, it was assumed that all the paint particles from the upper floors are transported to the El. 808'-0" floor (sump level).

The distribution of the paint debris was evaluated based on the flow paths available for transport from the upper floors. The flow paths correspond to the open areas in the upper floors where the curbing is not present. The quantity of paint transported through each opening will be proportional to the water flow through the opening. Tables 6.2-24 and 2.2-25 give the flow openings, their locations and the quantity of paint debris transported from each of the upper floors. The paint debris from the containment liner is assumed to be uniformly distributed at the 808'-0" elevation. The transport of paint debris on the 808'-0" elevation where the sumps are located is discussed in the following section.

6.2.4 Paint Transport at 808'-0" Elevation

Based on the critical velocities for paint transport discussed in Sections 6.2.1 and 6.2.3 and the available water velocities at the 808'-0" elevation, the transport potential for paint particles was evaluated. As discussed in Section 6.2.3, a very conservative critical velocity of 0.27 ft/sec was used for this evaluation.

Paint particles in any given zone of the containment were considered to have a potential for transport with the water flow towards the containment sumps if the available water velocity exceeded the critical velocity for transport. Figures 6.2-3 and 6.2-4 show the critical areas on the 808'-0" elevation of the containment, where the paint particles have a potential for transport. The critical areas are marked cross-hatched.

Figure 6.2-3 is based on the low water level and Figure 6.2-4 is for high water level.

For the purpose of this evaluation the following assumptions were used to determine paint transport at the 808'-0" elevation:

a. All the paint at 808'-0" elevation and the paint deposited from the upper levels (discussed in Section 6.2.3) is available for transport within the near sump zone Azimuth 45-0-315°.

b. Paint particles transported from critical areas continue to move from the critical areas until either the particle reaches the sump or enters a zone where the available flow velocity is less than the critical velocity for transport.

c. The water velocities used are based on the low water level in the containment.

d. No credit is taken for possible paint debris hideout at obstructions, corners and curbs.

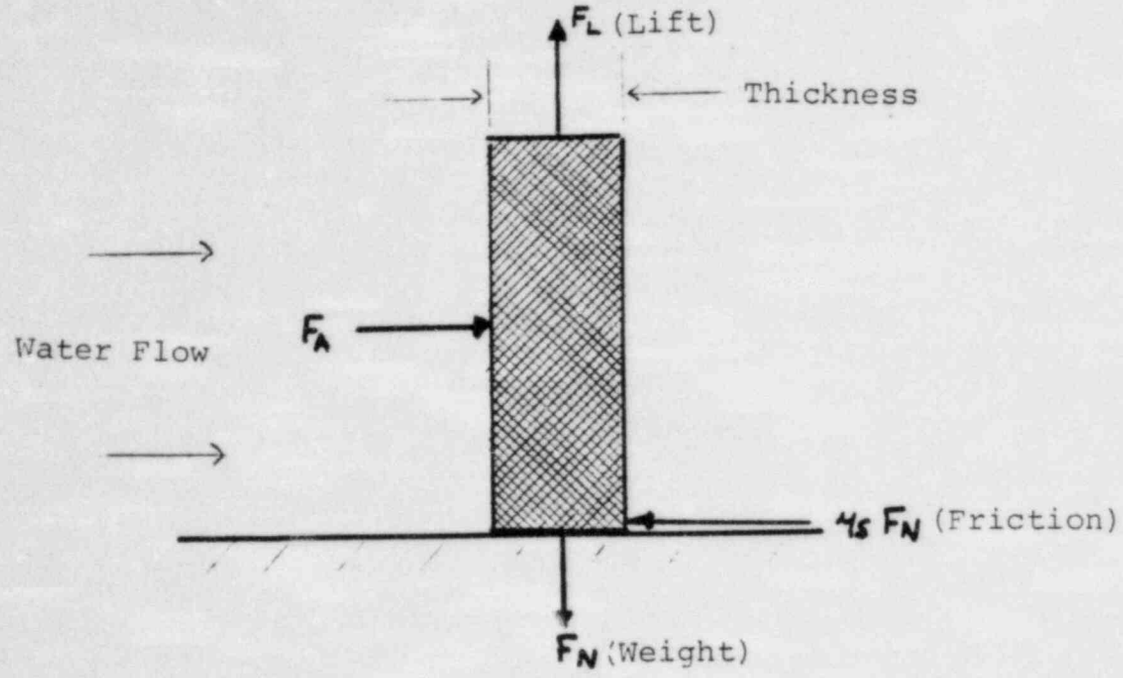

Side View

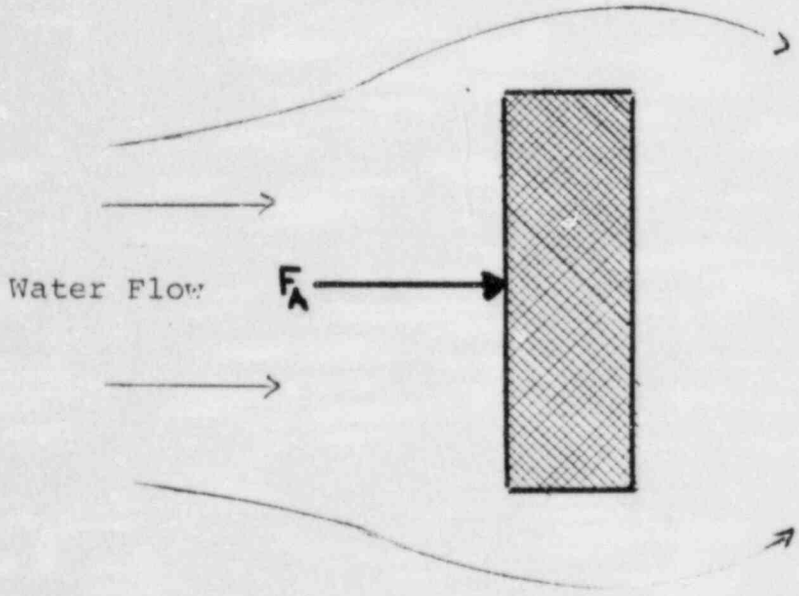

Plan View

FIGURE 6.2-1
TUMBLE TRANSPORT MODEL

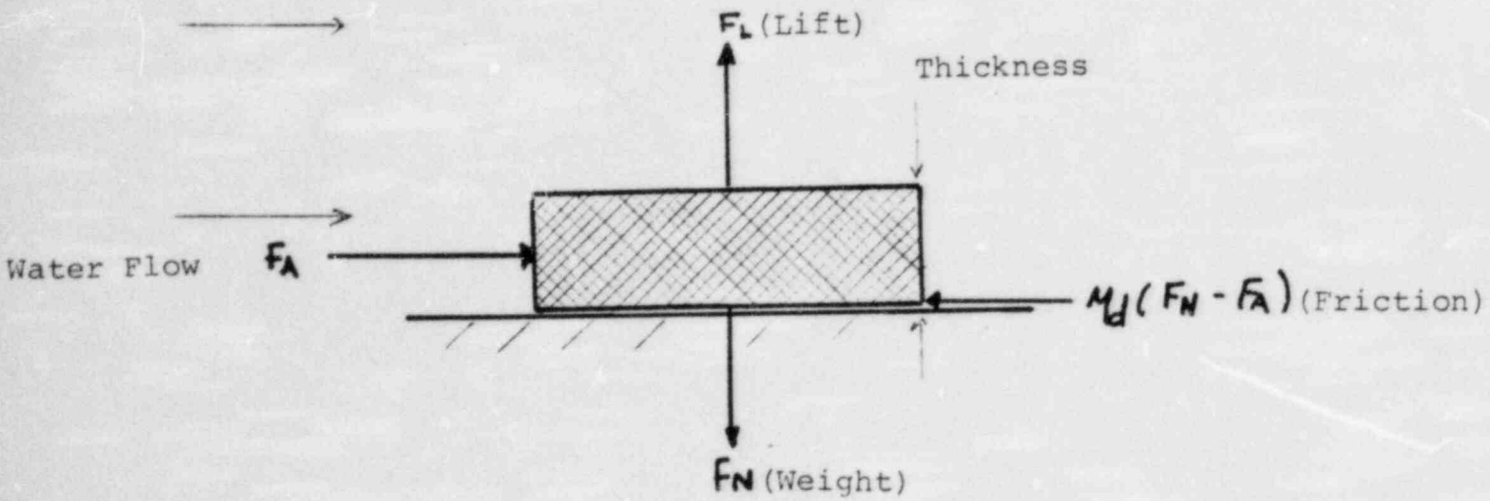

Side View

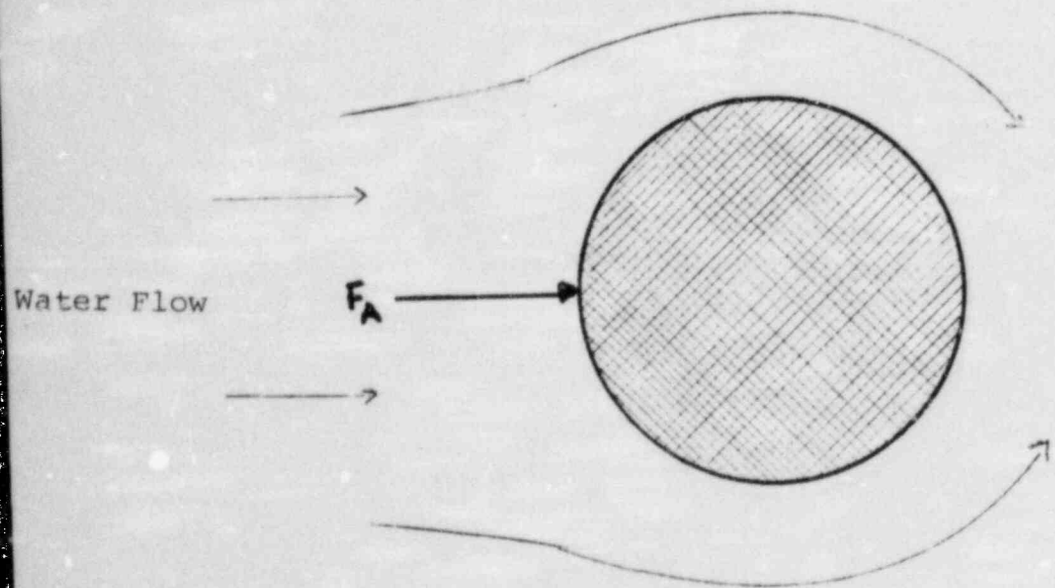

Plan View

FIGURE 6.2-2
SLIDE TRANSPORT MODEL

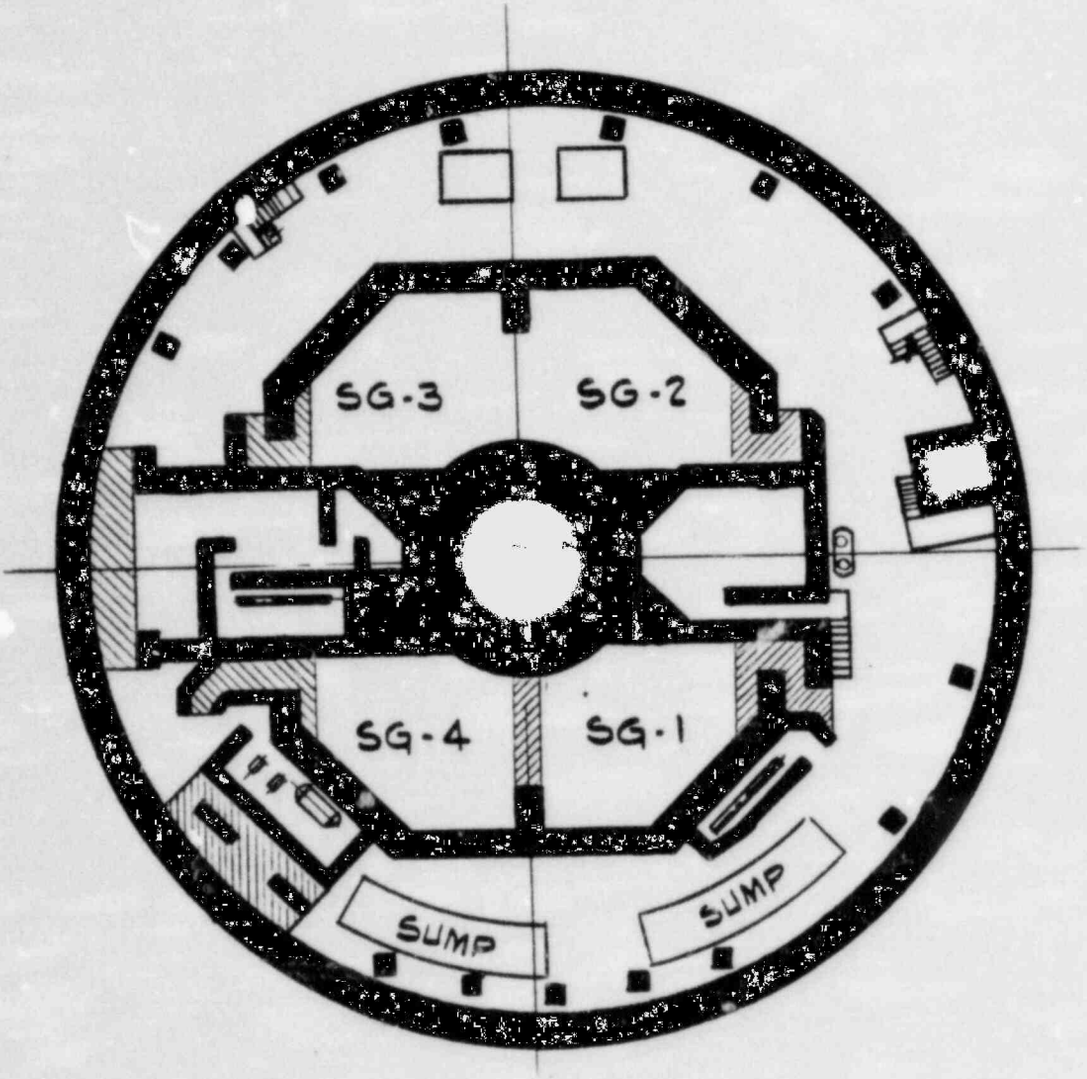

FIGURE 6.2-3
AREAS THAT EXCEED CRITICAL
VELOCITY @ ELEV. 808'-0"
LOW WATER LEVEL
TWO TRAINS OPERATING

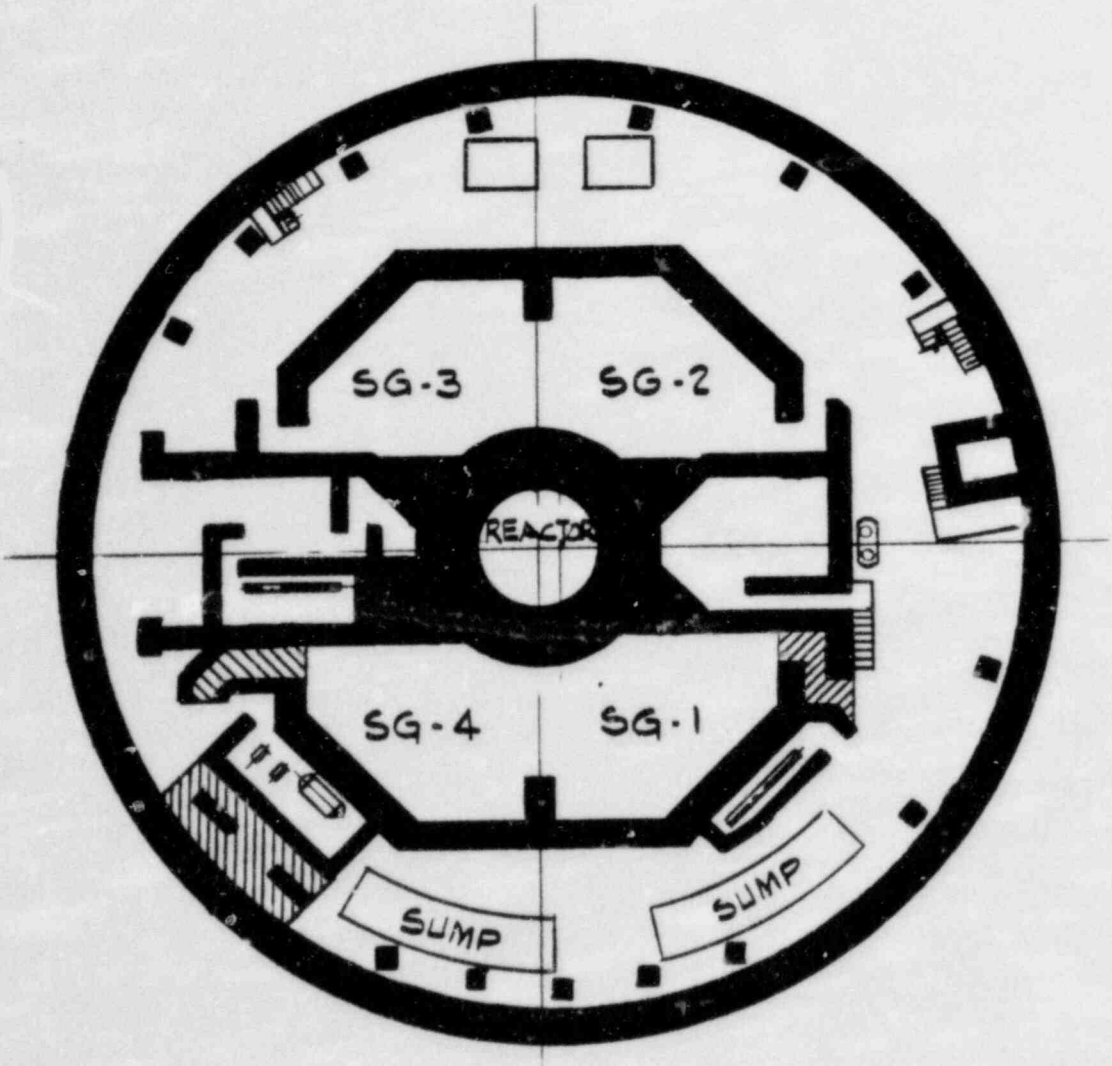

FIGURE 6.2-4
AREAS THAT EXCEED CRITICAL
VELOCITY @ ELEV. 808'-0"
HIGH WATER LEVEL
TWO TRAINS OPERATING

TABLE 6.1-1

QUANTITIES OF PAINT
IN CONTAINMENT

	TOTAL AREA SQ.FT.	ELEV.808 AREA SQ.FT.	ELEV.832 AREA SQ.FT.	ELEV.860 AREA SQ.FT.	ELEV.905 AREA SQ.FT.
LINER PLATE	145000	10174	11869	19076	103882
MISCELLANEOUS STEEL (NOTE1)	188080	47020	56424	56424	28212
CONCRETE SURFACES	285000	111150	85500	85500	2850
TOTAL	618080	168344	153793	161000	134944

NOTE 1. INCLUDES THE FOLLOWING:

HANGERS -	87300 SQ.FT.
NSSS EQUIPMENT -	25180 SQ.FT.
EQUIPMENT -	34600 SQ.FT.
CONDUIT SUPPORTS -	38500 SQ.FT.
MISCELLANEOUS -	2500 SQ.FT.

TABLE 6.2-1

TRANSPORT VELOCITY SUMMARY

PAINT THICKNESS = 10 MILS

Cont.pres PSI	60	Drag coef	1.1
Cont.temp F	307	Fric coef static	0.6
		Fric coef dynamic	0.42
Water density Lb/cf	57.0		
Viscosity water	0.000073		
Thickness Mils	10		

	SLIDE VELOCITY fps				
Paint den. lb/cf	90	100	120	150	200
Tumble vel. fps	0.131	0.149	0.180	0.219	0.272
Dia.in					
128	9.17	10.46	12.67	15.39	19.08
64	6.48	7.40	8.96	10.88	13.49
32	4.58	5.23	6.33	7.69	9.54
16	3.24	3.70	4.48	5.44	6.75
8	2.29	2.62	3.17	3.85	4.77
4	1.62	1.85	2.24	2.72	3.37
2	1.15	1.31	1.58	1.92	2.39
1	0.81	0.92	1.12	1.36	1.69
0.5	0.57	0.65	0.79	0.96	1.19
0.25	0.41	0.46	0.56	0.68	0.84
0.125	0.29	0.33	0.40	0.48	0.60
0.0625	0.20	0.23	0.28	0.34	0.4[illegible]

TABLE 6.2-2

TRANSPORT VELOCITY SUMMARY

PAINT THICKNESS = 5 MILS

Cont.pres PSI	60	Drag coef	1.1
Cont.temp F	307	Fric coef static	0.6
		Fric coef dynamic	0.42
Water density Lb/cf	57.0		
Viscosity water	0.000073		
Thickness Mils	5		

	SLIDE VELOCITY fps				
Paint den. lb/cf	90	100	120	150	200
Tumble vel. fps	0.092	0.105	0.128	0.155	0.192
Dia.in					
128	9.17	10.46	12.67	15.39	19.08
64	6.48	7.40	8.96	10.88	13.49
32	4.58	5.23	6.33	7.69	9.54
16	3.24	3.70	4.48	5.44	6.75
8	2.29	2.62	3.17	3.85	4.77
4	1.62	1.85	2.24	2.72	3.37
2	1.15	1.31	1.58	1.92	2.39
1	0.81	0.92	1.12	1.36	1.69
0.5	0.57	0.65	0.79	0.96	1.19
0.25	0.41	0.46	0.56	0.68	0.84
0.125	0.29	0.33	0.40	0.48	0.60
0.0625	0.20	0.23	0.28	0.34	0.42

TABLE 6.2-3

TRANSPORT VELOCITY SUMMARY

PAINT THICKNESS = 3 MILS

Cont.pres PSI	60	Drag coef	1.1
Cont.temp F	307	Fric coef static	0.6
		Fric coef dynamic	0.42
Water density Lb/cf	57.0		
Viscosity water	0.000073		
Thickness Mils	3		

	SLIDE VELOCITY fps				
Paint den. lb/cf	90	100	120	150	200
Tumble vel. fps	0.072	0.082	0.099	0.120	0.149
Dia.in					
128	9.17	10.46	12.67	15.39	19.08
64	6.48	7.40	8.96	10.88	13.49
32	4.58	5.23	6.33	7.69	9.54
16	3.24	3.70	4.48	5.44	6.75
8	2.29	2.62	3.17	3.85	4.77
4	1.62	1.85	2.24	2.72	3.37
2	1.15	1.31	1.58	1.92	2.39
1	0.81	0.92	1.12	1.36	1.69
0.5	0.57	0.65	0.79	0.96	1.19
0.25	0.41	0.46	0.56	0.68	0.84
0.125	0.29	0.33	0.40	0.48	0.60
0.0625	0.20	0.23	0.28	0.34	0.42

TABLE 6.2-4

TRANSPORT VELOCITY SUMMARY

PAINT THICKNESS = 10 MILS

Cont.pres PSI	20	Drag coef	1.1
Cont.temp F	250	Fric coef static	0.6
		Fric coef dynamic	0.42
Water density Lb/cf	58.8		
Viscosity water	0.000127		
Thickness Mils	10		

	SLIDE VELOCITY fps				
Paint den. lb/cf	90	100	120	150	200
Tumble vel. fps	0.125	0.144	0.175	0.214	0.266
Dia.in					
128	8.78	10.08	12.29	15.00	18.67
64	6.21	7.13	8.69	10.61	13.20
32	4.39	5.04	6.15	7.50	9.33
16	3.10	3.57	4.35	5.30	6.60
8	2.19	2.52	3.07	3.75	4.67
4	1.55	1.78	2.17	2.65	3.30
2	1.10	1.26	1.54	1.88	2.33
1	0.78	0.89	1.09	1.33	1.65
0.5	0.55	0.63	0.77	0.94	1.17
0.25	0.39	0.45	0.54	0.66	0.83
0.125	0.27	0.32	0.38	0.47	0.58
0.0625	0.19	0.22	0.27	0.33	0.41

TABLE 6.2-5

TRANSPORT VELOCITY SUMMARY

PAINT THICKNESS = 5 MILS

Cont.pres PSI	20	Drag coef	1.1
Cont.temp F	250	Fric coef static	0.6
		Fric coef dynamic	0.42
Water density Lb/cf	58.8		
Viscosity water	0.000127		
Thickness Mils	5		

	SLIDE VELOCITY fps				
Paint den. lb/cf	90	100	120	150	200
Tumble vel. fps	0.088	0.102	0.124	0.151	0.188
Dia.in					
128	8.78	10.08	12.29	15.00	18.67
64	6.21	7.13	8.69	10.61	13.20
32	4.39	5.04	6.15	7.50	9.33
16	3.10	3.57	4.35	5.30	6.60
8	2.19	2.52	3.07	3.75	4.67
4	1.55	1.78	2.17	2.65	3.30
2	1.10	1.26	1.54	1.88	2.33
1	0.78	0.89	1.09	1.33	1.65
0.5	0.55	0.63	0.77	0.94	1.17
0.25	0.39	0.45	0.54	0.66	0.83
0.125	0.27	0.32	0.38	0.47	0.58
0.0625	0.19	0.22	0.27	0.33	0.41

TABLE 6.2-6

TRANSPORT VELOCITY SUMMARY

PAINT THICKNESS = 3 MILS

Cont.pres PSI	20	Drag coef	1.1
Cont.temp F	250	Fric coef static	0.6
		Fric coef dynamic	0.42
Water density Lb/cf	58.8		
Viscosity water	0.000127		
Thickness Mils	3		

	SLIDE VELOCITY fps				
Paint den. lb/cf	90	100	120	150	200
Tumble vel. fps	0.068	0.079	0.096	0.117	0.146
Dia.in					
128	8.78	10.08	12.29	15.00	18.67
64	6.21	7.13	8.69	10.61	13.20
32	4.39	5.04	6.15	7.50	9.33
16	3.10	3.57	4.35	5.30	6.60
8	2.19	2.52	3.07	3.75	4.67
4	1.55	1.78	2.17	2.65	3.30
2	1.10	1.26	1.54	1.88	2.33
1	0.78	0.89	1.09	1.33	1.65
0.5	0.55	0.63	0.77	0.94	1.17
0.25	0.39	0.45	0.54	0.66	0.83
0.125	0.27	0.32	0.38	0.47	0.58
0.0625	0.19	0.22	0.27	0.33	0.41

TABLE 6.2-7

TRANSPORT VELOCITY SUMMARY

PAINT THICKNESS = 10 MILS

Cont.pres PSI	10	Drag coef	1.1
Cont.temp F	200	Fric coef static	0.6
		Fric coef dynamic	0.42
Water density Lb/cf	60.1		
Viscosity water	0.000194		
Thickness Mils	10		

	SLIDE VELOCITY fps				
Paint den. lb/cf	90	100	120	150	200
Tumble vel. fps	0.121	0.140	0.171	0.210	0.262
Dia.in					
128	8.50	9.82	12.03	14.73	18.38
64	6.01	6.94	8.50	10.42	13.00
32	4.25	4.91	6.01	7.37	9.19
16	3.00	3.47	4.25	5.21	6.50
8	2.12	2.45	3.01	3.68	4.59
4	1.50	1.74	2.13	2.60	3.25
2	1.06	1.23	1.50	1.84	2.30
1	0.75	0.87	1.06	1.30	1.62
0.5	0.53	0.61	0.75	0.92	1.15
0.25	0.38	0.43	0.53	0.65	0.81
0.125	0.27	0.31	0.38	0.46	0.57
0.0625	0.19	0.22	0.27	0.33	0.41

TABLE 6.2-8

TRANSPORT VELOCITY SUMMARY

PAINT THICKNESS = 5 MILS

Cont.pres PSI	10	Drag coef	1.1
Cont.temp F	200	Fric coef static	0.6
		Fric coef dynamic	0.42
Water density Lb/cf	60.1		
Viscosity water	0.000194		
Thickness Mils	5		

	SLIDE VELOCITY fps				
Paint den. lb/cf	90	100	120	150	200
Tumble vel. fps	0.086	0.099	0.121	0.148	0.185
Dia.in					
128	8.50	9.82	12.03	14.73	18.38
64	6.01	6.94	8.50	10.42	13.00
32	4.25	4.91	6.01	7.37	9.19
16	3.00	3.47	4.25	5.21	6.50
8	2.12	2.45	3.01	3.68	4.59
4	1.50	1.74	2.13	2.60	3.25
2	1.06	1.23	1.50	1.84	2.30
1	0.75	0.87	1.06	1.30	1.62
0.5	0.53	0.61	0.75	0.92	1.15
0.25	0.38	0.43	0.53	0.65	0.81
0.125	0.27	0.31	0.38	0.46	0.57
0.0625	0.19	0.22	0.27	0.33	0.41

TABLE 6.2-9

TRANSPORT VELOCITY SUMMARY

PAINT THICKNESS = 3 MILS

Cont.pres PSI	10	Drag coef	1.1
Cont.temp F	200	Fric coef static	0.6
		Fric coef dynamic	0.42
Water density Lb/cf	60.1		
Viscosity water	0.000194		
Thickness Mils	3		

	SLIDE VELOCITY fps				
Paint den. lb/cf	90	100	120	150	200
Tumble vel. fps	0.066	0.077	0.094	0.115	0.143
Dia.in					
128	8.50	9.82	12.03	14.73	18.38
64	6.01	6.94	8.50	10.42	13.00
32	4.25	4.91	6.01	7.37	9.19
16	3.00	3.47	4.25	5.21	6.50
8	2.12	2.45	3.01	3.68	4.59
4	1.50	1.74	2.13	2.60	3.25
2	1.06	1.23	1.50	1.84	2.30
1	0.75	0.87	1.06	1.30	1.62
0.5	0.53	0.61	0.75	0.92	1.15
0.25	0.38	0.43	0.53	0.65	0.81
0.125	0.27	0.31	0.38	0.46	0.57
0.0625	0.19	0.22	0.27	0.33	0.41

TABLE 6.2-10

TRANSPORT VELOCITY SUMMARY

DRAG COEFFICIENT = 1.5

Cont.pres PSI	10	Drag coef	1.5
Cont.temp F	200	Fric coef static	0.6
		Fric coef dynamic	0.42
Water density Lb/cf	60.1		
Viscosity water	0.000194		
Thickness Mils	3		

	SLIDE VELOCITY fps				
Paint den. lb/cf	90	100	120	150	200
Tumble vel. fps	0.057	0.066	0.080	0.098	0.123
Dia.in					
128	7.28	8.41	10.30	12.62	15.74
64	5.15	5.94	7.28	8.92	11.13
32	3.64	4.20	5.15	6.31	7.87
16	2.57	2.97	3.64	4.46	5.56
8	1.82	2.10	2.57	3.15	3.93
4	1.29	1.49	1.82	2.23	2.78
2	0.91	1.05	1.29	1.58	1.97
1	0.64	0.74	0.91	1.12	1.39
0.5	0.45	0.53	0.64	0.79	0.98
0.25	0.32	0.37	0.46	0.56	0.70
0.125	0.23	0.26	0.32	0.39	0.49
0.0625	0.16	0.19	0.23	0.28	0.35

TABLE 6.2-11

TRANSPORT VELOCITY SUMMARY

DRAG COEFFICIENT = 1.2

Cont.pres PSI	10	Drag coef	1.2
Cont.temp F	200	Fric coef static	0.6
		Fric coef dynamic	0.42
Water density Lb/cf	60.1		
Viscosity water	0.000194		
Thickness Mils	3		

	SLIDE VELOCITY fps				
Paint den. lb/cf	90	100	120	150	200
Tumble vel. fps	0.063	0.073	0.090	0.110	0.137
Dia.in					
128	8.14	9.40	11.51	14.11	17.60
64	5.75	6.65	8.14	9.97	12.44
32	4.07	4.70	5.76	7.05	8.80
16	2.88	3.32	4.07	4.99	6.22
8	2.03	2.35	2.88	3.53	4.40
4	1.44	1.66	2.04	2.49	3.11
2	1.02	1.17	1.44	1.76	2.20
1	0.72	0.83	1.02	1.25	1.56
0.5	0.51	0.59	0.72	0.88	1.10
0.25	0.36	0.42	0.51	0.62	0.78
0.125	0.25	0.29	0.36	0.44	0.55
0.0625	0.18	0.21	0.25	0.31	0.39

TABLE 6.2-12

TRANSPORT VELOCITY SUMMARY

DRAG COEFFICIENT = 0.9

Cont.pres PSI	10	Drag coef	0.9
Cont.temp F	200	Fric coef static	0.6
		Fric coef dynamic	0.42
Water density Lb/cf	60.1		
Viscosity water	0.000194		
Thickness Mils	3		

	SLIDE VELOCITY fps				
Paint den. lb/cf	90	100	120	150	200
Tumble vel. fps	0.073	0.085	0.104	0.127	0.159
Dia.in					
128	9.39	10.85	13.30	16.29	20.32
64	6.64	7.67	9.40	11.52	14.37
32	4.70	5.43	6.65	8.14	10.16
16	3.32	3.84	4.70	5.76	7.18
8	2.35	2.71	3.32	4.07	5.08
4	1.66	1.92	2.35	2.88	3.59
2	1.17	1.36	1.66	2.04	2.54
1	0.83	0.96	1.18	1.44	1.80
0.5	0.59	0.68	0.83	1.02	1.27
0.25	0.42	0.48	0.59	0.72	0.90
0.125	0.29	0.34	0.42	0.51	0.63
0.0625	0.21	0.24	0.29	0.36	0.45

TABLE 6.2-13

TRANSPORT VELOCITY SUMMARY

DRAG COEFFICIENT = 0.7

Cont.pres PSI	10	Drag coef	0.7
Cont.temp F	200	Fric coef static	0.6
		Fric coef dynamic	0.42
Water density Lb/cf	60.1		
Viscosity water	0.000194		
Thickness Mils	3		

	SLIDE VELOCITY fps				
Paint den. lb/cf	90	100	120	150	200
Tumble vel. fps	0.083	0.096	0.118	0.144	0.180
Dia.in					
128	10.65	12.30	15.08	18.47	23.04
64	7.53	8.70	10.66	13.06	16.29
32	5.33	6.15	7.54	9.23	11.52
16	3.77	4.35	5.33	6.53	8.15
8	2.66	3.08	3.77	4.62	5.76
4	1.88	2.18	2.67	3.27	4.07
2	1.33	1.54	1.88	2.31	2.88
1	0.94	1.09	1.33	1.63	2.04
0.5	0.67	0.77	0.94	1.15	1.44
0.25	0.47	0.54	0.67	0.82	1.02
0.125	0.33	0.38	0.47	0.58	0.72
0.0625	0.24	0.27	0.33	0.41	0.51

TABLE 6.2-14

TRANSPORT VELOCITY SUMMARY

FRIC.COEFF.DYNAM. = 0.1

Cont.pres PSI	10	Drag coef	1.1
Cont.temp F	200	Fric coef static	0.6
		Fric coef dynamic	0.1
Water density Lb/cf	60.1		
Viscosity water	0.000194		
Thickness Mils	3		

	SLIDE VELOCITY fps				
Paint den. lb/cf	90	100	120	150	200
Tumble vel. fps	0.066	0.077	0.094	0.115	0.143
Dia.in					
128	4.71	5.44	6.67	8.17	10.19
64	3.33	3.85	4.71	5.78	7.21
32	2.36	2.72	3.33	4.08	5.09
16	1.67	1.92	2.36	2.89	3.60
8	1.18	1.36	1.67	2.04	2.55
4	0.83	0.96	1.18	1.44	1.80
2	0.59	0.68	0.83	1.02	1.27
1	0.42	0.48	0.59	0.72	0.90
0.5	0.29	0.34	0.42	0.51	0.64
0.25	0.21	0.24	0.29	0.36	0.45
0.125	0.15	0.17	0.21	0.26	0.32
0.0625	0.10	0.12	0.15	0.18	0.23

TABLE 6.2-15

TRANSPORT VELOCITY SUMMARY

FRIC.COEFF.DYNAM. = 0.2

Cont.pres PSI	10	Drag coef	1.1
Cont.temp F	200	Fric coef static	0.6
		Fric coef dynamic	0.2
Water density Lb/cf	60.1		
Viscosity water	0.000194		
Thickness Mils	3		

	SLIDE VELOCITY fps				
Paint den. lb/cf	90	100	120	150	200
Tumble vel. fps	0.066	0.077	0.094	0.115	0.143
Dia.in					
128	6.38	7.37	9.03	11.06	13.80
64	4.51	5.21	6.38	7.82	9.76
32	3.19	3.68	4.51	5.53	6.90
16	2.26	2.61	3.19	3.91	4.88
8	1.59	1.84	2.26	2.77	3.45
4	1.13	1.30	1.60	1.96	2.44
2	0.80	0.92	1.13	1.38	1.72
1	0.56	0.65	0.80	0.98	1.22
0.5	0.40	0.46	0.56	0.69	0.86
0.25	0.28	0.33	0.40	0.49	0.61
0.125	0.20	0.23	0.28	0.35	0.43
0.0625	0.14	0.16	0.20	0.24	0.30

TABLE 6.2-16

TRANSPORT VELOCITY SUMMARY

FRIC.COEFF.DYNAM. = 0.3

Cont.pres PSI	10	Drag coef	1.1
Cont.temp F	200	Fric coef static	0.6
		Fric coef dynamic	0.3
Water density Lb/cf	60.1		
Viscosity water	0.000194		
Thickness Mils	3		

	SLIDE VELOCITY fps				
Paint den. lb/cf	90	100	120	150	200
Tumble vel. fps	0.066	0.077	0.094	0.115	0.143
Dia.in					
128	7.51	8.67	10.62	13.01	16.24
64	5.31	6.13	7.51	9.20	11.48
32	3.75	4.34	5.31	6.51	8.12
16	2.65	3.07	3.76	4.60	5.74
8	1.88	2.17	2.66	3.25	4.06
4	1.33	1.53	1.88	2.30	2.87
2	0.94	1.08	1.33	1.63	2.03
1	0.66	0.77	0.94	1.15	1.43
0.5	0.47	0.54	0.66	0.81	1.01
0.25	0.33	0.38	0.47	0.58	0.72
0.125	0.23	0.27	0.33	0.41	0.51
0.0625	0.17	0.19	0.23	0.29	0.36

TABLE 6.2-17

TRANSPORT VELOCITY SUMMARY

FRIC.COEFF.DYNAM. = 0.5

Cont.pres PSI	10	Drag coef	1.1
Cont.temp F	200	Fric coef static	0.6
		Fric coef dynamic	0.5
Water density Lb/cf	60.1		
Viscosity water	0.000194		
Thickness Mils	3		

	SLIDE VELOCITY fps				
Paint den. lb/cf	90	100	120	150	200
Tumble vel. fps	0.066	0.077	0.094	0.115	0.143
Dia.in					
128	9.02	10.42	12.77	15.64	19.51
64	6.38	7.37	9.03	11.06	13.80
32	4.51	5.21	6.38	7.82	9.76
16	3.19	3.68	4.51	5.53	6.90
8	2.26	2.61	3.19	3.91	4.88
4	1.59	1.84	2.26	2.77	3.45
2	1.13	1.30	1.60	1.96	2.44
1	0.80	0.92	1.13	1.38	1.72
0.5	0.56	0.65	0.80	0.98	1.22
0.25	0.40	0.46	0.56	0.69	0.86
0.125	0.28	0.33	0.40	0.49	0.61
0.0625	0.20	0.23	0.28	0.35	0.43

TABLE 6.2-18

TRANSPORT VELOCITY SUMMARY

FRIC.COEFF.DYNAM. = 0.6

Cont.pres PSI	10	Drag coef	1.1
Cont.temp F	200	Fric coef static	0.6
		Fric coef dynamic	0.6
Water density Lb/cf	60.1		
Viscosity water	0.000194		
Thickness Mils	3		

	SLIDE VELOCITY fps				
Paint den. lb/cf	90	100	120	150	200
Tumble vel. fps	0.066	0.077	0.094	0.115	0.143
Dia.in					
128	9.57	11.05	13.54	16.59	20.70
64	6.77	7.82	9.58	11.73	14.63
32	4.78	5.53	6.77	8.30	10.35
16	3.38	3.91	4.79	5.87	7.32
8	2.39	2.76	3.39	4.15	5.17
4	1.69	1.95	2.39	2.93	3.66
2	1.20	1.38	1.69	2.07	2.59
1	0.85	0.98	1.20	1.47	1.83
0.5	0.60	0.69	0.85	1.04	1.29
0.25	0.42	0.49	0.60	0.73	0.91
0.125	0.30	0.35	0.42	0.52	0.65
0.0625	0.21	0.24	0.30	0.37	0.46

TABLE 6.2-19

TRANSPORT VELOCITY SUMMARY
CONCRETE COATINGS

PAINT THICKNESS = 20 MILS

Cont.pres PSI	10	Drag coef	1.1
Cont.temp F	200	Fric coef static	0.6
		Fric coef dynamic	0.42
Water density Lb/cf	60.1		
Viscosity water	0.000194		
Thickness Mils	20		

	SLIDE VELOCITY fps				
Paint den. lb/cf	90	100	120	150	200
Tumble vel. fps	0.171	0.198	0.242	0.297	0.370
Dia.in					
128	8.50	9.82	12.03	14.73	18.38
64	6.01	6.94	8.50	10.42	13.00
32	4.25	4.91	6.01	7.37	9.19
16	3.00	3.47	4.25	5.21	6.50
8	2.12	2.45	3.01	3.68	4.59
4	1.50	1.74	2.13	2.60	3.25
2	1.06	1.23	1.50	1.84	2.30
1	0.75	0.87	1.06	1.30	1.62
0.5	0.53	0.61	0.75	0.92	1.15
0.25	0.38	0.43	0.53	0.65	0.81
0.125	0.27	0.31	0.38	0.46	0.57
0.0625	0.19	0.22	0.27	0.33	0.41

TABLE 6.2-20

TRANSPORT VELOCITY SUMMARY
CONCRETE COATINGS

PAINT THICKNESS = 30 MILS

Cont.pres PSI	10	Drag coef	1.1
Cont.temp F	200	Fric coef static	0.6
		Fric coef dynamic	0.42
Water density Lb/cf	60.1		
Viscosity water	0.000194		
Thickness Mils	30		

	SLIDE VELOCITY fps				
Paint den. lb/cf	90	100	120	150	200
Tumble vel. fps	0.210	0.242	0.297	0.364	0.454
Dia.in					
128	8.50	9.82	12.03	14.73	18.38
64	6.01	6.94	8.50	10.42	13.00
32	4.25	4.91	6.01	7.37	9.19
16	3.00	3.47	4.25	5.21	6.50
8	2.12	2.45	3.01	3.68	4.59
4	1.50	1.74	2.13	2.60	3.25
2	1.06	1.23	1.50	1.84	2.30
1	0.75	0.87	1.06	1.30	1.62
0.5	0.53	0.61	0.75	0.92	1.15
0.25	0.38	0.43	0.53	0.65	0.81
0.125	0.27	0.31	0.38	0.46	0.57
0.0625	0.19	0.22	0.27	0.33	0.41

TABLE 6.2-21

TRANSPORT VELOCITY SUMMARY

SAND PARTICLES

Cont.pres PSI	10	Drag coef	1.1
Cont.temp F	200	Fric coef static	0.6
		Fric coef dynamic	0.42
Water density Lb/cf	60.1		
Viscosity water	0.000194		

	SLIDE VELOCITY fps		
SAND DENSITY,lb/cf	87.36	112.32	137.28
PARTICLE SIZE, inches / mesh size			
0.0466 / 18	0.15	0.21	0.26
0.0365 / 22	0.14	0.19	0.23
0.0305 / 26	0.13	0.17	0.21
0.0258 / 30	0.12	0.16	0.19
0.0175 / 40	0.09	0.13	0.16
0.0107 / 60	0.07	0.10	0.12
0.007 / 80	0.06	0.08	0.10
0.005 / 100	0.05	0.07	0.09
0.0046 / 120	0.05	0.07	0.08
0.0042 / 140	0.05	0.06	0.08
0.0038 / 160	0.04	0.06	0.07
0.0033 / 180	0.04	0.06	0.07

NOTES

1. Specific gravity of sand as a raw material is considered as 1.4 to 2.2.

TABLE 6.3-22

TRANSPORT VELOCITY SUMMARY

ZINC DUST PARTICLES

Cont.pres PSI	10	Drag coef	1.1
Cont.temp F	200	Fric coef static	0.6
		Fric coef dynamic	0.42
Water density Lb/cf	60.1		
Viscosity water	0.000194		

		SLIDE VELOCITY fps	
ZINC DENSITY,lb/cf		443.04 (note 1)	249.6 (note 2)
PARTICLE SIZE, inches	microns		
0.001968	50	0.12	0.08
0.001374	40	0.11	0.08
0.001181	30	0.09	0.06
0.000787	20	0.08	0.05
0.000590	15	0.07	0.05
0.000393	10	0.05	0.04
0.000196	5	0.04	0.03
0.000098	2.5	0.03	0.02
0.000049	1.25	0.02	0.01
0.000024	0.625	0.01	0.01

NOTES

1. Density of zinc dust as a raw material.
2. Density of the dry coating film for inorganic zinc primer.

TABLE 6.2-23

SUMMARY OF CRITICAL TRANSPORT VELOCITIES
FOR PAINT PARTICLES[1]

Paint	Density lbs/cu.ft.	Velocities (ft/sec) vs Particle Size (Inches) 1/8	1/4	1/2	1
Carbozinc 11	6200[2]	>0.57	>0.81	>1.15	>1.62
Phenoline 305	90	0.27	0.38	0.53	0.7
Nutec 11	100[3]	>0.31	>0.43	>0.61	>0.8
Reactic 1201	90	0.27	0.38	0.53	0.7

Notes:

(1) At 200 F containment water temperature.
(2) Density 240 lbs/cu.ft.
(3) Density ranges from 100 to 128 lbs/cu.ft.

TABLE 6.2-24

PERIMETERS OF OPENINGS
ON UPPER ELEVATIONS

AZIMUTH RANGE	905 ELEV	860 ELEV	832 ELEV
0-45	0	0	23
45-90	0	0	0
90-135	0	0	14
135-180	3	6	6
180-225	36	20	28
225-270	23	26	20
270-315	0	22	0
315-360	0	0	19
	62	74	110

TABLE 6.2-25

COATINGS CONTRIBUTION
FROM UPPER ELEVATIONS

AZIMUTH RANGE	905 ELEV	860 ELEV	832 ELEV	TOTAL AT 808 ELEV. (NOTE 1)
COATINGS AVAILABLE	87800	128200	128200	76480
0-45	0	0	26805	46743
45-90	0	0	0	19938
90-135	0	0	16316	36254
135-180	4248	10395	6993	41573
180-225	50981	34649	32633	138200
225-270	32571	45043	23309	120861
270-315	0	38114	0	58051
315-360	0	0	22144	42081
TOTAL PAINT IN THE NEAR SUMP ZONE (AZIMUTH 0/45 AND 360/315)			:	88824

NOTE 1. CONTRIBUTION FROM LINER PLATE UP TO THE SPRING LINE AND PAINT AT THE 808 ELEV. ARE INCLUDED.

7.0 INSULATION DEBRIS GENERATION

7.1 Types of Insulation

Most of the thermal insulation inside the containment on both piping and equipment is of the reflective metallic type, composed of stainless steel. The high efficiency metallic thermal insulation is composed of fibrous media and very fine heat resistant particulate matter, totally encased in stainless steel. All antisweat insulation is fiberglass encapsulated in metal casing and is used on cold water piping.

All metallic insulation, with the exception of the reactor coolant pipe insulation inside the primary shield concrete, is designed to remain in place during an SSE. Figure 7.1-1 shows a typical metallic insulation for piping. Figure 7.1-2 shows the cross-section of a typical metallic insulation. Figure 7.1-3 shows the clamping arrangement for holding the metallic insulation panel in place. Table 7.1-1 gives the major dimensions, and thickness of each component.

The reflective metallic insulation assemblies are designed to withstand seismic forces resulting from acceleration of 3g in both horizontal directions and 3g in the vertical direction caused by the SSE. The insulation structural mounting frames and panel attachments to the mounting frames are designed to maintain their structural integrity during the SSE.

Sample panels of insulation were tested to confirm the design. In order to verify that the insulation meets the required seismic criteria, the insulation supplier has tested a typical assembly on a generic basis. The tests consisted of an initial sinusoidal input frequency between 3 and 100 Hz to determine the resonant frequency condition followed by an endurance test at the lowest resonant frequency. The insulation assembly was subjected to 10g's in both the horizontal and vertical directions. No damage or distortion to the structure was observed.

A series of pressurization tests were also performed to ensure that the insulation maintains its structural integrity under post-accident pressures as well as containment structural acceptance test and leakage rate test pressures. A thermal transient test was performed on sample insulation panels to ensure that the insulation maintains its structural integrity during post-accident temperature transients. This test consists of heating the sample panel to 650 F and quenching it with cold water.

7.2 Insulation Debris Generation

7.2.1 Identification of Accident

The initiating events for the insulation debris are the postulated LOCAs described in the FSAR. The design basis pipe break locations, their orientations, and their sizes have been determined. With this identification, an enveloping process was undertaken to locate breaks which have maximum potential for unacceptable debris generation. The following criteria were used to isolate the non-critical breaks for this evaluation:

- Breaks with barriers interposed between the break and the containment sumps were not considered if no flow path exists which would allow the transport of debris to the sumps.

- Breaks for which the expanding fluid jet does not impinge on insulated targets were not considered.

- Small diameter breaks in the same location and with effects similar to large diameter breaks were not considered.

- Analysis of longitudinal failures was required only in those cases whose postulated circumferential pipe failures do not target large areas of containment with insulated targets.

The mechanisms which were postulated for insulation debris generation are:

- Jet Impingement

- Pipe Whip

- Pipe Impact

Jet Impingement: Jet impingement is the most significant of the debris generation mechanisms for insulated pipe. All targets that intercept the jet resulting from the selected breaks were investigated. It was assumed, for conservatism, that all fibrous insulation within the vicinity of the break being investigated was dislodged and available for transport to the containment sumps. This is more conservative than NUREG/CR2791 which assumes that any insulation subject to a stagnation force in excess of 0.5 psi will result in dislodgement from the pipe. Further, NUREG/CR-2791 assumes the jet from the break covers a certain spray angle. For this report, it was conservatively assumed that all fibrous insulation in the break area is affected.

For reflective metallic insulation, one worst case primary coolant loop break in steam generator compartment #4 was

selected and evaluated for debris generation. Steam generator compartment #4 is the closest area to the sumps where such coolant pipe breaks can be postulated. Figure 7.2-1 shows the coolant loop postulated break locations for steam generator compartment #4. Break #7 in the hot leg pipe was determined to be the worst case for this evaluation. This makes the choice of this break the worst case for insulation transport and sump blockage potential. In addition the quantity of metallic insulation released was assumed to be from all the piping and equipment in this compartment except the topmost section of the steam generator.

The second category of worst case break considered for reflective metallic insulation was on the reactor coolant loop cold leg in steam generator compartment #4. It is a 10-inch branch line from the safety injection system. Figure 7.2-2 shows this break location. The jet portion and the targets were analyzed as part of the CPSES damage study of problem #DS1-17D, break #756LWR. The damage to the metallic insulation was calculated using all the components and piping within the jet impingement area up to 50 ft.

Pipe Whip: All insulation on the ruptured segment between the break location and the plastic hinge constitutes debris. However, for CPSES Unit 1 containment, the high energy lines are not insulated with fibrous insulation. Therefore, this concern does not have to be addressed for this type of insulation. For high efficiency insulation, where the insulation is wedged between the pipe whip restraint and the pipe, it is not possible for the insulation to be dislodged as a result of pipe whip. Therefore, no insulation debris will be created as a result of the pipe whip for fibrous and high efficiency insulation. The worst case pipe breaks considered for metallic insulation have pipe restraints which prevent pipe whip.

Pipe Impact: NUREG/CR-2791 assumes that five fabrication lengths of insulation on the impacted pipe are dislodged. This includes two lengths upstream and two lengths downstream of the impact point, and one length at the point of impact. For this analysis, as discussed above, all fibrous insulation in the vicinity of the break is dislodged. Again, this is more conservative than the NUREG/CR-2791 assumptions. No high-efficiency insulation debris can be generated by this mechanism. No metallic insulation is released by pipe impact because of the pipe restraints used to prevent pipe impact.

A field walkdown was performed in the containment of Unit 1 to determine which breaks had the greatest potential for generation of insulation debris. Twenty high energy pipe breaks were

selected for further investigation. The evaluation concentrates on the breaks which generate the maximum amount of debris and where debris transport to the sump is relatively direct. Two of the breaks release reflective metallic insulation and also cause activation of safety injection and containment sprays. The other breaks release fibrous insulation. The quantity of fibrous insulation used inside containment is limited to component cooling water and chilled water piping. This type of insulation is not located in any of the containment areas where high energy large breaks can release this insulation material to form debris. None of the breaks in the vicinity of the fibrous insulation are of the magnitude which would cause the activation of the safety injection or containment sprays. Therefore, the availability of the safeguards sumps is not required and sump blockage is not a concern. The quantities of debris generated are presented in Tables 7.2-1 through 7.2-5 for information purposes only.

High efficiency insulation was also evaluated. This insulation, which is a mineral wool type, 1/4-inch thick, is fully encapsulated in 1/8-inch thick sheeting of type 304 SS. The insulation is located at pipe whip restraints and in the gap between the restraints and the pipe.

7.2.2 Quantity of Insulation Debris

The quantities of fibrous insulation generated from various postulated breaks are shown on Tables 7.2-1 through 7.2-5. Short term transport of fibrous insulation was not analyzed because it was assumed to be transported to the sumps.

In the case of high efficiency insulation, it was conservatively assumed that insulation from five pipe whip restraints of safety injection pipes would be dislodged as a result of jet impingement from a pipe break. This resulted in the generation of about 40 square feet of high efficiency insulation.

The quantities of metallic insulation generated from the postulated breaks are shown on Tables 7.2-6 and 7.2-7. Table 7.2-6 is for primary coolant hot leg break. For purposes of this analysis reactor coolant loop breaks are not postulated as credible in view of the generic work done by Westinghouse regarding alternate pipe break criteria. For the purposes of this evaluation for debris effects, metallic insulation quantities given in Table 7.2-7 were used. These quantities are based on worst case break external to the reactor coolant loop. The metallic insulation debris generated by this break produced the maximum quantity of debris. NUREG-0897 Rev 1 (Draft) and NUREG/CR-3616 discuss the transport of metallic insulation materials. This information is based on experimental work done at Alden Research Laboratories during the second half of 1983. Based on these experiments, it is postulated by Alden Research

that metallic insulation inner foil can be transported at very low velocities.

In view of this new information, further evaluations were made for metallic insulation debris, its damage potential, and transport to the sump screens. In accordance with the recommendations of NUREG-0897 Revision 1 (Draft), it was postulated that all insulation within 7 pipe diameter lengths from the break will be completely destroyed to open up the metallic insulation. Figure 7.2-1 shows a typical metallic insulation section with all the sub-components. Table 7.2-8 gives the quantities of insulation that will be damaged in this manner and the area of the inner foil that will be released.

The short term transport of metallic insulation for this break does not have a direct pathway to the door openings in the steam generator compartments. However, for a conservative evaluation, it was assumed that all the insulation released in this manner will be propelled by the jet through the doorway for steam generator compartment #1.

7.3 Insulation Transport

The methodology described in this report is based on NUREG/CR-2791 and NUREG/CR-2982 Rev. 1. The evaluation of long term transport of debris involves only the metallic insulation because, (as discussed in Section 7.2.2) the fibrous insulation will not cause debris during a LOCA and the high efficiency insulation will sink to the floor.

The transport of the insulation debris occurs in two phases. The first phase relates to the transport of debris caused by the initiating event, such as pipe whip and jet impingement. This mechanism of transport is normally a transient, terminated by dislodging of all the insulation in the affected zone.

The second phase of transport begins with the recirculation of the sump water and continues as long as the ECCS recirculation is active.

Following a LOCA and the initiation of the ECCS, the containment will be flooded with water. All the water used for the initial phase of the ECCS is provided from the refueling water storage tank. At the end of this phase of ECCS operation, the water collected in the containment sumps is recirculated.

The transport mechanism for the debris is complex because of the various flow paths and hydraulic resistances present in the containment. In order to simplify the methodology, various assumptions were made to produce conservatively limiting conditions which reflect the long term debris transport. The major assumptions were:

a. Water cascading from the point of coolant loss and the containment spray will eventually flow to the containment sumps.

b. No stagnant areas exist within containment.

c. The force required to transport debris is a resultant of the friction between the debris and the floor, the normal force exerted by the debris and the buoyancy force.

7.3.1 Transport Evaluation

The long term transport evaluation for insulation material was done by a step-by-step methodology using the following criteria:

Step-1 Determine the flow of water to various zones in the containment during the recirculation phase of the ECCS and containment spray operation.

Step-2 Determine the minimum water level inside the containment for the postulated accident.

Step-3 Calculate flow velocities for each path to the ECCS sump inside the containment. The calculation is based on using open channel flow equations. The flow is apportioned to each parallel path based on equal pressure drops for each flow path.

Step-4 Using the flow velocities established in Step-3, determine the maximum velocity in each zone. Section 5.0 of this report discusses flow velocities.

Step-5 If the velocity calculated in Step-4 is less than the velocity required to move the metallic insulation, then the debris will not be transported to the sump screens.

Step-6 Based on the evaluation in Step-5. the quantity of insulation transported to the sump screens and the resulting sump affects are evaluated as discussed in Section 9.0.

The containment water levels are presented in Table 5.2-1 and flow velocities for each zone are presented in Tables 5.3-1 through 5.4-12 and 5.4-1.

Transport of insulation debris is dependent on the flow velocities inside the containment. The flow velocities at various zones inside the containment were calculated in Section 5.4. Table 7.3-1 summarizes these velocities in the sump zones. These velocities were calculated at high water level and low water level for one and two train ECCS system operation. The worst case for analysis will be the case which gives highest velocities, i.e., low water level and two train operation.

The fibrous insulation which can be released as debris is quantified in Section 7.2.2 (refer Tables 7.2-1 through 7.2-5). The accident scenarios for the fibrous insulation debris are all short term transients, which will not cause containment spray or ECCS system pumps to go into recirculation mode. Therefore, there will not be any requirement for the performance of

emergency sumps. In the absence of recirculation flow, the velocities of water at the sump level (EL 808.0 ft) will be essentially zero and no motion of debris can be postulated. Based on this evaluation, it was concluded that the fibrous insulation debris will not reach the sump and impact the safety of the plant.

The small quantity (40 sq.ft.) of high efficiency insulation (refer to Section 7.2.1) will not be transported to the sumps because it is fully encapsulated in 1/8-inch stainless steel sheeting. The maximum water velocity for any zone at the sump elevation (EL 808 ft) is less than 0.7 ft/sec and the minimum velocity required to transport this material is 2 ft/sec in accordance with NUREG-0869 and NUREG/CR-2791 (page A-23).

The quantity of metallic insulation calculated to be released is given in Tables 7.2-6 and 7.2-7. It was very conservatively assumed that the metallic insulation is transported through door openings to areas outside the steam generator compartment. The maximum velocity in the near sump areas of the containment is conservatively calculated to be 0.38 ft/sec at low water level and 0.30 ft/sec at high water level (refer Table 7.3-1). Using guidance from NUREG-0869, it was postulated that the metallic insulation will not be transported to the sumps because the water velocities inside the containment where metallic insulation debris is generated (zones 3 and 4) is considerably less than 2.0 ft/sec. In accordance with NUREG-0897 (dated April 1983) evaluation procedure, it was concluded that the metallic insulation will not be transported to the sump screens.

However, in view of the more recent information provided by NUREG-0897 Rev 1 (draft June 1984) and NUREG/CR-3616, more detailed study of the metallic insulation transport was performed in this evaluation.

The findings of the Alden Research Laboratory test data reported in NUREG-0897 Rev 1 and NUREG/CR-3616 are discussed below:

a. Transport velocities of metallic insulation components:

1) Single sheets of thin stainless steel materials (such as the 0.0025 - 0.004 inch thick foils used within reflective metallic insulation units) are transported at relative low water velocities, 0.2 - 0.5 ft/sec.

2) "As fabricated" reflective metallic insulation units required water velocities of 1.0 ft/sec or more for transport.

3) For all tested insulation material, transport of the test specimen was much slower than the flow velocity.

4) When several pieces of foil were tested simultaneously and interacted before reaching the screen, the group of foils ceased movement at the low flow velocities which had sustained motion of the individual foil pieces. Higher velocities, up to 1.8 ft/sec, were required to break up the group of foils and again initiate movement of individual foils.

5) The vertical side walls of the test flume were observed to hinder the transport of samples. Samples in contact with a wall were often pushed and folded against it, needing higher flow velocities to be dislodged.

6) Outer covers (0.037 inch thick) - When lying on the floor with their concave side up, the outer covers of the insulation units started to move at a flow velocity of approximately 0.7 ft/sec and moved continuously to the screen at a flow velocity of approximately 0.8 ft/sec. When lying with their concave side down, the outer covers did not move at a flow velocity of 1.8 ft/sec.

7) Inner covers - When lying with their concave side up, the inner covers moved at a flow velocity of approximately 0.7 ft/sec and reached the screen at a flow velocity of approximately 0.8 ft/sec. With the covers lying concave side down, these velocities were respectively 1.1 and 1.6 ft/sec.

8) End Covers - The end covers never moved, even at the highest flume flow velocity of approximately 2 ft/sec.

b. Transport and Blockage Modes

1) Thin foils (0.0025 - 0.004 inch thick) transported in an intermittent folding and tumbling manner, whether originally crumpled or not. Depending on the position and shape of the foils just upstream from the screen, the foils would either flip onto the screen to their full area or be pressed onto the screen in a folded position.

2) Neither the flexible thin foils, nor the relatively stiffer foils, ever became "water borne." A portion of the foil was always in contact with the test flume floor. Therefore, the screen was never blocked beyond the foil width or length. If the foil blocked the screen diagonally, the highest blockage would be the diagonal of a foil sheet.

3) Total blockage of the screen did not occur even when the total foil area in a given test was somewhat more than twice the wetted screen area. The maximum screen blockage observed was 80%. This factor is mainly due to the significant foil overlap that occurred in the screen blockage pattern.

Table 7.3-2 summarizes the findings of Alden Research Laboratories reported in NUREG/CR-3616.

The worst case water velocities in the near sump zones where metallic insulation debris is deposited (azimuth 60-300°) are less than 0.42 ft/sec. It can therefore be concluded that the only material which has any potential for transport of damaged components of metallic insulation will be the inner foils. The following discussion evaluates the transport potential for metallic insulation inner foil.

The quantity of inner foil that can be released is given in Table 7.2-8 (refer Section 7.2.2). The worst location of the foils at the end of short term transport resulting from the initiating event will be outside doorways from steam generator compartments 1 and 4. These areas correspond to channel no. 3 sub-channel A for steam generator compartment 1 and channel no. 4 sub-channel A for steam generator compartment B.

From Table 7.3-1, it can be seen that the worst case water flow velocities (low water level and 2 trains in operation) are

0.15 ft/sec at channel 3-A and 0.12 ft/sec at Channel 4-A. These two channel areas are relatively large areas 22 to 24 ft long with 128 to 144 sq.ft of flow area. Since the velocity required to transport the foil to the screens is 0.35 ft/sec (refer Table 7.3-2, item 5), it can be concluded that the inner foils will not be tranported to the screens. These foils will accumulate in the Channel 3A and 4A areas and tend to cluster into multiple foils and remain stationary.

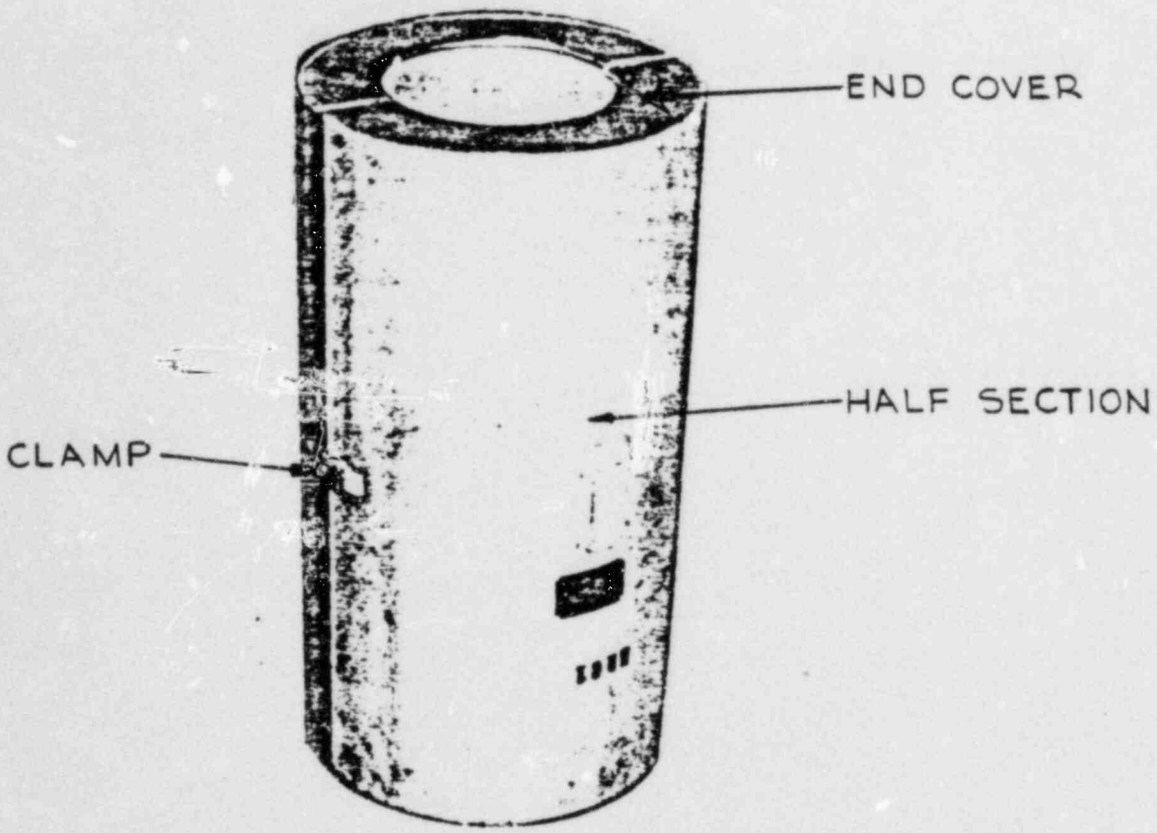

FIGURE 7.1-1
REFLECTIVE METALLIC INSULATION ASSEMBLY

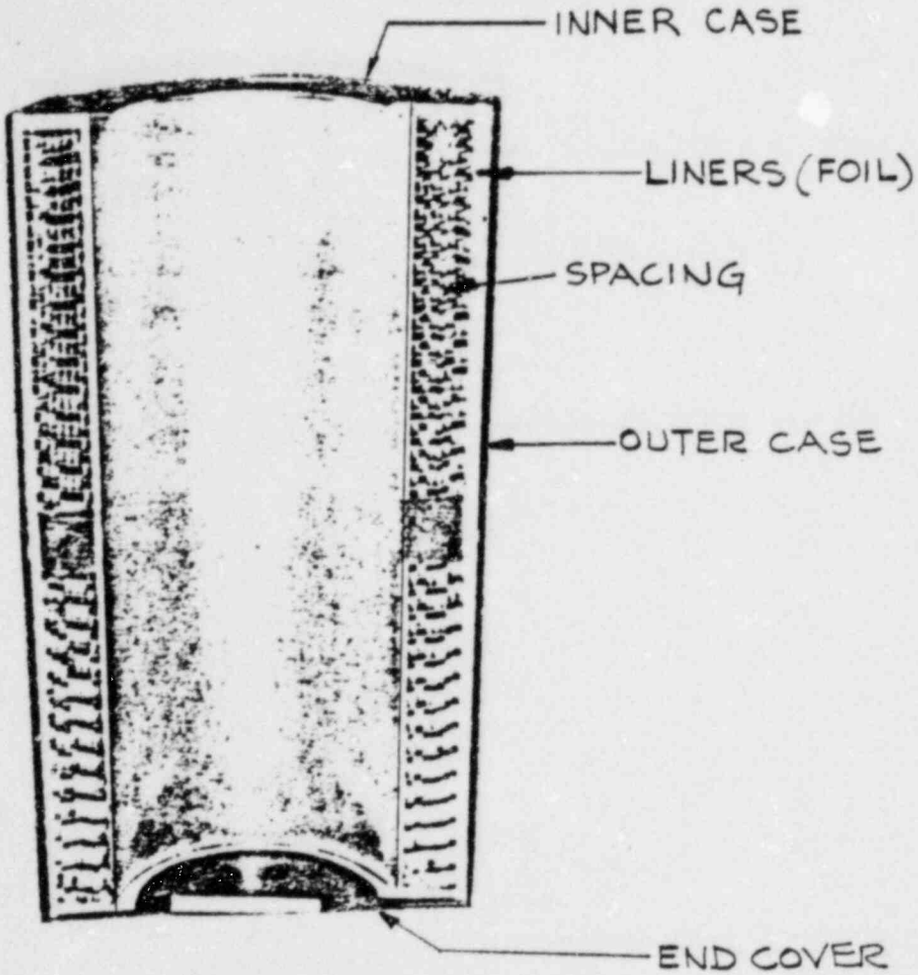

FIGURE 7.1-2
CROSS SECTION OF
INSULATION ASSEMBLY

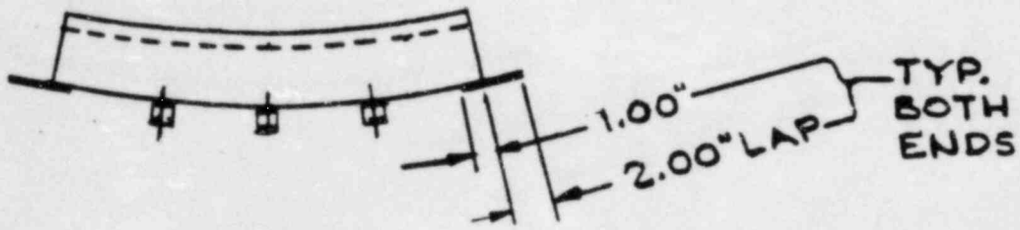

PLAN VIEW

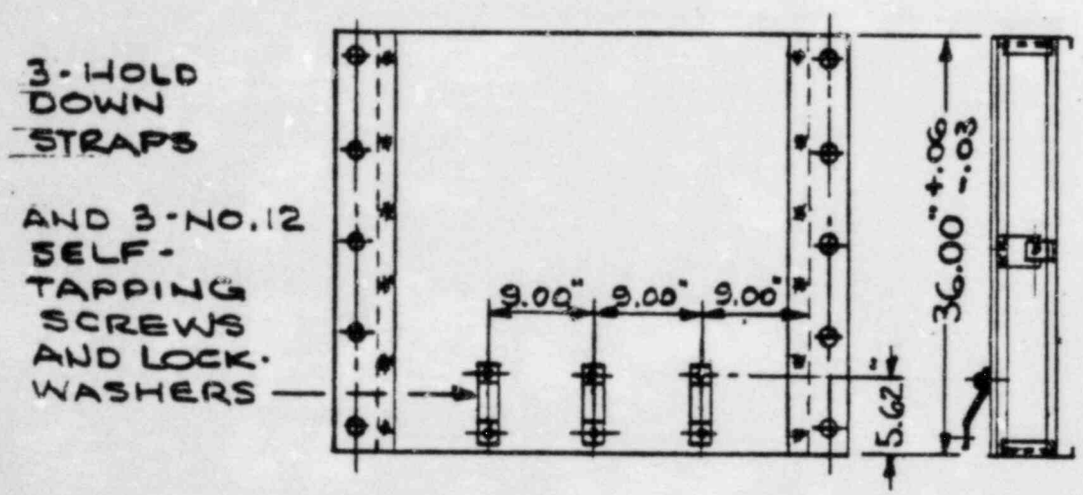

ELEVATION

END VIEW

FIGURE 7.1-3
METALLIC INSULATION PANEL

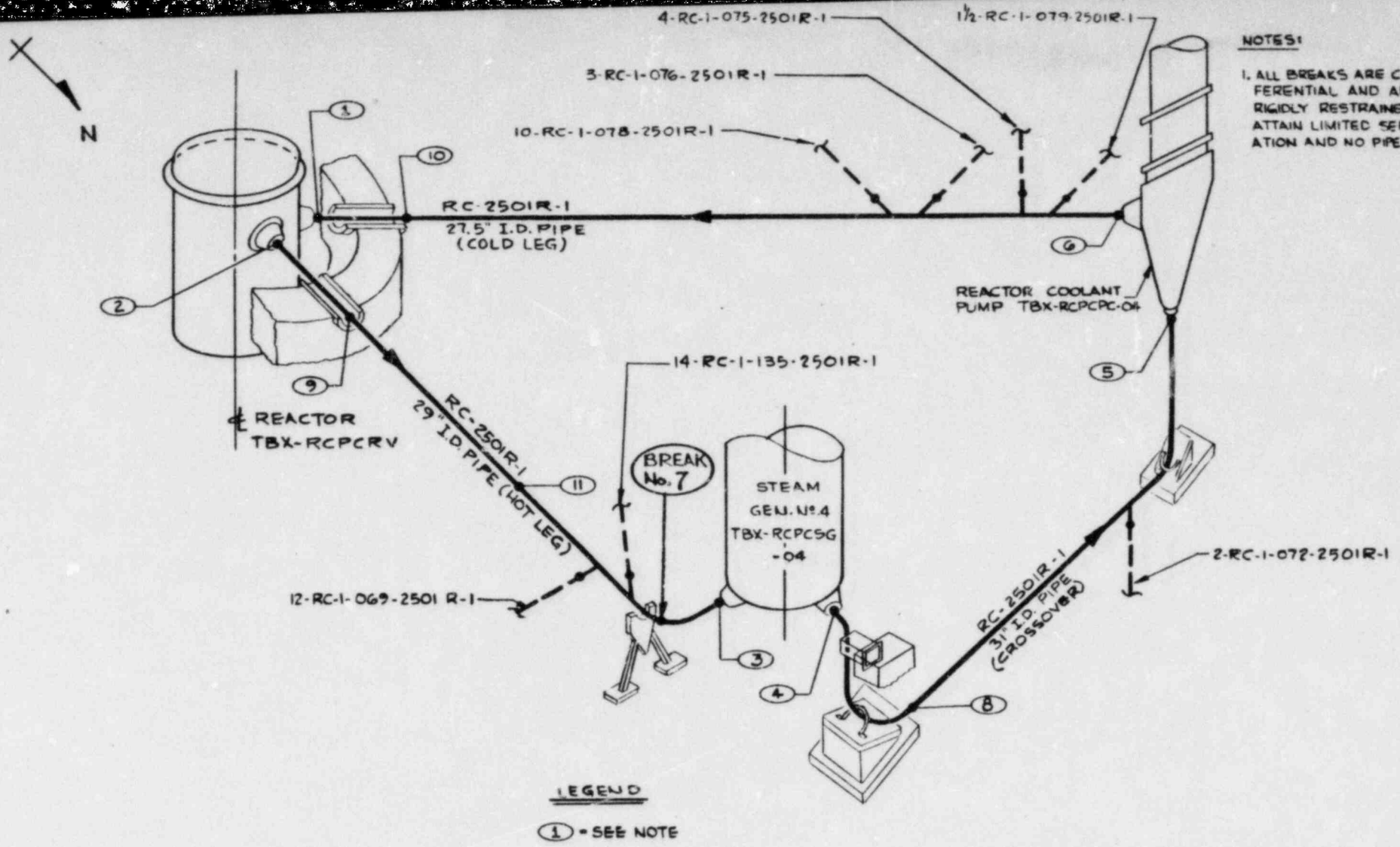

FIGURE 7.2-1
REACTOR COOLANT LOOP No. 4
BREAK POINTS AND RESTRAINT LOCATIONS

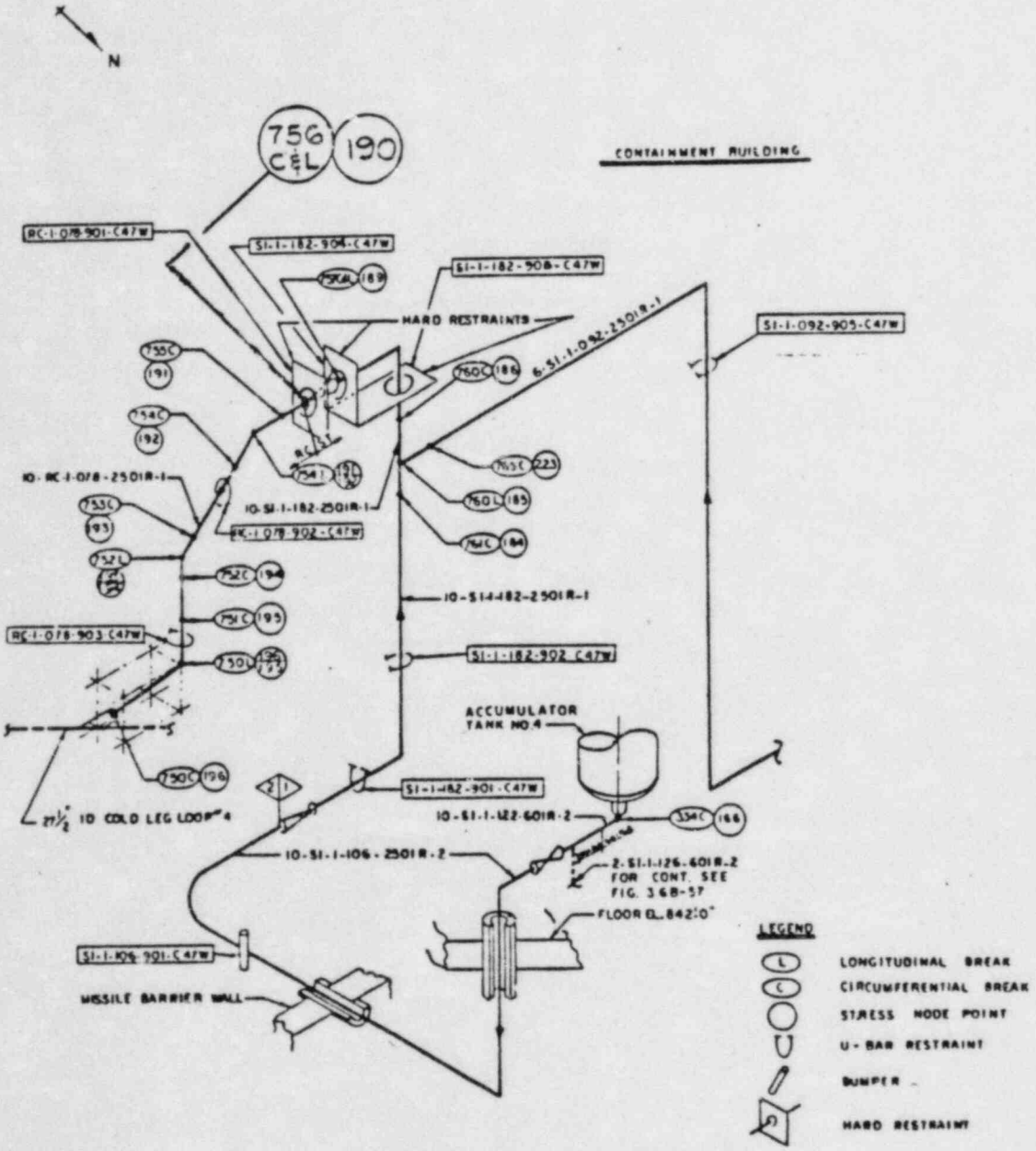

FIGURE 7.2-2
PROBLEM DSI-17D
SAFETY INJECTION SYSTEM
BREAK POINT AND
RESTRAINT LOCATIONS

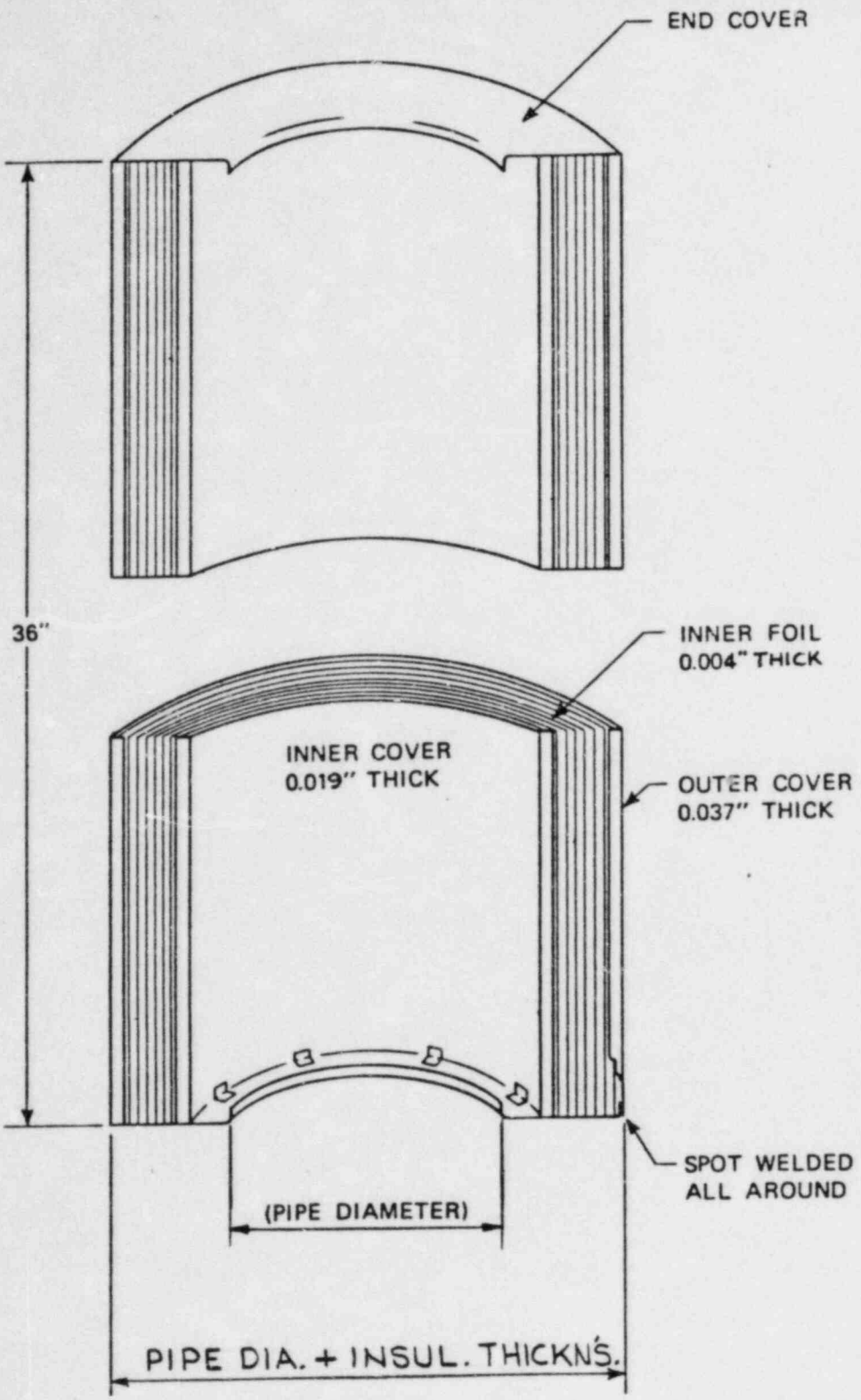

FIGURE 7.2-3

SCHEMATIC DRAWING OF REFLECTIVE METALLIC INSULATION UNIT

TABLE 7.1-1

INSULATION PANEL DIMENSIONS

ITEM	THICKNESS (INCHES)
Outer Case	0.037
Inner Case	0.019
Liners	0.004
Liner Spacing	0.33
Disc (End Cover)	0.019
Laps (Ends)	0.037

TABLE 7.2-1

FIBROUS INSULATION TAKE OFF

DRAWING NO. 2323-M1-0507

Case No.	Location	Line Size	Feet of Insulated Pipe	Square Feet of Insulation
1	El. Below 860'-0" Southwest Quadrant	3"	31	40.6
		6"	68	142.4
			Total	183.0
2	El. Below 860'-0" Northeast Quadrant	3/4"	43	31.0
		1"	29	22.8
		2"	74	77.5
		3"	163	213.2
		4"	141	221.4
		6"	109	228.2
			Total	794.1
3	El. Below 860'-0" Northeast Quadrant	3/4"	20'-0	14.4
		2"	3'-0	3.1
		3"	97'-0	126.9
		4"	160'-0	251.2
			Total	395.6
4	Part Plan El. 842'-0" Wall	3/4"	17'-0	12.3
		2"	44'-0	46.0
		3"	20'-0	26.2
		4"	185'-0	290.5
			Total	375.0

TABLE 7.2-2

FIBROUS INSULATION TAKE OFF

DRAWINGS NO. 2323-M1-0511

Case No.	Location	Line Size	Feet of Insulated Pipe	Square Feet of Insulation
1	El. Above 832'-6" 0° Near Cont. Wall	3/4"	20	14.4
		1"	21	16.5
		2"	65	68.1
		3"	16	20.9
		4"	172	270.0
		8"	50	130.9
			Total	521
2	El. Above 832'-6" 315° Azimuth	3/4"	32	23
		1"	11	8.6
		2"	38	40.0
		3"	52	68.1
		4"	126	197.8
		6"	115	240.7
		8"	26	68.0
			Total	646
3	El. Above 832'-6" 19° Azimuth	3/4"	38	27.3
		1"	10	7.8
		2"	37	38.7
		3"	46	60.2
		4"	111	174.3
		8"	12	31.4
			Total	340

TABLE 7.2-3

FIBROUS INSULATION TAKE OFF

DRAWING NO. 2323-M1-0511-01

Case No.	Location	Line Size	Feet of Insulated Pipe	Square Feet of Insulation
1	El. Below 832'-6" Northwest Quadrant of Cont.	1"	40	31.4
			Total	31.4
2	El. Below 832'-6" West Side of Cont.	1"	22	17.3
		2"	51	53.4
			Total	70.7
3	El. Below 832'-6" Southwest Quadrant of Cont.	1"	5	4.0
		2"	66	69.2
		4"	91	142.9
			Total	216.1

TABLE 7.2-4

FIBROUS INSULATION TAKE OFF

DRAWING NO. 2323-M1-0513

Case No.	Location	Line Size	Feet of Insulated Pipe	Square Feet of Insulation
1	El. Below 836' Reactor Coolant Pump No. 01	1-1/2"	2	2.0
		2"	37	38.8
			Total	40.8
2	El. Below 836' Reactor Coolant Pump No. 02	1-1/2"	2	2.0
		2"	44	46.0
			Total	48.0
3	El. Below 836' Reactor Coolant Pump No. 03	1-1/2"	2	2.0
		3"	30	39.3
			Total	41.3
4	El. Below 836' Reactor Coolant Pump No. 04	1-1/2"	2	2.0
		2"	23	24.1
			Total	26.1

TABLE 7.2-5

FIBROUS INSULATION TAKE OFF

DRAWING NO. 2323-M1-0513-01

Case No.	Location	Line Size	Feet of Insulated Pipe	Square Feet of Insulation
1	El. 835'-0" Stm. Gen. No. 1 Compt.	3/4"	51	36.8
		2"	11	11.6
		3"	90	117.8
		4"	15	23.6
			Total	189.8
2	El. 836'-0" Stm. Gen. No. 4 Compt.	3/4"	38	27.4
		2"	44	46.1
		3"	144	188.3
		4"	7	11.0
			Total	272.8
3	El. 836'-0" Stm. Gen. No. 2 Compt.	3/4"	44	31.7
		2"	11	11.6
		3"	95	124.3
		4"	11	17.3
			Total	184.9
4	El. 836'-0" Stm. Gen. No. 3 Compt.	3/4"	56	40.4
		3"	138	180.6
		4"	12	18.9
			Total	239.9

TABLE 7.2-6

METALLIC INSULATION DAMAGE FROM R.C. LOOP PIPE BREAK

STEAM GENERATOR COMPT. NO. 4

Piping or Equip.	Area Damaged (ft^2)	No. of Foil Liners
Stm. Gen. No. 4	2670	10
R.C. Pump No. 4	328	13
27 1/2" Cold Leg	71.43	10
29" Hot Leg	132.47	13
31" Crossover	325.42	14
Containment Spray	62.60	5
RTD	61.52	7
Feed Water	346.16	5
Miscellaneous Piping:		
Reactor coolant	601.87	5-10
Residual heat	61.02	3
Safety injection removal	25.66	2
Main Steam	153.19	5 & 8
Total	4839.34 ft^2	
Total area of insulation foil =	46,600 ft^2	

TABLE 7.2-7

METALLIC INSULATION DAMAGE FROM 10" R.C. PIPE BREAK

STEAM GEN. COMPT. NO. 4

Piping or Equip.	Area Damaged (ft^2)	No. of Foil Liners
Stm. Gen. No. 4	46.70	10
29" Hot Leg	132.47	13
RC Pipe	18.77	10
SI Piping	7.26	2
MS Pipe	3.04	5
Total	89.49 ft^2	
Total area of insulation foil =	815.64 ft^2	

TABLE 7.2-8

REFLECTIVE METALLIC INSULATION
LOCATED WITHIN 7 PIPE DIA. OF JET
FROM PIPE BREAK 756 LWR

Line No. or Equip.	Area Hit By Jet	No. of Foil Liners
1-RC-1-156-2501R-2	2.072 ft^2	7
1 1/2-SI-1-202-2501R-1	.548 ft^2	2
STM. GEN. #4	6.925 ft^2	10
Total	9.545 ft^2	

Total foil area - 84.85 ft^2

TABLE 7.3-1

WATER VELOCITIES IN CHANNELS
APPROACHING THE SUMPS
(ft/sec)

Channel[1] No.	Sub-Channel[1] No.	Water Level			
		High		Low	
		One Train	Two Trains	One Train	Two Trains
3	A	0.05	0.11	0.07	0.15
3	B	0.09	0.18	0.12	0.25
4	A	0.04	0.09	0.06	0.12
4	B	0.15	0.30	0.21	0.42
4	C	0.06	0.11	0.08	0.16

Notes:

1. See Figure 5.4-1 for the channel locations
2. See Figure 5.4-4 for the sub-channel locations

TABLE 7.3-2

TRANSPORT AND BLOCKAGE TEST RESULTS

Sample Description	Velocity to initiate motion (ft/sec)	Velocity to transport to screen (ft/sec)	Comments
1. Undamaged unit (half assembly)			
concave side up	1.0	1.0	Either flipped on screen or got stuck partially flipped
concave side down	above 2.2		Never moved.
2. Outside Cover (0.037" thick)			
concave side up	0.7	0.8	Same blockage mode as undamaged units.
concave side down	above 1.8		
3. Inside Cover (0.015" thick)			
concave side up	0.7	0.8	With both initial positions, covers flipped against the screen on arrival and got flattened against it by the flow force.
concave side down	1.1	1.6	

Table 7.3-2 (Continued)

Sample Description	Velocity to initiate motion (ft/sec)	Velocity to transport to screen (ft/sec)	Comments
4. End Covers	above 2		Never moved.
5. 0.0040 inch foil (36 x 36 inches) uncrumpled	0.25	0.40	Folding and tumbling transport mode, occasionally sliding. Flips on screen upon arrival, often folded.
crumpled	0.25	0.35	Folding and tumbling or sliding transport mode.
multiple sheets (2 crumpled 2 uncrumpled)	0.25	0.9 to 1.1	Foil interactions often create jams needing higher velocities to break up. Signficant overlapping on screen. Blockage up to about 80% observed.

8.0 NEAR SUMP EFFECTS

This section of the report summarizes the results of analyses conducted to study the behavior of paint flecks which become dislodged in the event of paint failure and fall to the surface of the pool of water existing at the containment lower floor during the post-LOCA recirculation mode.

As will be evident from the results of these analyses, only paint which is located near the ECCS sumps or can be washed to the pool surface in the vicinity of the sumps (including the paint on the containment liner segment defined between the azimuthal angles of 30 and 330° which can be washed down by the action of the containment spray water) has the potential for adversely affecting the performance of the sump.

This section of the report is subdivided into two subsections. The first subsection addresses the theories employed to describe the motion of the paint particles through the pool of water. The second subsection considers the propensity for particles reaching the screen to stick to it and result in partial or full clogging of the ECCS sump fine screens.

8.1 Motion of Paint Fragments Through the Pool of Water

a. Introduction

Motion of paint fragments through the pool water is affected by many parameters including fragment size, shape, density, and water velocity. In general, however, the principal characteristics of the fragment motion are related to the local Reynolds number and the fragment mass moment of inertia.

For very low local Reynolds numbers ($N_R < 1.0$), paint fragments (herein idealized as thin disks) will move through the water maintaining their original orientation, i.e., the pitch angle with which they begin their descent through water. This particular type of behavior can be described by a theory which maintains the initial angle of the fragment constant throughout its descent through the water. Since the local Reynolds number is defined as:

$$N_R = \frac{Wd}{\gamma}$$

where W is the particle relative velocity (relative to the water), d is the fragment (disk) diameter, and γ is the kinematic viscosity of water, values of N_R less equal to one exist only in regions of low fragment velocity and/or virtually stagnant pool conditions. These conditions would not simultaneously exist for fragments which exceed 1/8 inch diameter (particles having diameters less than 1/8 inch will not clog the ECCS sump screens).

For higher local Reynolds numbers ($1<N_R<100$), the motion of the fragment is characterized by an initial adjustment occurring as its travel begins through water, whereby any initial orientation will adjust itself to an attitude normal to the velocity resultant from pool drift and gravity.

For yet higher local Reynolds numbers ($100<N_R$), the motion will be characterized by a periodic pitching (flutter) which persists throughout the descent of the fragment. The pitching oscillations are damped in the case of the low local Reynolds numbers ($1 N_R < 100$) and hence the adjustment mentioned above results, but are not damped for $100<N_R1$ (or the damping is very small). In the case of the smallest and lightest fragment that cannot pass through the ECCS sump screens, i.e., a 1/8-inch disk, 5 mils thick, with 90 lb/ft^3 density, the local Reynolds number is generally above 250. Hence unstable oscillations can be expected to persist until the fragment reaches the bottom of the pool or the ECCS screens, whichever occurs first.

Finally, Reference 14 notes that the type of motion that can be expected is also influenced by the mass moment of inertia of the fragment. The latter is given by

$$I = md^2$$

where m is the fragment mass which equals $\rho_\rho \frac{\pi d^2}{4} t$ (P_ρ = fragment density, d = fragment (disk) diameter and t = fragment 4 thickness).

When the dimensionless mass moment of inertia of the fragment defined as

$$I^* = I/\rho_w d^5$$

where $p_w d5$ is proportional to the mass moment of inertia of a rigid sphere of water about its diameter d, exceeds 10^{-2}, tumbling motion of the fragment can be expected for $N_R < 100$. The tumbling motion probability is increased for progressively higher N_R.

For the 1/8-inch fragment, the dimensionless moment of inertia is approximately 3×10^{-3} and $N_R \simeq 250$; thus, no tumbling is expected. As the fragment size increases, the local Reynolds number increases (for instance a 1/2-inch-diameter fragment will have a Reynolds number of 1000), but the dimensionless mass moment of inertia decreases; hence, tumbling is also not to be expected. However, if the size of the fragment remains the same, i.e., 1/8 inches, but the thickness is increased to about 15 mils (about the maximum expected), then the fragment may tumble.

Because of the uncertainty inherent in the behavior of the fragment as it travels through the water, all of the motions described above have been studied, so that the most conservative type of motion, ie that resulting in the longest horizontal distance travelled, could be selected. The theory and results for each type of motion are described below.

b. Analysis of Motion With Constant Angle

This analysis assumes that the paint fragment is idealized as a disk which hits the pool surface at any incident angle. Conservatively, and because of surface tension effects (particles smaller than 1/8" will break through the surface with difficulty), small paint fragments (i.e., 1/8-inch diameter, 5 mils thick) are assumed to be momentarily arrested at the water surface, then to start their travel through the water at the angle of impact with zero initial velocity. Any angle of impact is assumed to be equally probable since for travel in air (or together with spray droplets) the local Reynolds number is high and the dimensionless mass moment of inertia (with respect to air) is also large and hence tumbling motion would be expected.

Referring to Figure 8.1-1, the equations describing the motion of the paint fragment through water when the pitch angle is assumed constant are the following:

$$\rho_P V_P \frac{du}{dt} = \rho_P V_P g - \rho_w V_P g - \frac{C_D(\phi)}{2} \rho_w A_{proj} \sin\beta \; W^2$$

$$- \frac{C_L(\phi)}{2} \rho_w A_{proj} \cos\beta \; W^2$$

$$\rho_P V_P \frac{du}{dt} = -\frac{C_D(\phi)}{2} \rho_w A_{proj} \cos B \; W^2 + \frac{C_L(\phi)}{2} \rho_w A_{proj} \sin\beta W^2$$

$$W^2 = u^2 + (V_o - v)^2$$

$$A_{proj} = \frac{d^2}{4} \sin(\phi)$$

Herein u = vertical component of the fragment velocity

defined as positive downward

v = horizontal component of the fragment velocity

P_ρ = paint density (assumed to be the minimum - 90 lb/ft^3)

P_W = water density (60 lb/ft^3 at 200°F)

W = fragment relative velocity

V_o = velocity of pool water toward the screen (0.08 ft/sec)

C_D = Drag coefficient which varies with ϕ

C_L = Lift coefficient which varies with ϕ

B = angle from pool surface to the velocity vector

The equations describing the motion of the paint particle have been written for a two dimensional problem only. Strictly speaking, the problem is tridimensional, and under the assumption of constant angle with presence of lift, a particle can travel sideways with respect to the direction of the pool drift velocity. However, if one assumes that lift is negligible, then side motion can be considered negligible, and the problem reduces to a two dimensional problem.

The value of C_D for the circular disk is described as a sine function of the incident angle of the disk relative to flow. It has a maximum value of 1.9 when the disk is oriented normal to the relative velocity vector and a minimum value of $C_D = .074/N_R^{0.2}$ when the disk is parallel to the flow (Reference 15). The lift coefficient, C_L, is, conservatively assumed to be negligible for consistency with the observations of References 14 and 16, which found it to be so for low Reynolds numbers. However, comments by W.W. Willmarth to Reference 16 point out that if the motion is accompanied by large oscillation, appreciable lift is developed. Hence, neglect of lift may not be entirely justifiable.

As will be shown later inclusion of lift results in lesser horizontal distance travelled by the fragment.

The results of the constant angle analysis, indicated on Figure 8.1-2, show that if the initial incident angle assumed for the disk approaches 90°, the relatively large downward vertical velocity dominates over the pool "drift" (recirculated pool velocity) velocity so that the fragment does not travel horizontally a significant distrance.

While mathematically this result is correct, physically it may be unrealistic because the actual behavior at the local Reynolds

numbers ($N_R \simeq 250$) is expected to result in an adjustment of the pitch angle.

As Reference 14 indicates, at the local Reynolds numbers of interest, the fragment will tend to orient itself in the most stable equilibrium state (unless large oscillations are present). This state is defined as that which would have the largest dimension being normal to the relative velocity, i.e., the disk will move in a perpenticular position to the velocity that propels it (or drags it).

The results of this analysis show that only paint contained within a distance of 8.6 feet of the edge of the screens has the potential for reaching the screen (i.e., bottom of screen from 9.5 ft. pool surface). Moreover, since the angle remains constant, not all paint within this area will reach the screen, but only a certain fraction.

That fraction is related to the angle with which the paint fragment hits the surface. Since, as will be discussed later, this is not the most conservative mode of paint transport, discussion of the quantity of paint transported in this fashion is deferred to a later subsection of this section.

c. Oscillatory Motion of Fragment

The second analytical method employs the same equations as the method described in Item b above, but adds one additional equation which describes the rotation of the particle fragment. This equation is

$$\frac{d^2\theta}{dt^2} = - \frac{LW^2}{d^2} \left(\frac{C_D}{2t_p} \frac{\rho_w}{\rho_p} \sin \phi + \frac{C_L}{2t_p} \frac{\rho_w}{\rho_w} \cos\phi \right)$$

Here t_ρ is the paint fragment thickness, and L is the distance from the fragment center of mass to the center of applied pressure. This distance is given by

$$L = \frac{0.44d\alpha}{\Pi^2} \quad \text{where } \alpha = 90^o - |\phi|$$

Using the two equations given in Item b, plus the third equation given above, the maximum horizontal distance travelled by the fragment as a function of its initial angle of descent is given in Figure 8.1-2. As this figure shows, the maximum distance which the fragment can travel is the same as computed by the first method. However, proportionately more paint located within this distance away from the edge of the screen can reach the

screen, since paint which begins its travel at angles near 90° can now reach the screen from distances farther away than calculated in the prior method.

In the results shown in Figure 8.1-2 lift has been neglected. As Reference 17 indicates, lift may be present when large oscillation occur. Analyses performed with consideration of lift indicate that in general lift will reduce the maximum horizontal distance that a particle can travel. Because of the large uncertainty associated with the choice of a value for lift coefficients, no credit can obviously be taken for the effect. However, one can intuitively understand this effect by visualizing that since the particle will travel substantially with its face aligned normal to its motion (on the average since the particle oscillates about this position), it presents an angle of attack to lift which causes lift to reduce its forward motion.

The equation describing the rotation of the paint particle about its center mass contains no damping term. This is considered appropriate for the range of Reynolds numbers of interest and when lift is neglected. As the amplitude of the oscillation increases and lift becomes pronounced, the absence of a damping term will probably lead to incorrect solutions (this is one of the reasons why lift has been ignored). Actually, the damping term would not be a true damping, but rather a virtual mass effect, whereby the effect of hydrodynamic mass introduced by the angular acceleration through a large rotation is to add an inertia term which opposes the rotation of the fragment. Figure 8.1-3 illustrates the trajectory of a 1/8-inch paint fragment descending through a pool of water with a drift velocity of 0.8 fps. Two trajectories are shown. One trajectory assumes no lift, and the other assumes a large lift coefficient. As previously stated, little confidence can be placed on the accuracy of the latter. However, its behavior tends to confirm that lift will reduce the horizontal distance travelled.

The frequency of oscillation of the particle illustrated in Figure 8.1-3 is 4.17 sec-1. Reference 16 provides an equation from which the expected frequency of oscillation of disks falling through a medium can be predicted from the equation.

$$n(\text{frequency of oscillation}) = 0.169\, W(\rho_w C_D/\pi\rho_p td)^{\frac{1}{2}} \text{sec}^{-1}$$

herein all symbols have been previously defined, one computes that for a particle 1/8 inch in diameter falling with a velocity approximately equal to 0.8 fps, its frequency of oscillation should be about 4.53 sec^{-1}.

d. Tumbling Fragments

The third analysis performed assumes that the fragment tumbles as it descends through the water. For tumbling, the fragment is idealized as a sphere having an equivalent mass as the disk (a sphere having a diameter equal to the disk would travel a much shorter distance horizontally).

Under this assumption the equations of motion are considerably simplified since there is no preferred orientation. This sphere corresponding to the 1/8-inch paint fragment is computed to travel horizontally a maximum distance of 2-1/2 feet.

Drag for the sphere in the range of Reynolds numbers of interest is approximated by

$$C_D = \frac{24}{N_R} \left(1 + \frac{3}{16} N_R\right)^{\frac{1}{2}}$$

8.2 Analysis of Potential for Sump Clogging

If one conservatively assumes that any paint fragment larger than the minimum screen opening which reaches the screen surface sticks to the surface, and further conservatively assumes that no fragment overlays another fragment, then results of the analysis employing method a) (Item (b) above indicate that a large percentage of the fine screens can be blocked.

The precise amount of screen blockage depends on may factors, including the amount of paint, insulation and other debris which may have been transported to the screen by mechanisms described in other sections of this report. This section however, demonstrates that regardless of mechanism of transport, i.e., global transport from other containment areas as addressed in the other sections of this report, which clogs the lower portion of the screens, or local transport through the pool in the immediate vicinity of the sumps, as addressed in this section, which clogs a significant percentage of the upper portion of the screens, there will remain on the top portion of the screen a band estimated to be a minimum of 2 inches wide, which will be free of paint. This is not the only area of the screen free of paint, debris, etc. The maximum amount of sump clogging resulting from failure of all paint in containment will be 94 percent. Results of the full scale test conducted by Western Canada Ltd. have shown that this percentage of blockage is acceptable from the standpoint of sump performance and NPSH requirements of the ECCS pumps.

The 94 percent is a composite figure, since as will be shown later there are other areas of the screen which will only be partly blocked. To understand how the 94 percent composite figure is derived, it is necessary to understand the precise

geometry of the top portion of the sump. This geometry is shown in Figure 8.2-1.

The top of the sump rack is a solid steel plate which extends more than 1 foot outward from the fine screen, and approximately 8 inches outward from the course screens.

A distance of 5-3/8 inches separates the fine and coarse screens (5.5 inches from outer edge); and a solid plate connects the bottom of the fine screen frame to the bottom of the coarse screen frame.

The top of the fine screens is a solid plate extending downward approximately twelve inches. Likewise, the coarse screens are separated from the top plate by a gap, which is approximately ten inches. The top of the coarse screen consists of a solid plate 2-11/16 inches wide.

The results of the analyses in this section indicate that at the beginning, when the screens are relatively free and the inlet velocity at the fine screen is 0.08 fps, the descent of the smallest paint particles through the pool (1/8 inch, 5 mils thick) takes place at approximately 45° trajectory. As particles accumulate against the screen (including debris from the other transport mechanism described in other sections), the inlet velocity at the fine screen itself will increase, although farther away from the fine screen (i.e., just outside the coarse screens) the velocity will not change nearly as much. Ultimately, as the fine screens become blocked to the maximum extent, the inlet velocity reaches a value of about 1.3 fps at the fine screens.

At this point the flow through the fine screens behaves as two dimensional flow through an orifice of diameter equal to the screen open band. Particles of paint which fall in the pool immediately adjacent to the top plate edge would fall at most along a 45° trajectory until they experience the increased velocities in the region influenced by the orificing effect of the severely blocked fine screens. Those particles which are brought in the vicinity of the lower edge of the coarse screen frame will then be transported at an angle defined as

$$\alpha = \tan^{-1} \frac{U_s}{V_\infty}$$

Where U_s is the terminal velocity of the particle modelled as a sphere, since for the higher Reynolds numbers the particle will tend to tumble, and V_∞ is the average of the flow velocity over the distance travelled. Solution for this angle is iterative since V_∞ depends on the size of the orifice which in turn is dictated by the angle.

At an orifice size of 2 inches the velocity at the fine screen inlet is about 1.3 fps and the velocity at the coarse screens inlet is about .4 fps. At these higher velocities the particle fragment will tumble and behave more as an equivalent sphere. For a 1/8 inch particle the vertical velocity component will be about 0.3 fps. From the moment the particle crosses the coarse screen its trajectory will be defined along a parabola roughly bounded by an angle given by α = tan 0.3/0.8 or 20 degrees where 0.8 fps is the average velocity over the distance travelled.

Since 5.5 (distance separating two screens) times tan 20° is 2.0 inches, this dimension is the band width of the top of the fine screens which is computed to remain free of paint debris.

In addition to the free band of fine screens that would remain on all sides of the sump, there is some additional area of the screen which will not be blocked.

The screen facing the steam generator wall is computed to be not completely blocked. Most of the paint on concrete walls is computed not to reach the screen because of its relatively large thickness (≃25-30 mils). Of the remainder of the paint a fraction consisting of approximately 35 ft of paint from the ceiling plus about 30 ft of paint on pipes, supports, etc., is computed to reach the screen over about half its width. The remainder of the width is completely clogged by the ceiling paint and support paint. If there were no other debris against that side of the sump, the screen open area would be about 25 ft^2. With debris covering the bottom half of the screen, only about 12.5 ft^2 would remain open. This figure is equally applicable to either sump. Together with the free area at the very top of the screen, the total free area would be approximately 24 ft^2. This blockage would not impair the capacity of the ECCS sump to function, since as stated in Section 4, 19 ft^2 is sufficient.

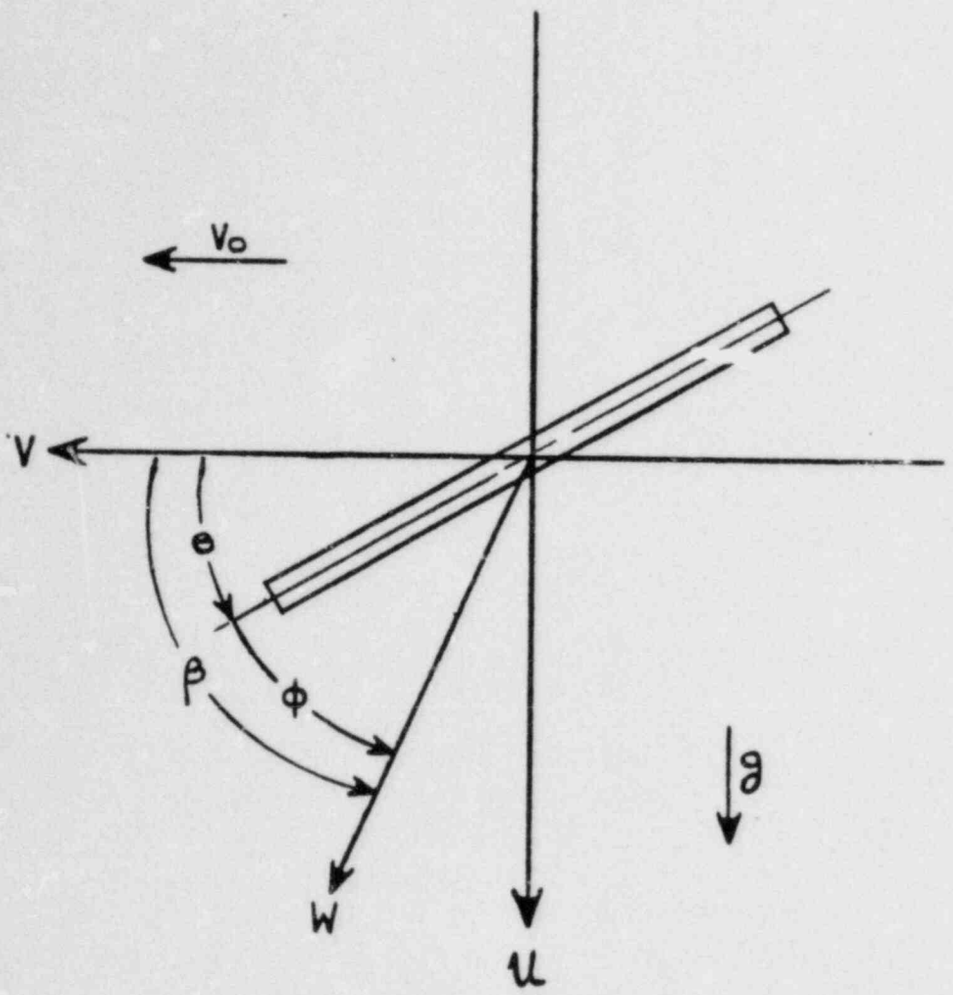

FIGURE 8.1-1
CHIP MOTION WITH CONSTANT ANGLE

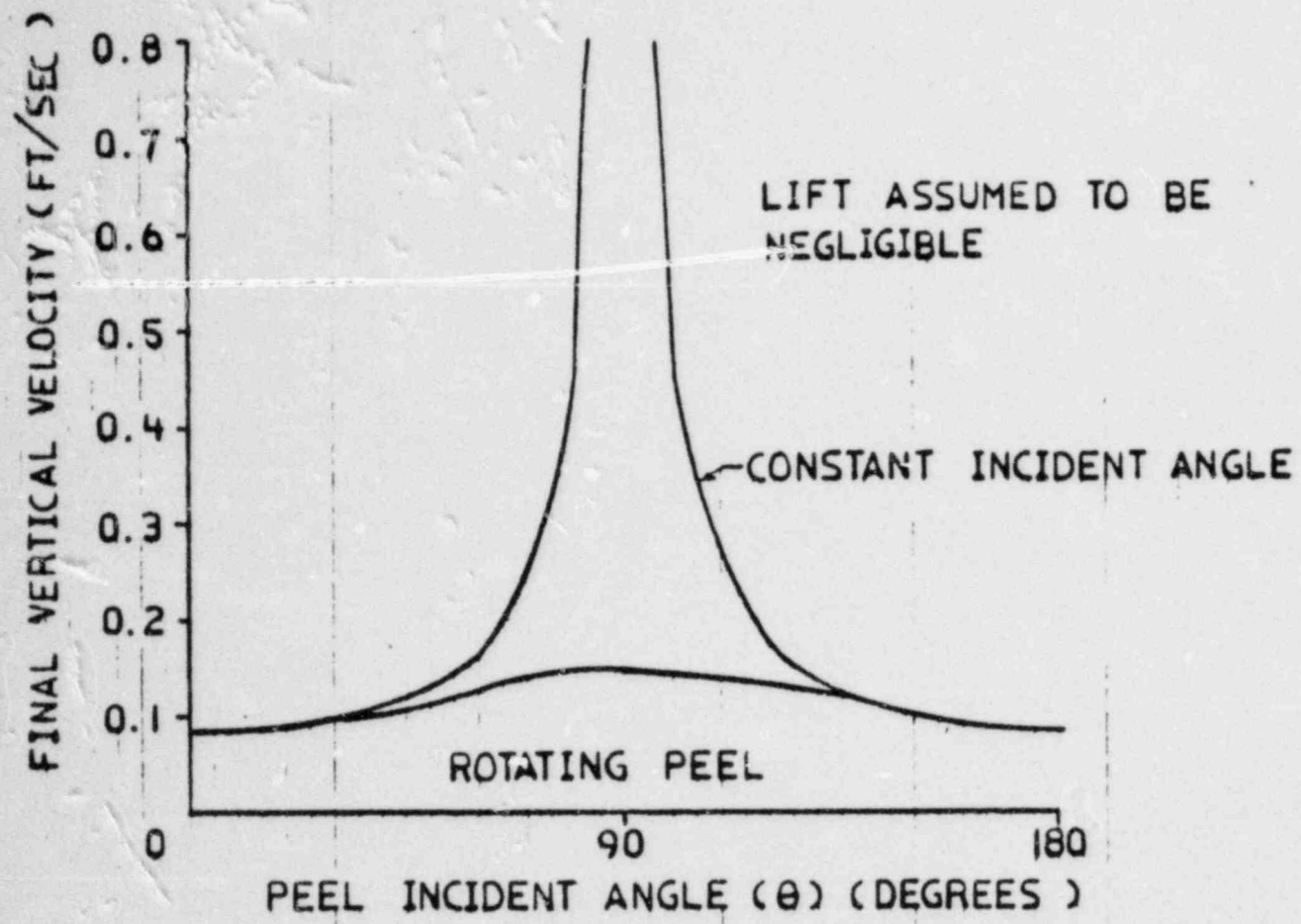

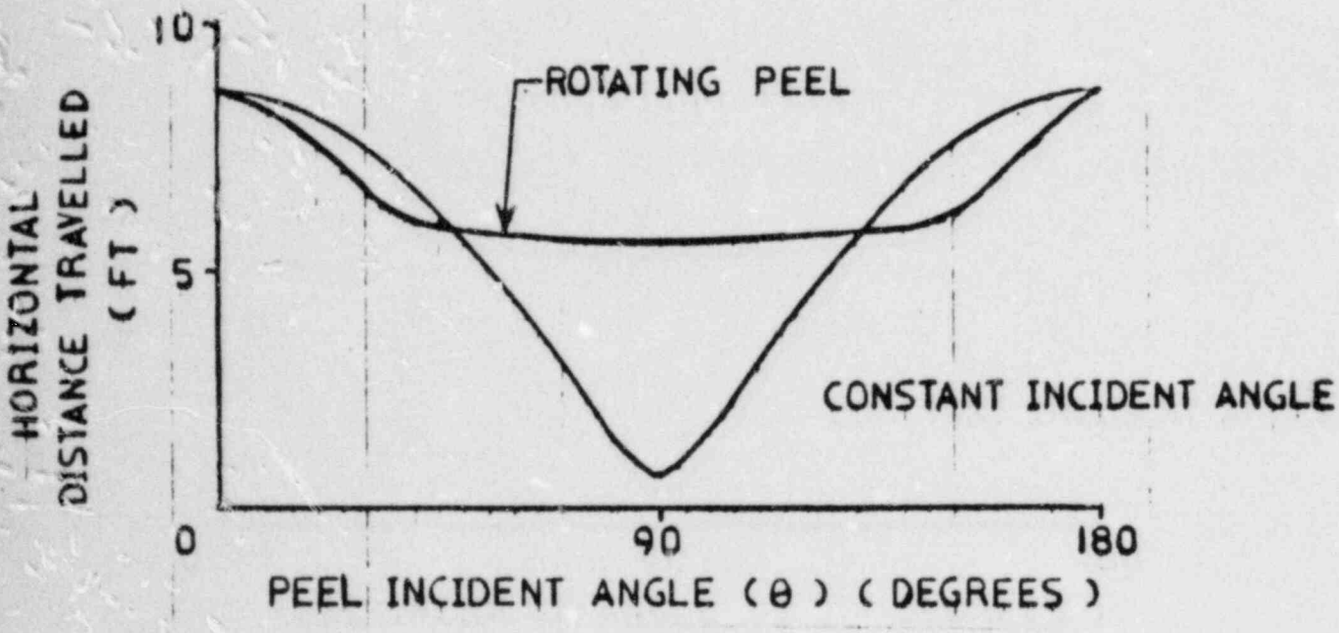

FIGURE 8.1-2
CONSTANT ANGLE ANALYSIS RESULTS

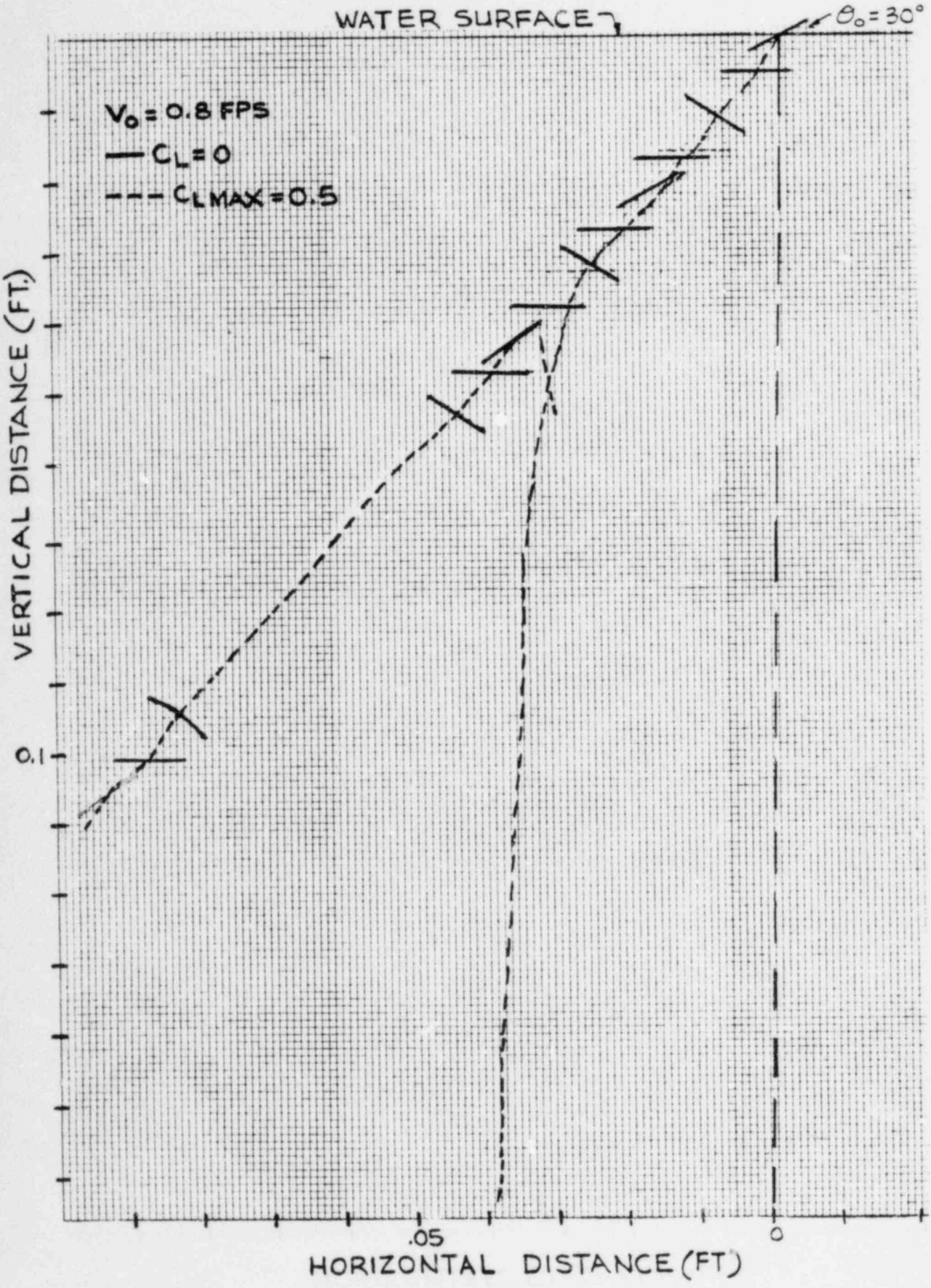

FIGURE 8.1-3
OSCILLATING MOTION OF PAINT FRAGMENT

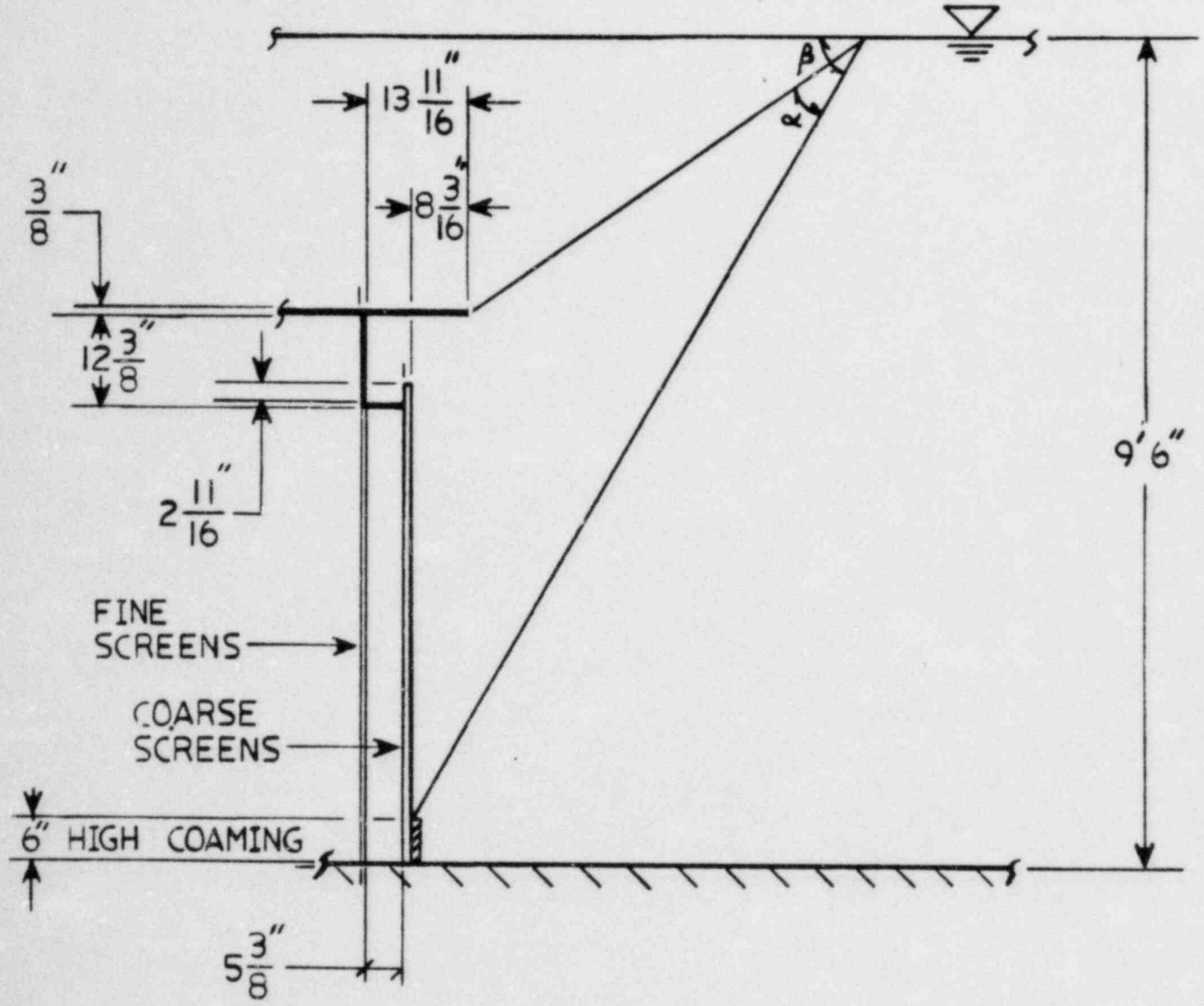

FIGURE 8.2-1
SUMP GEOMETRY

9.0 DEBRIS EFFECTS ON EMERGENCY SUMPS

Each of the two containment recirculation sump screens has a total through-flow area of 386 ft^2. The sump screen design is in accordance with the requirements of Regulatory Guide 1.82 with a through-screen velocity of 0.11 fps. Figure 3.2-2 shows the arrangement of the Emergency Sumps.

The NPSH for RHR/SI pumps and containment spray pumps during the recirculation phase is given in Table 4.1-2.

Blockage of the sumps by debris will tend to increase the pressure losses across the sump screens. The increase in pressure losses will depend on the extent of the blockage and the porosity of the debris. The increase in pressure losses will reduce the available pump NPSH. This can have an adverse effect on the operation of the recirculation pumps, if it exceeds the margin between available and required NPSH.

For totally impermeable debris, the pressure loss across the sump screens was calculated based on the area available for flow, excluding the projected blockage area.

The evaluation of fibrous insulation debris generation shows that there are no zones inside the containment where such insulation can fail to cause debris coincident with a demand for the emergency sump operation.

The insulation debris transport analysis discussed in Section 7.3 determined that the high efficiency insulation and metallic insulation will not be transported to the sump screens.

Any paint debris that is transported to the sump by sliding along the concrete surface will accumulate on the floor. This is because the water velocity at the screens is much lower than the velocity required to put the debris into suspension. However, for a conservative first approximation, to determine if pressure losses were excessive, it was assumed that the screens will be blocked by the paint particles forming a heap next to the screens with an angle of repose of 45 degrees. Figure 9-2 shows a graph of the quantity of paint accumulation at the sump screens corresponding to different levels of sump screen blockage.

The quantity of paint that has any potential for transport to the sump screens is the paint in the sump area itself as discussed in Section 6.2 Paint Debris Transport.

Table 6.2-25 gives about 89,000 sq. ft., as the quantity of paint that can accumulate in the near sump zone (azimuth 45-0/360 - 315°). This quantity includes:

a. All the paint debris from upper floors of the containment which can be transported to the near sump zone.

b. All the paint on the containment liner in the sector for the near sump zone up to the spring line.

c. All the paint between elevations 808' and 832' in the near sump zone.

The 89,000 sq. ft. of paint in the near sump zone will consist of concrete and steel coatings. For a conservative estimate of the volume of paint debris, it was assumed that most of this coating is from concrete surfaces with an average paint thickness of 20 mils. It was also conservatively assumed that the bulk density of the paint debris is only 50 percent of the actual density. Based on these conservative assumptions, the volume of paint debris in the near sump area was calculated to be about 300 cubic feet. This amount of debris constitutes about 50 percent sump screen blockage.

From Figure 9-2, it can be concluded that about 35 percent of the sump screens will be blocked if all the coating were from steel surfaces and about 50 percent blockage if all the coatings were from concrete surfaces. This amount of blockage must be combined with the blockage from near field effects as determined from Section 8. As can be seen from the last paragraph of section 8, this combination leads to the conclusion that 24 square feet of screen area is available. Using data from Table 4.1.3, the head loss through the screens is estimated to be 0.4 feet. Because of this loss, the elevation of water in the containment required to supply the minimum NPSH to the ECCS pumps is increased. Using data from table 4.1.2, the NPSH margin for these pumps will be as shown in Table 9-1.

Based on the above evaluations for insulation and paint debris effects on the emergency sump performance, the following conclusions were arrived at:

a. Insulation has no potential for forming debris which can block the sump screens.

b. Paint debris accumulating in the near sump area resulting from all the coating systems failing in the containment cannot result in unacceptable sump screen blockage.

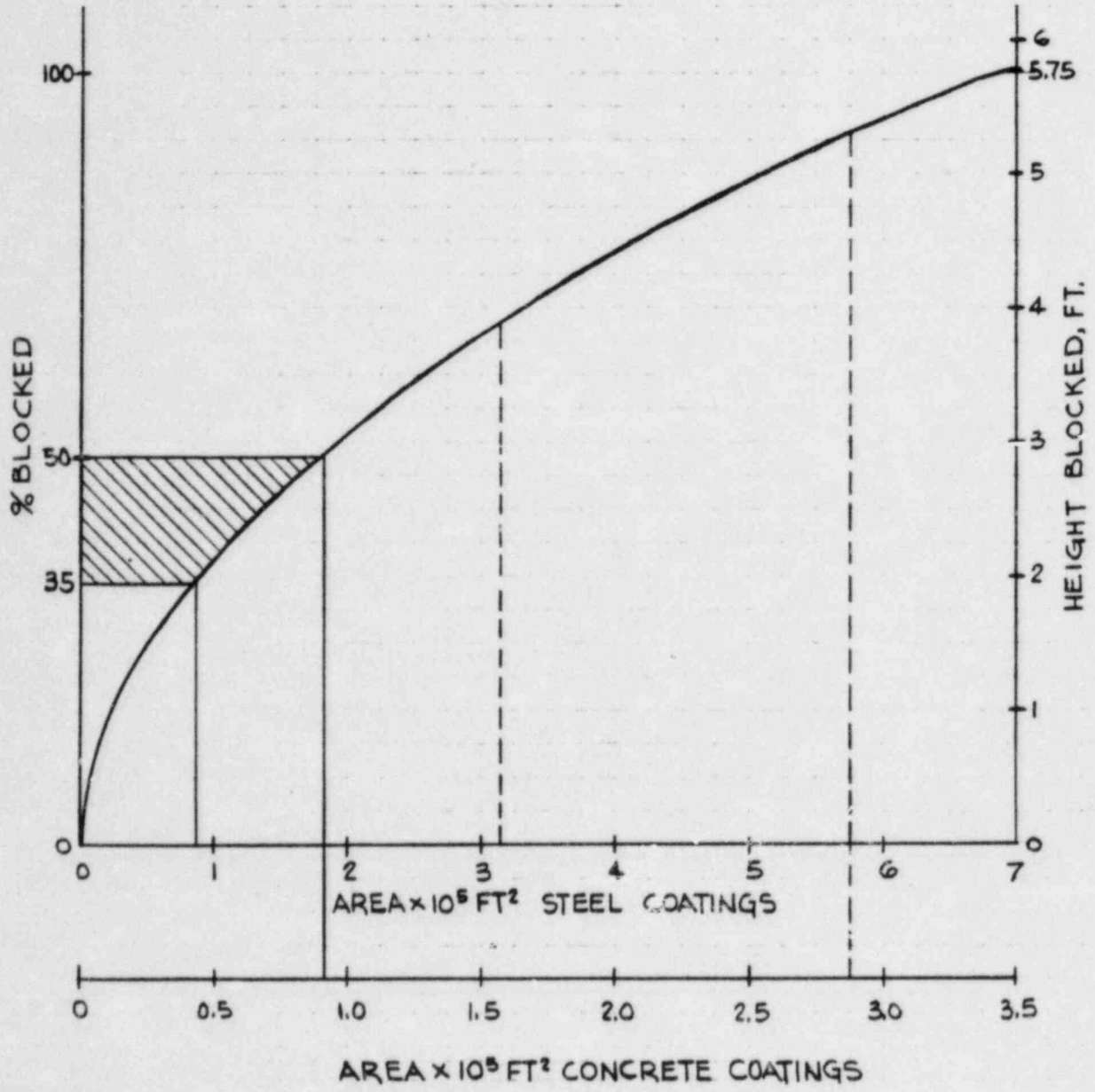

FIGURE 9.1
PAINT AREA VS. % BLOCKED SCREEN

TABLE 9-1

SPRAY AND RHR PUMP NPSH

PARAMETER	Pump CSS	RHR
Loss through screen with 24 ft^2 area, feet	0.4	0.4
Water elevation to supply required NPSH, feet[1]	1.02	2.6
Water elevation available, feet[1]	6.83	6.83
NPSH margin, feet	5.81	6.63

NOTE:

[1] Feet above containment floor (EL. 808 ft)

APPENDIX 1

APPENDIX
TO
REPORT ON EVALUATION OF PAINT
AND CONTAINMENT EMERGENCY SUMP PERFORMANCE
BY GIBBS & HILL, INC.

WESTINGHOUSE EVALUATION OF PAINT DEBRIS EFFECTS
ON THE CPSES EMERGENCY CORE COOLING SYSTEM

INTRODUCTION

Westinghouse was requested to evaluate the CPSES Emergency Core Cooling System (ECCS) to determine if the system function/components would be degraded by the ingestion of paint debris postulated to be present in the containment sump following a large break Loss of Coolant Accident (LOCA). This evaluation was made based on the following assumptions:

a. Carboline Carbozinc-11 fails during the LOCA and releases zinc to the ECCS.

b. The zinc remains suspended in the ECCS coolant.

c. Leachable chloride from all containment paint has the potential to reach the ECCS.

Using the above assumptions an in-depth review was made of the ECCS and its critical components to determine what potential corrosion/erosion degradation effects might be expected. Also, no deleterious effects are postulated in the reactor core for the material concentrations assumed in this evaluation.

A chemical analysis of all containment paints was made to determine the amount of leachable chlorides which could potentially be absorbed into the ECCS.

Evaluation of the Emergency Core Cooling System, Potential Degradation

The Emergency Core Cooling System and its critical operating components which include the high and medium head injection pumps, the low head Residual Heat Removal (RHR) pumps, valves, orifices and RHR heat exchangers were evaluated for potential corrosion and erosion degradation associated with the failure of the Carboline Carbozinc-11 paint at LOCA conditions and the subsequent ingestion of zinc into the ECCS. Zinc particles in the range of two to 50 microns were assumed to be present in the coolant water and remained in suspension during the post-accident ECCS operating sequences. Leachable chlorides from all the containment paints were also assumed to be absorbed into the ECCS coolant.

The in-depth evaluation of the ECCS and its critical components failed to identify any condition or component that would experience significant erosion or corrosion damage. Chemical analysis of the six paints used in containment identified potential chloride concentration levels which are significantly below those levels which could cause stress corrosion cracking problems in sensitized austenitic stainless steel.

If the zinc assumed to be present in the ECCS coolant should settle/drop out of suspension a major portion of the drop out

would occur in the reactor vessel lower plenum where flow velocities are expected to be ≤ .1 ft/sec during ECCS recirculation. The available drop out volume of the reactor vessel lower plenum is > 300 ft^3 and would adequately contain all the zinc which could be ingested into the ECCS.

Containment Paint Chemical Analysis Results

The impurity contribution of the various containment paint systems to contamination of the Emergency Core Cooling System (ECCS) assuming all paint leachables are released to the ECCS was calculated assuming the following parameters:

Volume of Fluid in Containment	550,000 gallons
Metal Paint Volume	7.85×10^6 cm^3
Concrete Paint Volume	2.02×10^7 cm^3
Touch-Up Paint Volume	Insignificant compared to the above volumes.

The analyzed chloride content of the various containment paints, their contribution to the total chlorides and the total chlorides contained in these paints are presented in Table 1.

The total chlorides from the paint systems (6,192 grams) would result in an ECCS coolant chloride concentration of 3.0 ppm. This value is significantly lower than the 96.5 ppm concentration level below which no cracking of sensitized austenitic stainless steel would occur in 12 months when exposed at 150°F to a solution of boric acid and sodium hydroxide at pH 8.5. This 96.5 ppm value is obtained using two plots presented in WCAP-7628,Stress Corrosion Testing, D.D. Whyte, 1978, and which conservatively assumes that the slope of the chloride concentration versus time to crack plot is the same at high pH (8.5) as at low pH (4.5). This value was calculated to be 96.5 ppm of chloride. Since the total chloride leachables from all containment paint would result in only a 3.0 ppm concentration, no stress corrosion cracking of any of the austenitic stainless steels would occur.

Effects of Fluoride Content of Paint on Corrosion

If any fluoride ions were present in the paints, no fluoride cracking of sensitized stainless steel would occur since it would form fluoroborates which do not crack stainless steel.

TABLE 1

Material	Chloride Concentration, ppm	Total Weight of Paint, grams	Total Chloride Released, grams
Metal Paint			
Phenoline-305	170 to 180	7.25×10^6	1269
Carbozinc-11	70 to 80	1.0×10^7	750
Concrete Paint			
Nutec-11S + 11 + 1201	95 to 120	3.9×10^7	4173
Touch-Up Paint			
Carboline-191	250 to 300	Insignificant compared to above quantities.	

Total paint chloride which would be potentially released = 6,192 grams.

Summary and Conclusions

The evaluation of the ECCS and its critical operating components revealed no potential erosion or corrosion degradation with respect to the postulated ingestion of zinc into the ECCS. The conclusions resulting from this evaluaiton and the related containment paint chemical analysis are as follows:

- No significant erosion or corrosion damage to the ECCS or to its critical components.
- Leachable chloride concentration levels (for all containment paints) which could enter the ECCS are significantly below the chloride concentration levels which could cause cracking in sensitized austenitic stainless steel.
- No fluoride cracking of sensitized stainless steel will occur since any fluoride ion, if present, would form fluoroborates which have no effect on stainless steel.
- No deleterious effects are postulated in the reactor core for the material concentrations assumed in this evaluation.

REFERENCES

1) ANSI N101.2 - 1972 Protective Coatings (Paints) for Light Water Nuclear Reactor Containment Facilities

2) SSPC, Volume 1, Steel Structures Painting Manual, Chapter 23 - 1982

3) ASTM D772-47, Standard Method of Evaluating Degree of Flaking (Scaling) of Exterior Paints, Volume 06.01 - 1984

4) ASTM E714-56, Standard Method of Evaluating Degree of Blistering of Paints, Volume 06.01 - 1984

5) ASTM D660-44, Standard Method of Evaluating Degree of Checking of Exterior Paints, Volume 06.01 - 1984

6) NUREG/CR -2791

7) Regulatory Guide 1.82

8) Western Canada Hydraulic Laboratory Report, Dated November 1981

9) Open Channel Hydraulics, Vente Chow, McGraw Hill, 1959

10) Handbook of Hydraulics, Brater King, McGraw Hill, 5th Edition, 1963

11) Design of Small Dams, U.S. Department of Interior, Bureau of Reclamation, U.S. Government Printing Office, 1974

12) NUREG - 0897, Rev. 1 (Draft), June 1984

13) NUREG/CR - 3616

14) W.W. Willmarth, N.E. Hawk, and R.L. Harvey, "Steady and Unsteady Motions and Wakes of Freely Falling Disks," The Physics of Fluids, 7, 2, 197-208 (1964).

15) B. McCormick "Aerodynamics, Aeronautics, and Flight Mechanics," John Wiley & Sons, New York, 1979.

16) E.K. Marchildon, A. Clamen, W.H. Gauvin, "Oscillatory Motion of Freely Falling Disks," Physics of Fluids, 9, 2018 (1964).

17) A.W.W. Willmarth "Reply to Comments by E.K. Marchildon, A. Clamen, and W.H. Gauvin," The Physics of Fluids, 9, 2019 (1964).